CFD Analysis of Flow and Heat Transfer through Natural Convection in Co-axial Cylinders with effect of shape of Cylinder

A Project Report

Submitted by

Ram Kaistha (R900213034)

D. Vinay Kumar (R900213021)

B. Sai Nagendra (R900213017)

In partial fulfilment of the requirements
For the award of the degree of
BACHELOR OF TECHNOLOGY
In
CHEMICAL ENGINEERING WITH SPECIALIZATION IN REFINING & PETROCHEMICALS)

Under the guidance of

Dr. Krunal Madhukar Gangawane
Assistant Professor
Department of Chemical Engineering

DEPARTMENT OF CHEMICAL ENGINEERING

APRIL, 2017

COLLEGE OF ENGINEERING STUDIES
UNIVERSITY OF PETROLEUM AND ENERGY STUDIES, DEHRADUN

DECLARATION BY SCHOLAR

I hereby declare that this submission is my own and that, to the best of my knowledge and belief, it contains no material previously published or written by another person nor material which has been accepted for the award of any other Degree or Diploma of the University or other Institute of Higher learning, except where due acknowledgement has been made in the text.

DUGGINENI VINAY KUMAR (R900213021)

RAM KAISTHA (R900213034)

BADDIREDDY SAI NAGENDRA (R900213017)

CERTIFICATE

This is to certify that the thesis titled **CFD Analysis of Flow and Heat Transfer through Natural Convection in Co-axial Cylinders with effect of shape of Cylinder** submitted by **Duggineni Vinay Kumar (R900213021), Ram Kaistha (R900213034), Baddireddy Sai Nagendra (R900213017)**, to the University of Petroleum & Energy Studies, for the award of the degree of **BACHELOR OF TECHNOLOGY** in Chemical Engineering is a bonafide record of project work carried out by them under my supervision and guidance. The content of the thesis, in full have not been submitted to any other Institute or University for the award of any other degree or diploma.

Dr. Krunal Madhukar Gangawane

Assistant Professor-SG

Department of Chemical Engineering

ACKNOWLEDGEMENT

The successful completion of the report could not have been possible without the help and guidance of our mentor. We would like to take this opportunity to express my sincere and humble acknowledgements towards him.

We would like to thank our mentor **Dr. Krunal Madhukar Gangawane** who have helped us in gathering the information and training us in Ansys which led to the successful completion of this report.

We would also like to thank other staff members at the University for creating an environment conductive for understanding this kind of a study. Finally we would like to express my sincere gratitude to our Professor's, for helping us to undertake this Project and constantly encouraging me to interact with the experts and make the best use of the immense opportunities available at the University.

Duggineni Vinay Kumar

Ram Kaistha

Baddireddy Sai Nagendra

NOMENCLATURE

Nusselt Number (Nu)

Prandtl Number (Pr)

Grashoff Number (Gr)

Blockage

Computational Fluid dynamics (CFD)

Finite Volume

Natural Convection

Forced Convection

Newtonian & Non-Newtonian Fluids

Dilatant Fluids

Pseudo Plastic Fluids

Dynamic (μ) & Kinematic Viscosity (ν)

Thermal Conductivity (K)

Coefficient of Thermal Conductivity (β)

Specific Heat Capacity (C_p)

Buoyancy

Density (ρ)

Temperature Function

Stream Function

ABSTRACT

Natural convection from isolated sources has been investigated for years, and heat transfer correlations for most basic geometries can be retrieved from heat transfer handbooks. Natural convection in enclosures has also been the subject of intensive research efforts, and its fundamentals are now summarized in monographs and review works. In such a context, major problems are the prediction of the flow regimes and patterns, and the effect of confinement on heat transfer performances. This, in turn, implies the reliability of heat transfer correlations as derived for isolated sources. Buoyancy-induced flows play a central role in a number of practical applications, including environmental thermal control, nuclear design, solar heating, and the cooling of electronic devices. More generally, almost all technologies involving passive heat transfer as the main source of thermal dissipation rely upon natural convection effects. The Boussinesq approximation for buoyancy has successfully been used in analytical and numerical studies of natural convection. By applying this approximation, two dimensionless variables are present in the non-dimensionalized governing equations, i.e. the Grashof (or Rayleigh) and Prandtl numbers. Parametric studies on Grashof and Prandtl-number dependence of steady-state and unsteady features of natural convection can been presented over a wide range of both numbers. Numerical results of natural convection in enclosures can also been extensively documented for various geometries and boundary conditions. Numerical simulations were performed for three values of the ratio between the cylinder radius and the cavity side, the aspect ratio, and four values of the Rayleigh number. The finite-volume method adopted involved the use of structured boundary-fitted quadrilateral meshes, to solve the momentum and energy equations in their steady-state formulation. Flow patterns and thermal fields in all configurations were presented, alongside with profiles of the average Nusselt number in between the enclosure walls and the cylinder surface.

TABLE OF CONTENTS

LIST OF TABLES

LIST OF FIGURES

CHAPTER 1

INTRODUCTION

1.1 Computational fluid dynamics (CFD)

Computational fluid dynamics or CFD [1][2][3] is the analysis of systems involving fluid flow, heat transfer and associated phenomena such as chemical reactions by means of computer-based simulation. The technique is very powerful and spans wide range of industrial and non-industrial application areas. Computers are used to perform the calculations required to simulate the interaction of liquids and gases with surfaces defined by boundary conditions. With high-speed supercomputers, better solutions can be achieved. Ongoing research yields software that improves the accuracy and speed of complex simulation scenarios such as transonic or turbulent flows. Initial experimental validation of such software is performed using a wind tunnel with the final validation coming in full-scale testing. Some examples are:

- Aerodynamics of aircraft and vehicles:-lift and drag
- Hydrodynamics of ships
- Power plant:-combustion in internal combustion engines and gas turbines
- Turbomachinery:-flows inside rotating passages, diffusers etc.
- Electrical and electronic engineering:-cooling of equipment including microcircuits
- Chemical process engineering:-mixing and separation, polymer moulding
- External and internal environment of buildings:-wind loading and heating/ventilation
- Environmental engineering:-distribution of pollutants and effluents
- Hydrology and oceanography:-flows in rivers, estuaries, oceans
- Meteorology:-weather prediction
- Biomedical engineering:-blood flows through arteries and veins

Computational Fluid Dynamics (CFD) provides a qualitative (sometimes even quantitative) prediction of fluid flows by means of

- Mathematical modelling (partial differential equations)
- Numerical methods (discretization and solution techniques)
- Software tools (solvers, pre- and post-processing utilities)

CFD enables scientists and engineers to perform ‘numerical experiments’ (I.e. computer simulations) in a ‘virtual flow laboratory’.

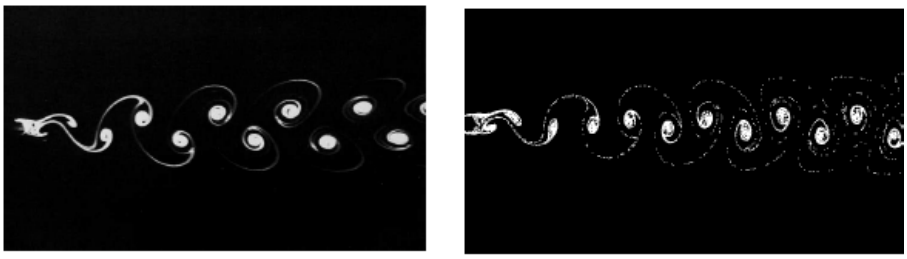

real experiment CFD simulation

© An introduction to CFD-Versteeg and Malalasekera-2nd Ed.

1.2 CFD Methodology

CFD codes are structured around the numerical algorithms that can tackle fluid flow problems. In order to provide easy access to their solving power all commercial CFD packages include sophisticated user interfaces to input problem parameters and to examine the results. Hence all codes contain three main elements: (i) a pre-processor, (ii) a solver and (iii) a post-processor. We briefly examine the function of each of these elements within the context of a CFD code.

Pre-processor:-

Pre-processing consists of the input of a flow problem to a CFD program by means of an operator-friendly interface and the subsequent transformation of this input into a form suitable for use by the solver. The user activities at the pre-processing stage involve:

• Definition of the geometry of the region of interest: the computational domain

• Grid generation – the sub-division of the domain into a number of smaller, non-overlapping sub-domains: a grid (or mesh) of cells (or control volumes or elements)

• Selection of the physical and chemical phenomena that need to be modelled.

• Definition of fluid properties

• Specification of appropriate boundary conditions at cells which coincide with or touch the domain boundary

The solution to a flow problem (velocity, pressure, temperature etc.) is defined at nodes inside each cell. The accuracy of a CFD solution is governed by the number of cells in the grid. In general, the larger the number of cells, the better the solution accuracy. Both the accuracy of a solution and its cost in terms of necessary computer hardware and calculation time are dependent on the fineness of the grid.

Solver:-

There are three distinct streams of numerical solution techniques: finite difference, finite element and spectral methods. We shall be solely concerned with the finite volume method, a

special finite difference formulation that is central to the most well-established CFD codes: CFX/ANSYS, FLUENT, PHOENICS and STAR-CD. In outline the numerical algorithm consists of the following steps:

• Integration of the governing equations of fluid flow over all the (finite) control volumes of the domain

• Discretisation – conversion of the resulting integral equations into a system of algebraic equations

• Solution of the algebraic equations by an iterative method

The first step, the control volume integration, distinguishes the finite volume method from all other CFD techniques. The resulting statements express the (exact) conservation of relevant properties for each finite size cell. This clear relationship between the numerical algorithm and the underlying physical conservation principle forms one of the main attractions of the finite volume method and makes its concepts much simpler to understand by engineers than the finite element and spectral methods. The conservation of a general flow variable φ, e.g. a velocity component or enthalpy, within a finite control volume can be expressed as a balance between the various processes tending to increase or decrease it. In words we have:

$$\begin{bmatrix}\text{Rate of change of } \phi \text{ in the control volume with respect to time}\end{bmatrix} = \begin{bmatrix}\text{Net rate of increase of } \phi \text{ due to convection into the control volume}\end{bmatrix} + \begin{bmatrix}\text{Net rate of increase of } \phi \text{ due to diffusion into the control volume}\end{bmatrix} + \begin{bmatrix}\text{Net rate of creation of } \phi \text{ inside the control volume}\end{bmatrix}$$

Post-processor:-

As in pre-processing, a huge amount of development work has recently taken place in the post-processing field. Due to the increased popularity of engineering workstations, many of which have outstanding graphics capabilities, the leading CFD packages are now equipped with versatile data visualisation tools. These include:

• Domain geometry and grid display

• Vector plots

• Line and shaded contour plots

• 2D and 3D surface plots

• Particle tracking

• View manipulation (translation, rotation, scaling etc.)

• Colour PostScript output

More recently these facilities may also include animation for dynamic result display, and in addition to graphics all codes produce trusty alphanumeric output and have data export facilities for further manipulation external to the code. As in many other branches of CAE, the graphics output capabilities of CFD codes have revolutionised the communication of ideas to the non-specialist.

The fundamental basis of almost all CFD problems are the Navier–Stokes equations, which define many single-phase (gas or liquid, but not both) fluid flows. These equations can be simplified by removing terms describing viscous actions to yield the Euler equations.

CHAPTER 2

MOTIVATION

Natural convective heat transfer from a body to a finite space enclosing it has received increased attention in recent years. Applications have included nuclear reactor design, cooling of electronic equipment, aircraft cabin insulation and thermal storage systems [4]. At the same time, as the rapid development of computer ability since early 1980s, numerical simulation has become an effective alternative for solving engineering problems involving fluid flow and heat transfer. Instead of conducting laboratory experiments, a great many numerical efforts have been made in studying transient natural convection between two horizontal parallel plates, in rectangular/square, triangular, cylindrical and odd-shaped enclosures and enclosures of arbitrary cross-sectional geometry. Among the promising numerical schemes, finite-difference/volume-based method has been most widely used and some other numerical approaches have been proven to be applicable, such as finite element analysis and accelerated full-multigrid method. Effects of natural convection in horizontal enclosures with inner bodies has attracted increased attention. Typical geometries include horizontal annuli between two concentric cylinders or squares and spherical shells between two concentric or eccentric spheres. The numerical investigation of natural convection in a horizontal air-filled cylindrical enclosure with a concentric triangular cylinder under steady state condition has been also done. The effects of Prandtl number of steady state natural convection in the same geometry was later studied. In order to extend the existing knowledge, natural convection in such geometries is numerically studied in the present project [5].

CHAPTER 3

OBJECTIVES

Through our project we will analyse:

1. Flow and Heat Transfer characteristics in Co-Axial cylinders with effect of shape of inner cylinder
2. Determination of Average Nusselt Number (Nu)
3. Comparison of different characteristics using Newtonian and Non-Newtonian Fluids

CHAPTER 4

LITERATURE REVIEW

4.1 The finite volume method

The finite volume method (FVM) [6] is a method for representing and evaluating partial differential equations in the form of algebraic equations. Similar to the finite difference method or finite element method, values are calculated at discrete places on a meshed geometry. "Finite volume" refers to the small volume surrounding each node point on a mesh. In the finite volume method, volume integrals in a partial differential equation that contain a divergence term are converted to surface integrals, using the divergence theorem. These terms are then evaluated as fluxes at the surfaces of each finite volume. Because the flux entering a given volume is identical to that leaving the adjacent volume, these methods are conservative. Another advantage of the finite volume method is that it is easily formulated to allow for unstructured meshes. The method is used in many computational fluid dynamics packages.

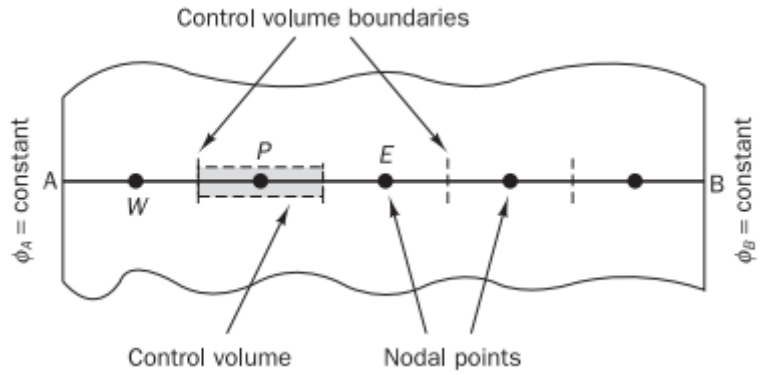

Figure 4.1.1

© An introduction to CFD-Versteeg and Malalasekera-2nd Ed.

Step 1: Grid generation

The first step in the finite volume method is to divide the domain into discrete control volumes. Let us place a number of nodal points in the space between A and B. The boundaries (or faces) of control volumes are positioned mid-way between adjacent nodes. Thus each node is surrounded by a control volume or cell. It is common practice to set up control volumes near the edge of the domain in such a way that the physical boundaries coincide with the control volume boundaries. At this point it is appropriate to establish a system of notation that can be used in future developments. The usual convention of CFD methods is shown in Figure 2.

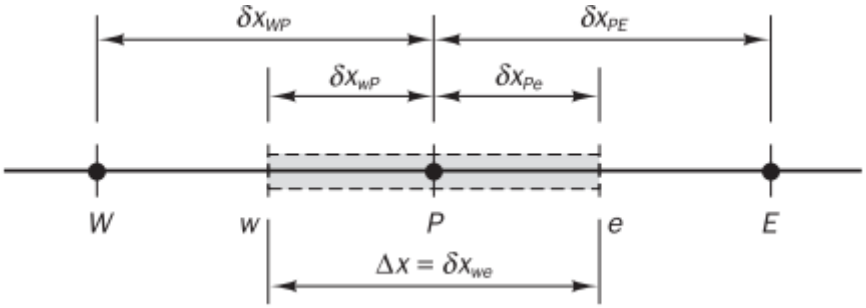

Figure 4.1.2

© An introduction to CFD-Versteeg and Malalasekera-2nd Ed.

A general nodal point is identified by P and its neighbours in a one dimensional geometry, the nodes to the west and east, are identified by W and E respectively. The west side face of the control volume is referred to by *w* and the east side control volume face by *e*. The distances between the nodes W and P, and between nodes P and E, are identified by δx_{wP} and δx_{Pe} respectively. Similarly distances between face *w* and point P and between P and

face e are by δx_{wP} and δx_{Pe} respectively. Figure 2 shows that the control volume width is Δx $=\delta x_{we}$.

Step 2: Discretisation

The key step of the finite volume method is the integration of the governing equation (or equations) over a control volume to yield a discretised equation at its nodal point P. It is a very attractive feature of the finite volume method that the discretised equation has a clear physical interpretation.

Step 3: Solution of equations

Discretised equations must be set up at each of the nodal points in order to solve a problem. For control volumes that are adjacent to the domain boundaries the general discretised equation is modified to incorporate boundary conditions. The resulting system of linear algebraic equations is then solved to obtain the distribution of the property at nodal points. Any suitable matrix solution technique may be enlisted for this task. The techniques of dealing with different types of boundary conditions will be explained in detail later of the project.

4.2 Natural and forced convection

Convection heat transfer requirements:-

The heat transfer by convection requires a solid-liquid interface, a temperature difference the solid surface and the surrounding fluid and a motion of the fluid. The process of heat transfer by convection would occur when there is a movement of macro-particles of the fluid in space from a region of higher temperature to lower temperature [7].

Convection heat transfer mechanism:-

Let us imagine a heated solid surface, say a plane wall at a temperature T_s placed in an atmosphere at temperature T_∞. Since all real fluids are assumed to be viscous, the fluid particles adjacent to the solid surface will stick to the surface. The fluid particle at A, which is at a lower temperature, will receive heat energy from the plate by conduction. The internal energy of the particle would increase and when the particle moves away from the solid surface (wall or plate) and collides with another particle at B which is at ambient temperature, it will transfer a part of its energy to the B and the temperature at B would increase. This way heat energy is transferred from the heated plate to the surrounding fluid. Therefore the

process of heat transfer by convection involves a combined action of heat conduction, energy storage and the transfer of energy by mixing motion of fluid particles.

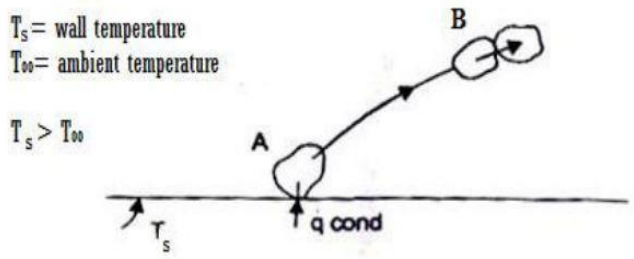

Figure 4.2.1: principle of heat transfer by convection

Main purpose of convective heat transfer analysis is to determine:

- Flow field
- Temperature field in fluid
- Heat transfer coefficient, h

There are two types of convection heat transfer:

- Natural or Free convection
- Forced convection

Natural Convection:-

Natural convection [8] is a mechanism, or type of heat transport, in which the fluid motion is not generated by any external source (like a pump, fan, suction device, etc.) but only by density differences in the fluid occurring due to temperature gradients. In natural convection, fluid surrounding a heat source receives heat, becomes less dense and rises. The surrounding, cooler fluid then moves to replace it. This cooler fluid is then heated and the process continues, forming a convection current; this process transfers heat energy from the bottom of the convection cell to top. The driving force for natural convection is buoyancy, a result of differences in fluid density. Because of this, the presence of a proper acceleration such as arises from resistance to gravity, or an equivalent force (arising from acceleration, centrifugal force or Coriolis Effect), is essential for natural convection.

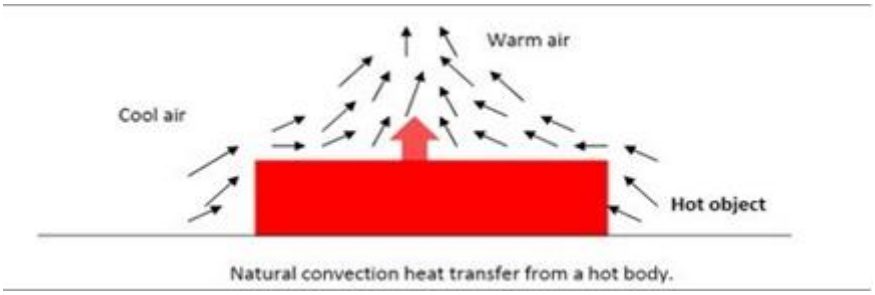

Figure 4.2.2: Natural convection

Grashof number is frequently arises in the study of situations of natural or free convection.

Grashof number:

The Grashof number (Gr) is a dimensionless number in fluid dynamics and heat transfer which approximates the ratio of the buoyancy to viscous force acting on a fluid. It frequently arises in the study of situations involving natural convection. It is named after the German Engineer Franz Grashof.

The Grashof number is:

$Gr = g\beta (T_s - T_\infty) L^3 / \upsilon^2$

Where

g=acceleration due to gravity. SI units: m/s^2 ,

B= coefficient of thermal expansion, (equal to approximately 1/T, for ideal gases)

T_s = surface temperature. SI units: K

T_∞ = bulk temperature SI units: K

L=vertical length SI units: m

ν = kinematic viscosity (SI units: m^2 /s)

Prandtl number:

The Prandtl number (Pr) or Prandtl group is dimensionless group, named after the German physicist Ludwig Prandtl, defined as the ratio of momentum diffusivity to thermal diffusivity. That is, the Prandtl number is given as:

$Pr = \nu / \alpha$ = momentum diffusivity / thermal diffusivity

Where

ν = Kinematic viscosity, $\nu = \mu / \rho$, (SI units: m^2 /s)

α =Thermal diffusivity, α = k/ (ρ Cp), (SI units: m^2 /s)

Where

μ= Dynamic viscosity, (SI units: Pa s = N s/m^2)

k = Thermal conductivity, (SI units: W/m-K)

ρ = Density, (SI units: kg/m^3)

Cp = Specific heat, (SI units: J/kg-K)

4.3 Non-Newtonian fluid:

A **Non-Newtonian fluid**[9] is a fluid that does not follow Newton's law of viscosity. Most commonly, the viscosity (the measure of a fluid's ability to resist gradual deformation by shear or tensile stresses) of non-Newtonian fluids is dependent on shear stress or shear rate history. Some non-Newtonian fluids with shear-independent viscosity, however, still exhibit normal stress-differences or other non-Newtonian behavior. Many salt solutions and molten polymers are non-Newtonian fluids, as are many commonly found substances such as ketchup, custard and toothpaste.

In a Newtonian fluid, the relation between the shear stress and the shear stress is linear, passing through the origin, the constant of proportionality being the coefficient of viscosity. In a non-Newtonian fluid, the relation between the shear stress and the shear stress is different and can even be time-dependent (time dependent viscosity). Therefore, a constant coefficient of viscosity cannot be defined.

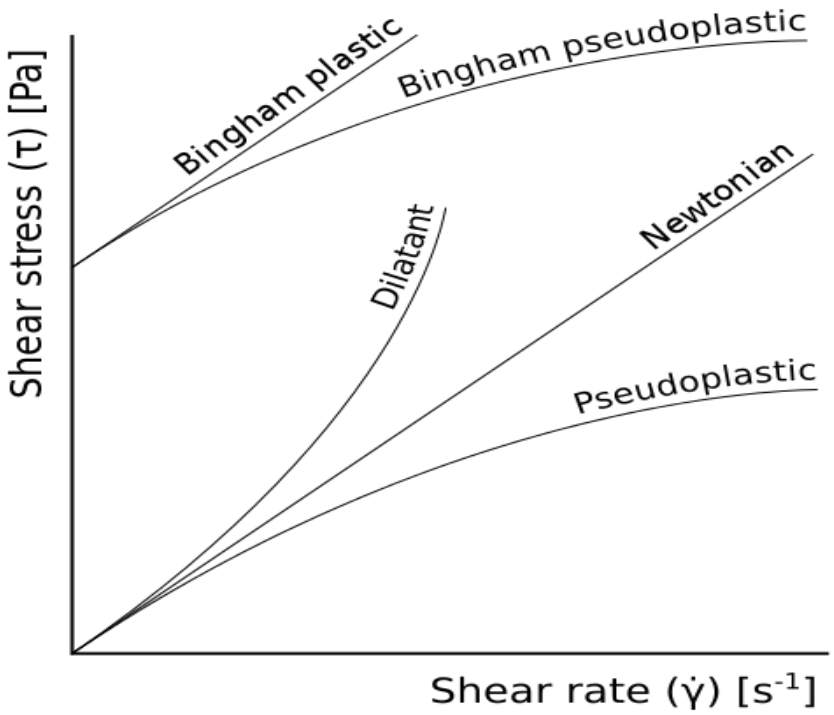

Figure 4.3.1: Classification of Fluids with shear stress as a function of shear strain.

Shear thickening fluid:

The viscosity of a shear thickening fluid, or dilatant fluid, appears to increase when the shear rate increases. Corn starch dissolved in water is a common example: when stirred slowly it looks milky, when stirred vigorously it feels like a very viscous liquid.

$$T=\mu\,(du/dy)^{n;}\ n>1$$

Shear thinning fluid:

A familiar example of the opposite, a shear thinning fluid, or pseudo plastic fluid, is wall paint: The paint should flow readily off the brush when it is being applied to a surface but not drip excessively. Note that all thixotropic fluids are extremely shear thinning, but they are significantly time dependent, whereas the colloidal "shear thinning" fluids respond instantaneously to changes in shear rate. Thus, to avoid confusion, the latter classification is more clearly termed pseudo plastic.

Another example of a shear thinning fluid is blood. This application is highly favored within the body, as it allows the viscosity of blood to decrease with increased shear strain rate.

$$T=\mu\,(du/dy)^{n};\ n<1$$

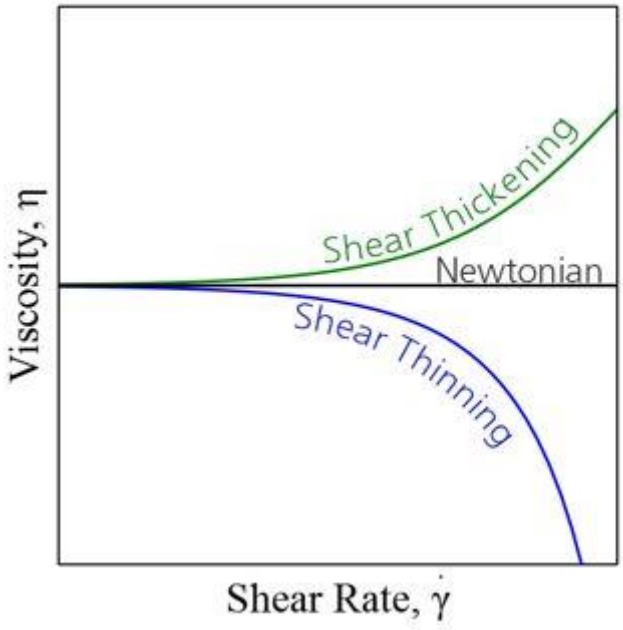

Figure 4.3.2: Viscosity vs Shear rate Behaviour

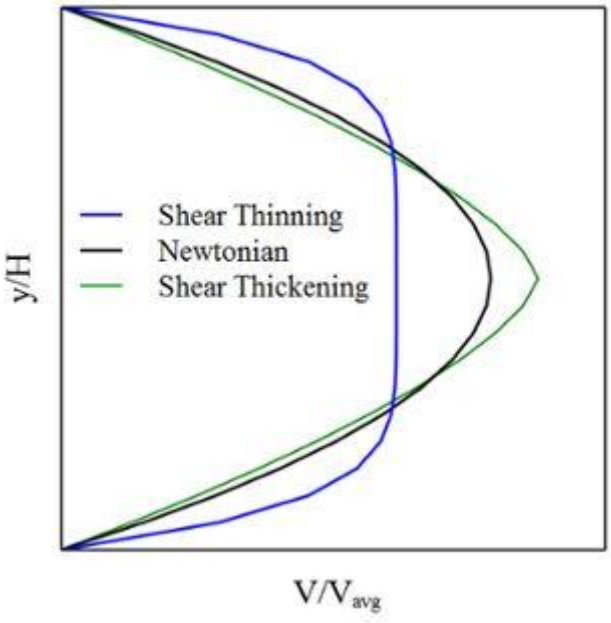

Figure 4.3.3: Distance from Centre vs Velocity graph

CHAPTER 5

METHODOLOGY

5.1 Problem formulation

The physical domain being considered is a horizontal annulus confined by an inner cylinder and its circular cylindrical enclosure. Without loss of generality, the cross section of the inner cylinder is assumed to be coaxially placed and are extremely long in the axial direction. Therefore, a two-dimensional cross-sectional domain is considered. Gravity is assumed to act along the negative y-direction. The aspect ratio and characteristic length of the model are defined as the ratio and gap between the outer and inner radii, i.e. AR = Rout/Rin and L = Rout - Rin, respectively. Initially, air confined in the annulus is quiescent and is isothermally kept at a temperature Tout, which is also the temperature imposed on the outer circular wall. The temperature on the inner triangular wall is suddenly improved to Tin and uniformly maintained at this value. Such temperature gradient, Tin - Tout, between the two cylinders serves as the driving force for natural convection. The entire physical domain is initially at a uniform temperature Tout = 300 K. At t = 0 s, a temperature Tin = 301 K that is higher than Tout is applied suddenly on the inner wall, and this temperature is maintained for t > 0 s. Hydro-dynamically, no-slip boundary conditions are adopted on both walls. It is evident that the Prandtl and Grashoff numbers are the two parameters that govern the problem. The governing equations and definitions of dimensionless numbers for the present model and properties of fluid are assumed to be varied and evaluated at 301 K. As a result, the Prandtl number ($Pr = \bar{\upsilon}/\alpha$) is varied in this study (Pr = 1/10/100) and the Grashoff number ($Gr = g\beta$ (Tin - Tout) $L^3/\bar{\upsilon}^2$) is only able to be varied by changing the β ($10^3 - 10^6$) values. This ensures that the natural convective flow is inherently in laminar regime. In order to simplify the problem, some assumptions are made such as air is an incompressible, Newtonian fluid with constant properties, heat conduction obeys the Fourier's law and viscous dissipation and radiative heat transfer are neglected.

5.2 Computational details

The commercial finite-volume-based CFD code Fluent (version 17) is employed to perform the numerical study. The computational domain is created and meshed using the geometry drawer and mesher. Thin boundary layers that consist of structured quadrilateral cells are generated in between inner and outer walls. In discretizing the governing equations, the second-order implicit scheme is used for the temporary terms and the QUICK scheme is adopted for both momentum and energy equations. The commercial code ANSYS Fluent has been widely used by many researchers for solving and investigating steady-state natural convection heat transfer in the same geometry under consideration. Therefore, a validation test of the code is not required for the present study.

According to the above assumptions, the following formulas are obtained [10]:

K(W/m-K)	g(m/s$^{2)}$	μ(Pa s)	Cp (J/kg-K)	ΔT(K)	ρ (kg/m$^{3)}$	L (m)
1	-10	1	=Pr	1	1	100

Continuity equation:

$$\frac{\partial \rho}{\partial t} + \nabla.(\rho V) = 0$$

Momentum equation:

$$\frac{\partial(\rho V)}{\partial t} + \nabla.(\rho VV) = \nabla.\tau + \rho g$$

Energy equation:

$$\frac{\partial(\rho cT)}{\partial t} + \nabla.(\rho VcT) = \nabla.(k \nabla T)$$

Where Û is the fluid velocity vector.

Where ∇ · [τ] is divergence of the shear force tensor.

Where K is thermal conductivity (W/m-K)

ΔT= Temp. Difference (K)

ρ= Density

t= Time

c= Specific heat capacity (J/kg-K)

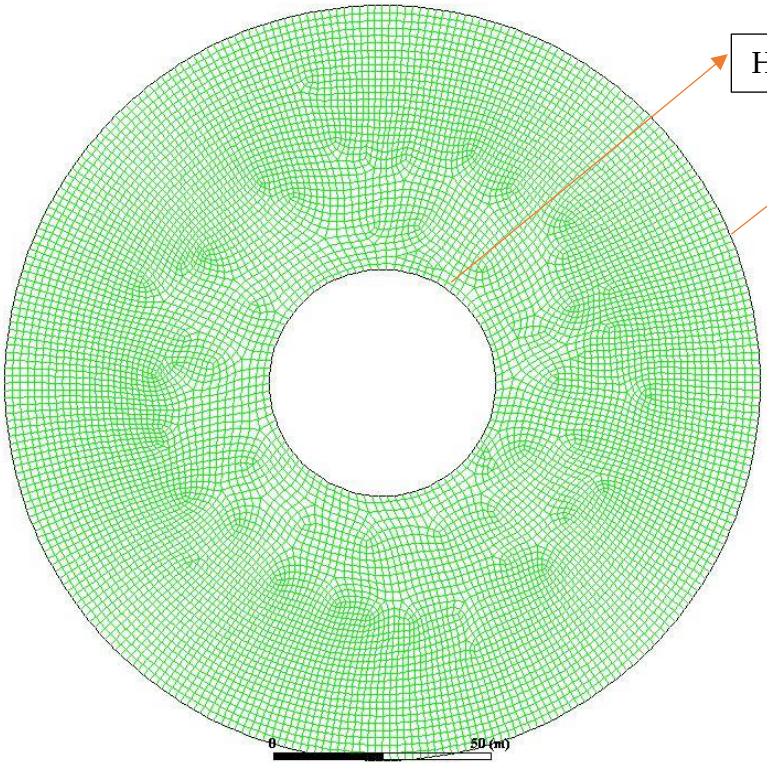

Fig 5.2.1: Co-axial meshed cylinder-Blockage 30%

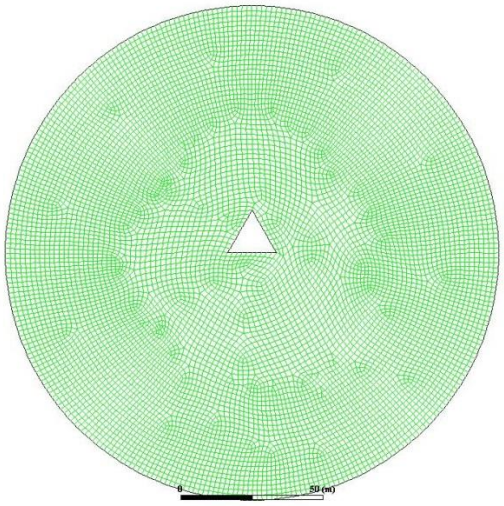

Fig 5.2.2: Co-axial meshed prism inside cylinder-blockage-10%

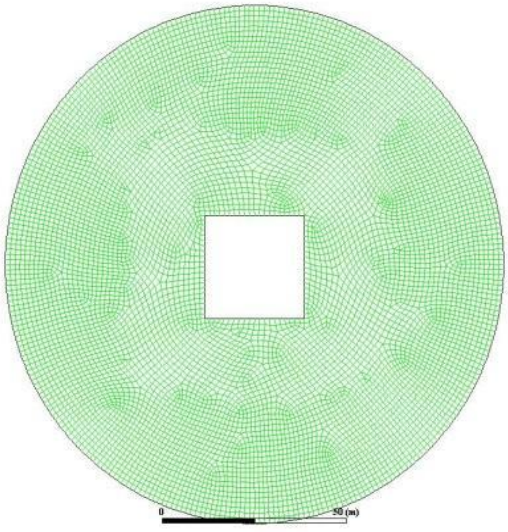

Fig 5.2.3: Co-axial meshed cube inside cylinder-blockage-20%

CHAPTER 6

RESULTS & DISCUSSION

1. Analysis of 2-Dimensional co-axial cylinders with effect of circle, cube and triangular cylinders were carried out for different Prandtl and Grashoff numbers.

2. Average Nusselt Number of above mentioned is computed through Ansys Fluent.

3. Isotherms and stream function plots are extracted.

4. Analysis of plots is done to verify the best fit.

5. The above effects are studied for both Newtonian and Non-Newtonian fluids.

T.No.6.1.1 Average Nusselt Number data for co-axial cylinders

Pr=1	**Average Nusselt number (Nu)**			
Blockage(%)/Gr	1000	10000	100000	1000000
10	0.2124113	0.23815376	0.42280174	0.65468618
20	0.30388759	0.32266369	0.57582456	0.95398295
30	0.4062233	0.41533453	0.67153608	1.1881372
Pr=100	**Average Nusselt number (Nu)**			
Blockage(%)/Gr	1000	10000	100000	1000000
10	0.4243616	0.67969811	1.130722	2.017505
20	0.5792855	0.97167391	1.6572361	3.0422349
30	0.6795458	1.1950602	2.0488469	3.8505703

Pr=Prandtl Number

Gr= Grashoff Number

Nu = Nusselt Number

T.No.6.1.2 Avg. Nusselt number data of Co-axial 2-D Cube inside Cylinder

Pr=1	**Average Nusselt number (Nu)**			
Blockage(%)/Gr	1000	10000	100000	1000000
10	0.2282885	0.2527611	0.4502328	0.7072245
20	0.338258	0.3530599	0.6066634	1.031342
30	0.4705101	0.4765372	0.683759	1.246825
Pr=100	**Average Nusselt number (Nu)**			
Blockage(%)/Gr	1000	10000	100000	1000000
10	0.4507718	0.7294387	1.320397	2.785322
20	0.614121	1.054949	1.6572361	2.8669527
30	0.6994956	1.280128	2.264826	3.2648883

T.No.6.1.3 Avg. Nusselt Number data Co-axial 2-Dimensional prism inside cylinder

Pr=1	**Average Nusselt number (Nu)**			
Blockage(%)/Gr	1000	10000	100000	1000000
10	0.1969681	0.2201362	0.3860093	0.597648
20	0.2758589	0.2939644	0.5226475	0.858542
30	0.3633752	0.3734866	0.6012625	1.064587
Pr=100	**Average Nusselt number (Nu)**			
Blockage(%)/Gr	1000	10000	100000	1000000
10	0.3910827	0.6308852	1.130849	2.522768
20	0.5258479	0.8767417	1.494592	2.86074
30	0.6060075	1.069164	1.859856	3.681076

Non-Newtonian Fluids Nusselt number data

T.No.6.1.4 Average Nusselt Number data for co-axial cylinders (n=0.2)

Pr=1/0.2	Average Nusselt number (Nu)			
Blockage(%)/Gr	1000	10000	100000	1000000
10	0.212103	0.21210298	0.21210298	0.24277841
20	0.3036828	0.30368278	0.30368278	0.35371862
30	0.4061274	0.40612738	0.40612738	0.42632976
Pr=100/0.2	Average Nusselt number (Nu)			
Blockage(%)/Gr	1000	10000	100000	1000000
10	0.212103	0.21210298	0.21210307	0.55812179
20	0.3036828	0.30368278	0.30368291	0.80976592
30	0.4061274	0.40612738	0.40612744	0.98687644

T.No.6.1.5 Avg. Nusselt number data of Co-axial 2-D Cube inside Cylinder (n=0.2)

Pr=1/0.2	Average Nusselt number (Nu)			
Blockage(%)/Gr	1000	10000	100000	1000000
10	0.2280007	0.2280007	0.2280008	0.6460997
20	0.3380493	0.3380542	0.3381103	0.8926909
30	0.4704303	0.4714303	0.4404304	1.100261

Pr=100/0.2	Average Nusselt number (Nu)			
Blockage(%)/Gr	1000	10000	100000	1000000
10	0.2280007	0.2280007	0.2280008	0.6460997
20	0.3380493	0.3380542	0.3381103	0.8926909
30	0.4704303	0.4714303	0.4404304	1.100261

T.No.6.1.6 Avg. Nusselt Number data Co-axial 2-Dimensional prism inside cylinder (n=0.2)

Pr=1/0.2	**Average Nusselt number (Nu)**			
Blockage(%)/Gr	1000	10000	100000	1000000
10	0.1966793	0.2146329	0.5358213	0.386986
20	0.2756453	0.3248476	0.7137332	1.172541
30	0.3632564	0.3881214	0.8254348	1.92189

Pr=100/0.2	**Average Nusselt number (Nu)**			
Blockage(%)/Gr	1000	10000	100000	1000000
10	0.1966793	0.1966793	0.1966793	0.5279329
20	0.2756453	0.2756453	0.2756454	0.7458847
30	0.3632564	0.3632564	0.3632564	0.8736717

T.No.6.1.7 Average Nusselt Number data for co-axial cylinders (n=0.6)

Pr=1/0.6	**Average Nusselt number (Nu)**			
Blockage(%)/Gr	1000	10000	100000	1000000
10	0.212103	0.21210299	0.21212044	0.2443089
20	0.3036828	0.3036828	0.30369519	0.32815306
30	0.4061274	0.40612739	0.40613307	0.41724893

Pr=100/0.6				
Blockage(%)/Gr	1000	10000	100000	1000000
10	0.212103	0.2121835	0.29756028	0.64953316
20	0.3036828	0.30373901	0.38883585	0.92900026
30	0.4061274	0.40615282	0.45320129	1.1404307

T.No.6.1.8 Avg. Nusselt number data of Co-axial 2-D Cube inside Cylinder (n=0.6)

Pr=1/n=0.6	**Average Nusselt number (Nu)**			
Blockage(%)/Gr	1000	10000	100000	1000000
10	0.2280007	0.2280007	0.2280171	0.2583915
20	0.3380492	0.3380589	0.3380492	0.3566306
30	0.4704303	0.4704304	0.4704344	0.4780691
Pr=100/n=0.6	**Average Nusselt number (Nu)**			
Blockage(%)/Gr	1000	10000	100000	1000000
10	0.2280007	0.2280762	0.3133347	0.7041698
20	0.3380492	0.3380932	0.4066476	0.9978824
30	0.4704304	0.4704485	0.500694	1.227161

T.No.6.1.9 Avg. Nusselt Number data Co-axial 2-Dimensional prism inside cylinder (n=0.6)

Pr=1/0.6	**Average Nusselt number (Nu)**			
Blockage(%)/Gr	1000	10000	100000	1000000
10	0.1966793	0.1966793	0.1966947	0.2243618
20	0.2756453	0.2756453	0.2756577	0.2981671
30	0.3632564	0.3632564	0.3632631	0.374819

Pr=100/0.6	**Average Nusselt number (Nu)**			
Blockage(%)/Gr	1000	10000	100000	1000000
10	0.1966793	0.1967501	0.2722752	0.6103384
20	0.2756454	0.2757012	0.3517717	0.8420663
30	0.3632564	0.3632862	0.407283	1.017791

T.No.6.1.10 Average Nusselt Number data for co-axial cylinders (n=1.4)

Pr=1/1.4	**Average Nusselt number (Nu)**			
Blockage(%)/Gr	1000	10000	100000	1000000
10	0.2121045	0.21214251	0.21314989	0.23620269
20	0.3036839	0.30370902	0.3043682	0.3210292
30	0.406128	0.40614015	0.4064564	0.41474561
Pr=100/1.4	**Average Nusselt number (Nu)**			
Blockage(%)/Gr	1000	10000	100000	1000000
10	0.2255693	0.33106223	0.48722478	0.69878051
20	0.3129229	0.43315813	0.68066742	0.99704346
30	0.4106313	0.49929773	0.82230632	1.2249647

T.No.6.1.11 Avg. Nusselt Number data Co-axial 2-Dimensional prism inside cylinder (n=1.4)

Pr=1/1.4	**Average Nusselt number (Nu)**			
Blockage(%)/Gr	1000	10000	100000	1000000
10	0.1966807	0.1967173	0.1976797	0.2189386
20	0.2756465	0.2756735	0.2763717	0.2928349

30	0.3632571	0.3632729	0.3636718	0.3730996
Pr=100/1.4	**Average Nusselt number (Nu)**			
Blockage	1000	10000	100000	1000000
10	0.2092304	0.3052065	0.3052085	0.4477742
20	0.2849988	0.3951362	0.6155197	0.8976035
30	0.3685671	0.4514176	0.7348063	1.098168

T.No.6.1.12 Avg. Nusselt number data of Co-axial 2-D Cube inside Cylinder (n=1.4)

Pr=1/n=1.4	**Average Nusselt number (Nu)**			
Blockage(%)/Gr	1000	10000	100000	1000000
10	0.2280021	0.2280375	0.2289755	0.2509223
20	0.33805	0.3380693	0.3385755	0.3515642
30	0.4704307	0.4704387	0.470643	0.4759367
Pr=100/n=1.4	**Average Nusselt number (Nu)**			
Blockage(%)/Gr	1000	10000	100000	1000000
10	0.2406733	0.3500084	0.5186214	0.7466347
20	0.345201	0.454339	0.724329	1.06568
30	1.307174	0.8611595	0.5317045	0.4733215

6.2 Tec plots of isotherms and stream functions

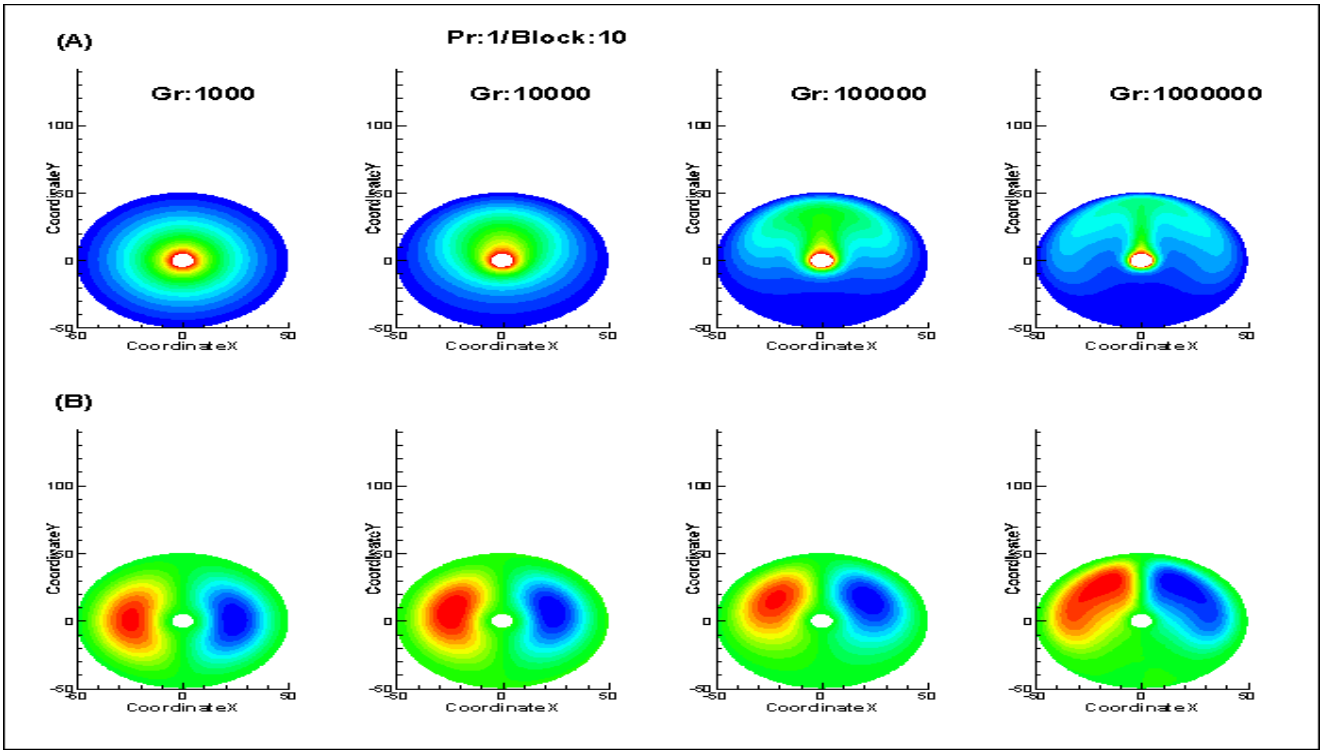

Fig.6.2.1 (A) Temperature profile, (B) Stream Function (Blockage=10%, Pr=1)

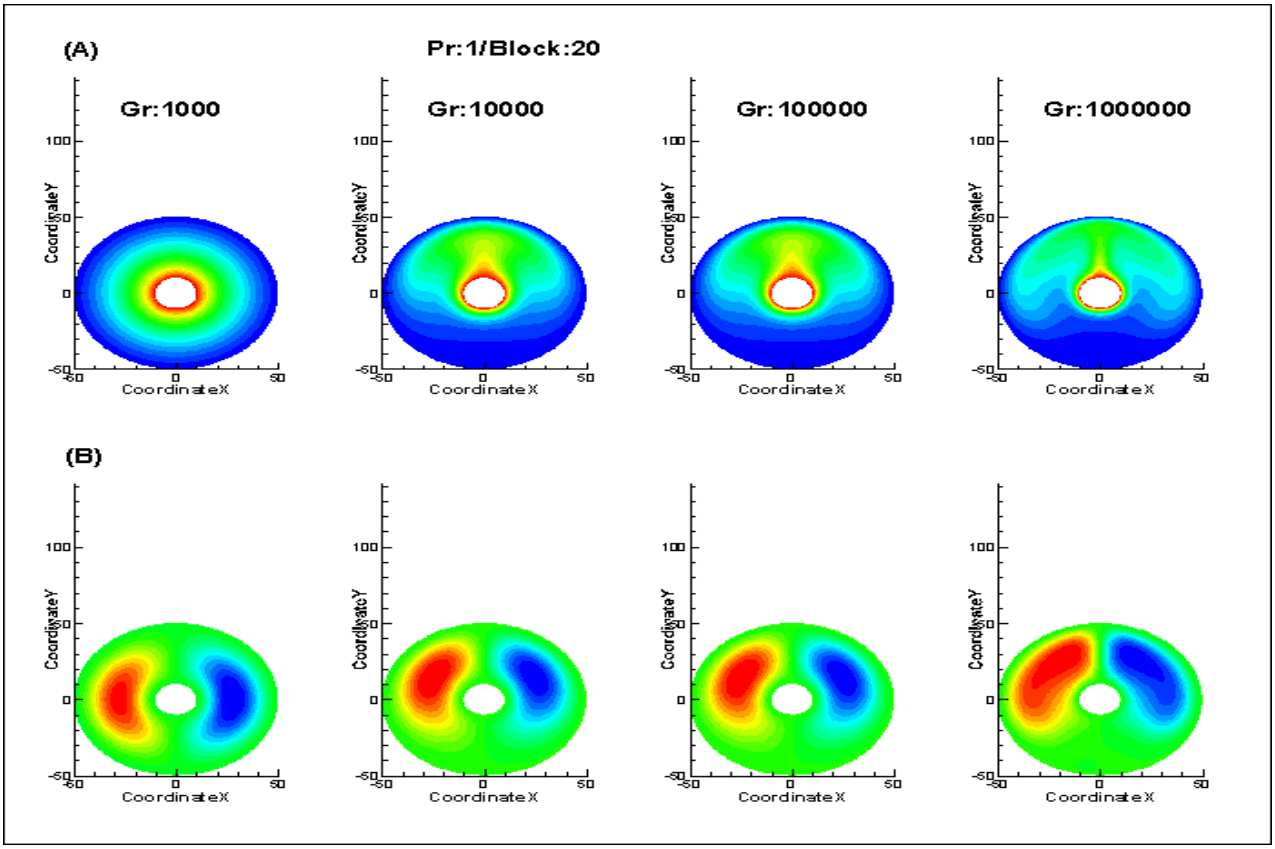

Fig.6.2.2 (A) Temperature profile, (B) Stream Function (Blockage=20%, Pr=1)

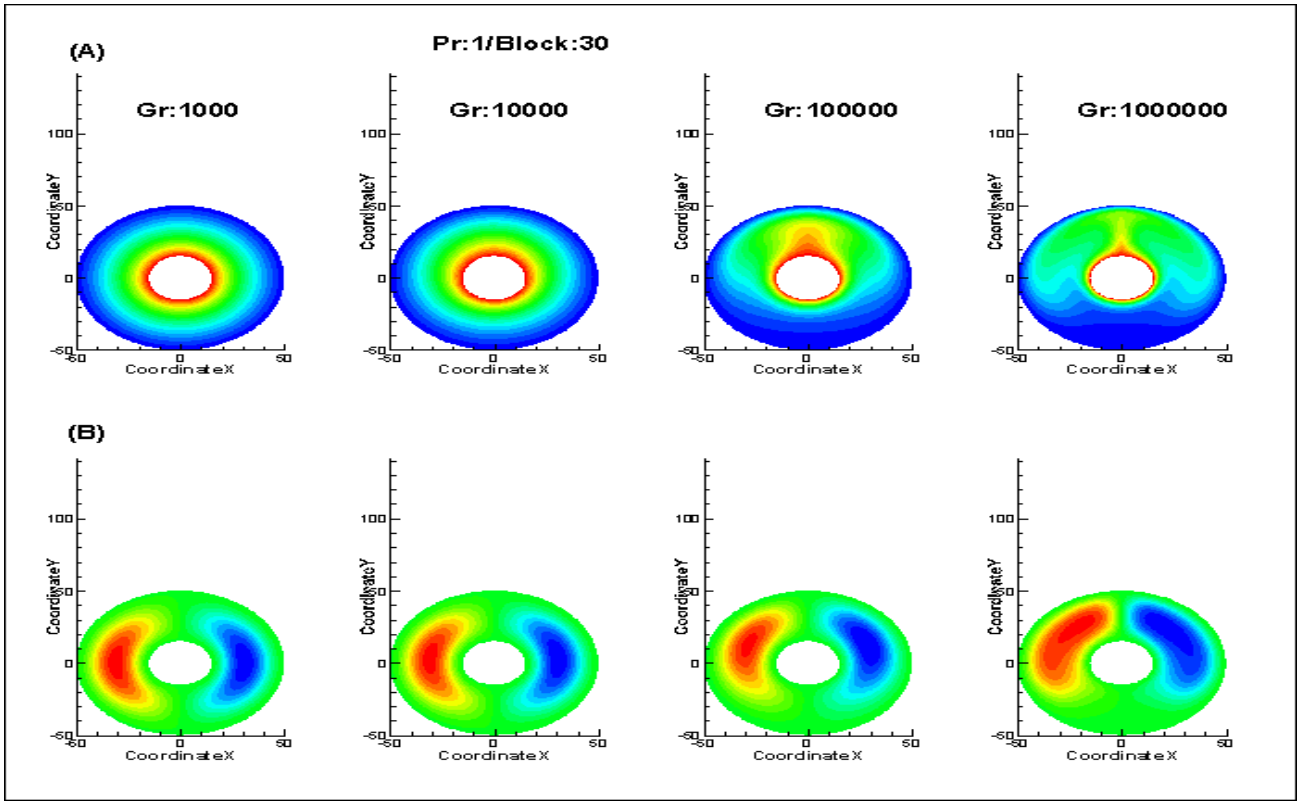

Fig. 6.2.3 (A) Temperature profile, (B) Stream Function (Blockage=30%, Pr=1)

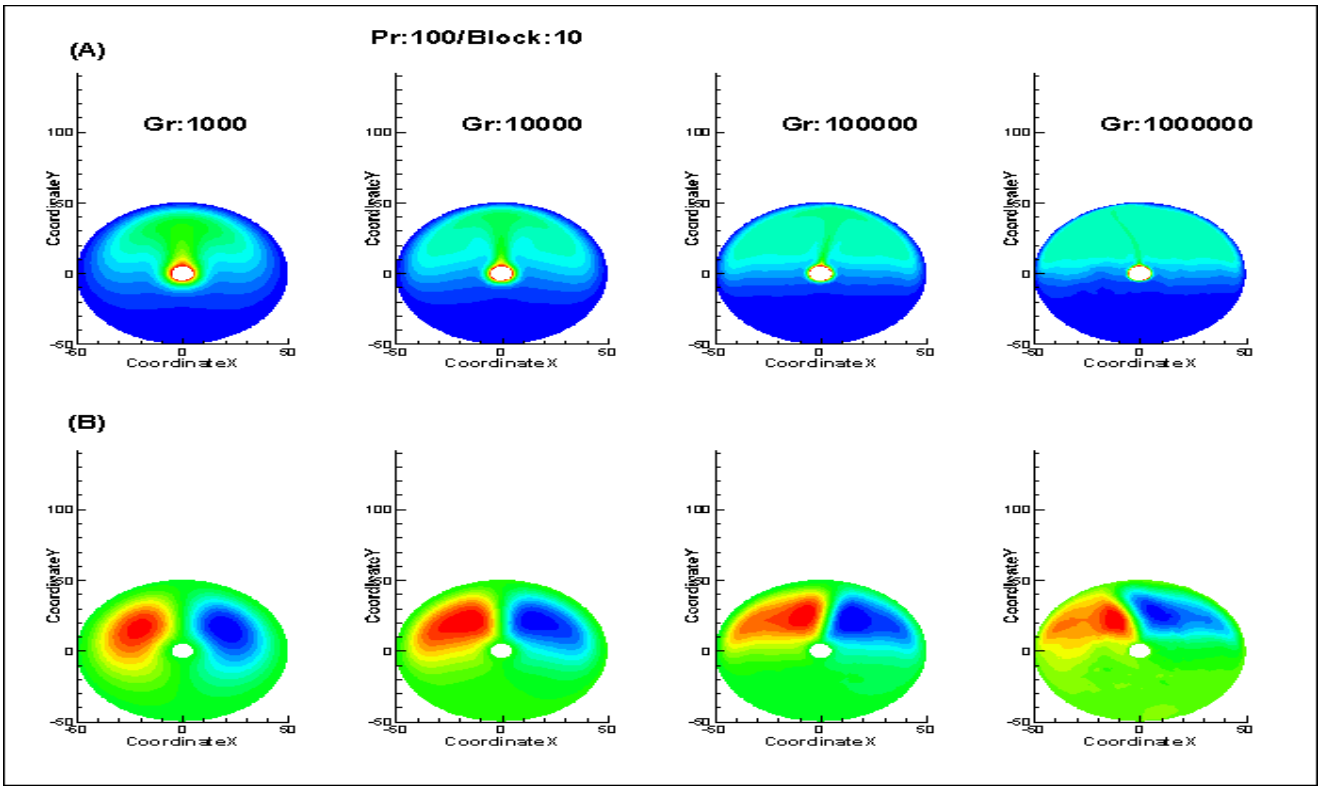

Fig.6.2.4 (A) Temperature profile, (B) Stream Function (Blockage=10%, Pr=100)

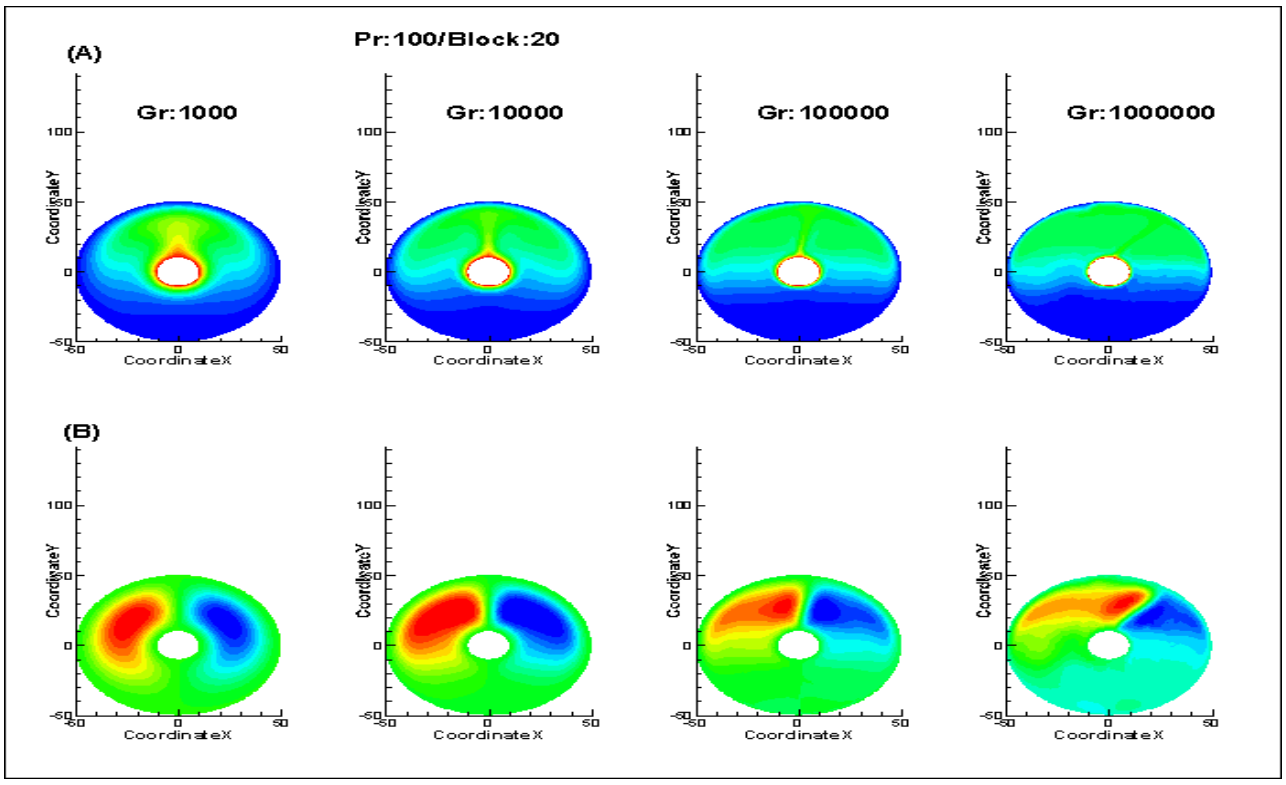

Fig.6.2.5 (A) Temperature profile, (B) Stream Function (Blockage=20%, Pr=100)

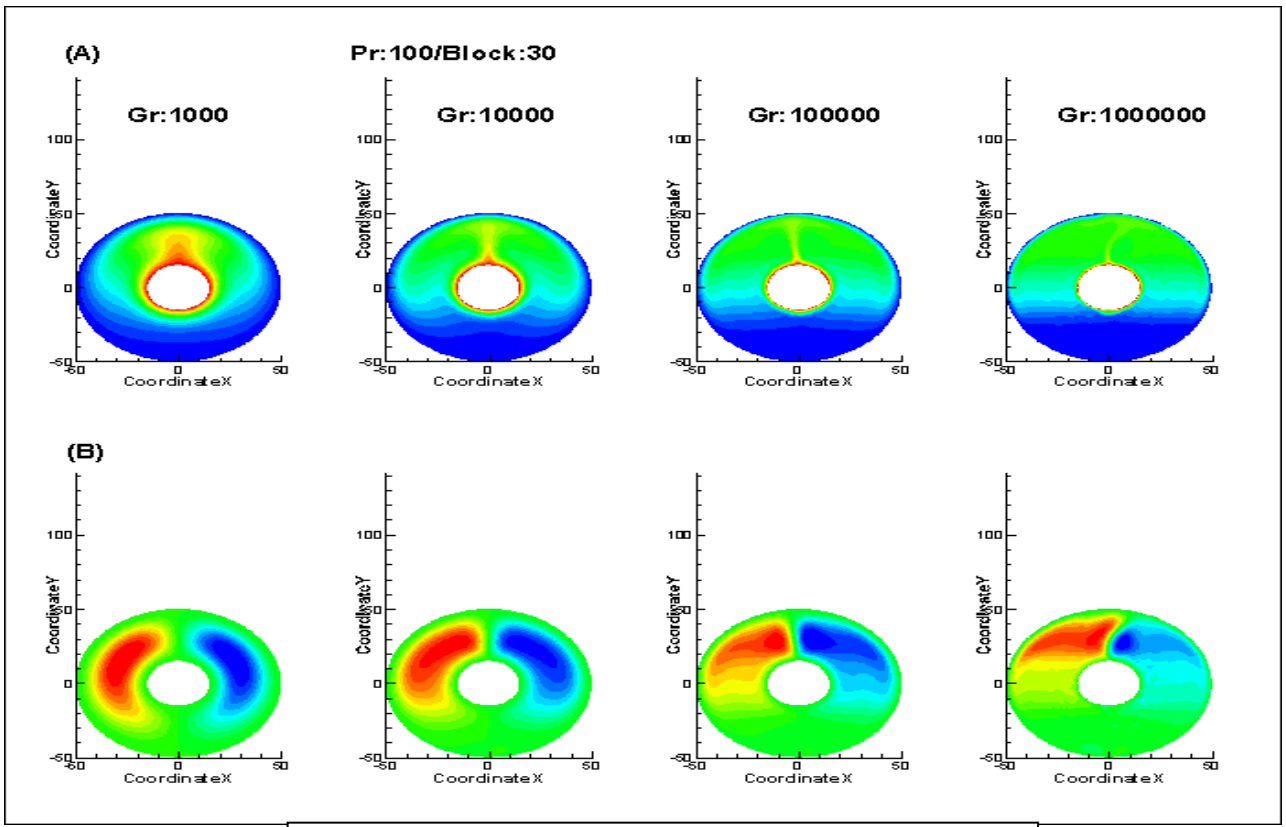

Fig.6.2.6 (A) Temperature profile, (B) Stream Function (Blockage=30%, Pr=1)

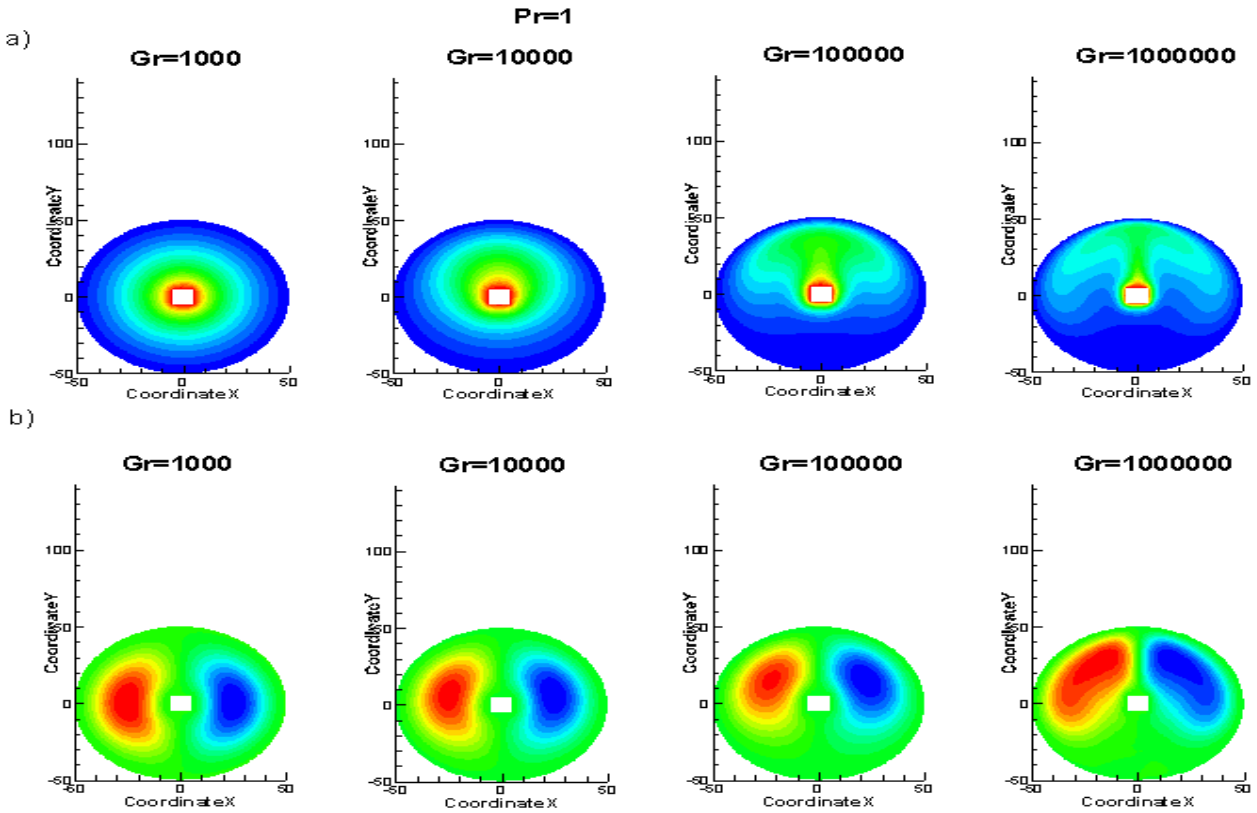

Fig. 6.2.7 (A) Temperature profile, (B) Stream Function (Blockage=10%, Pr=1)

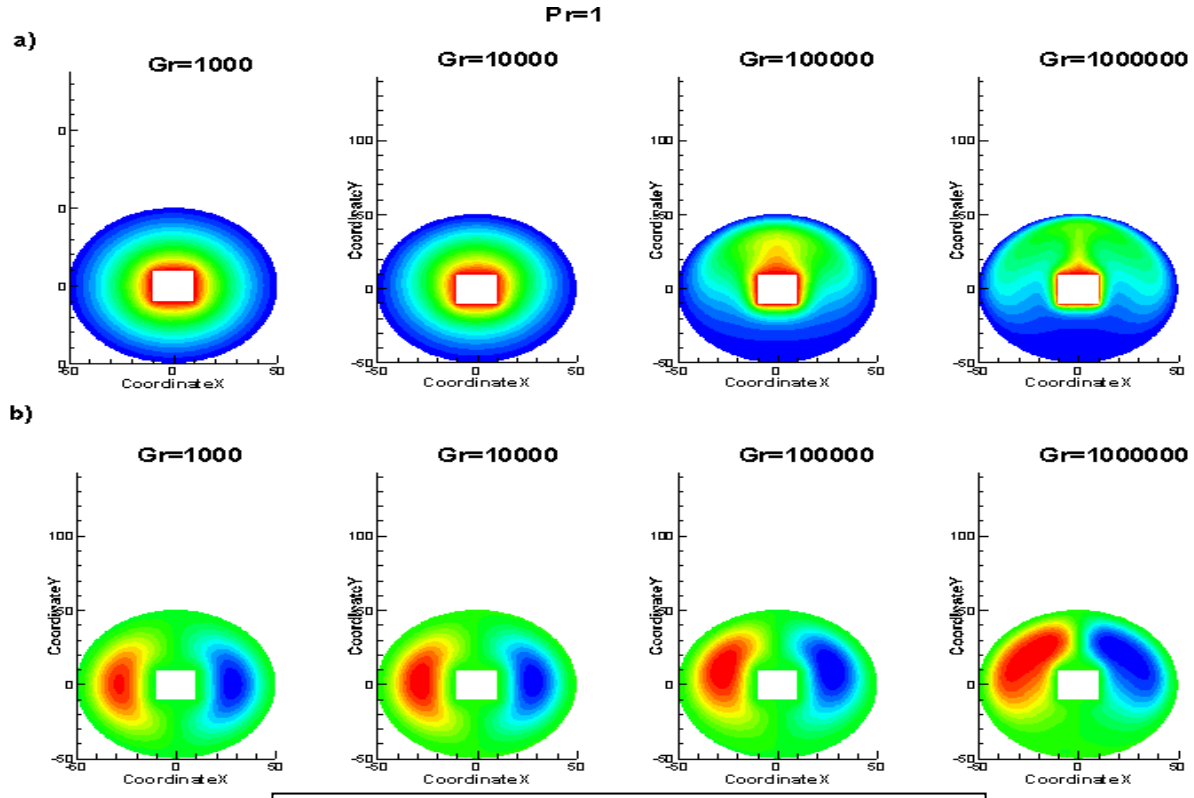

Fig. 6.2.8 (A) Temperature profile, (B) Stream Function (Blockage=20%, Pr=1)

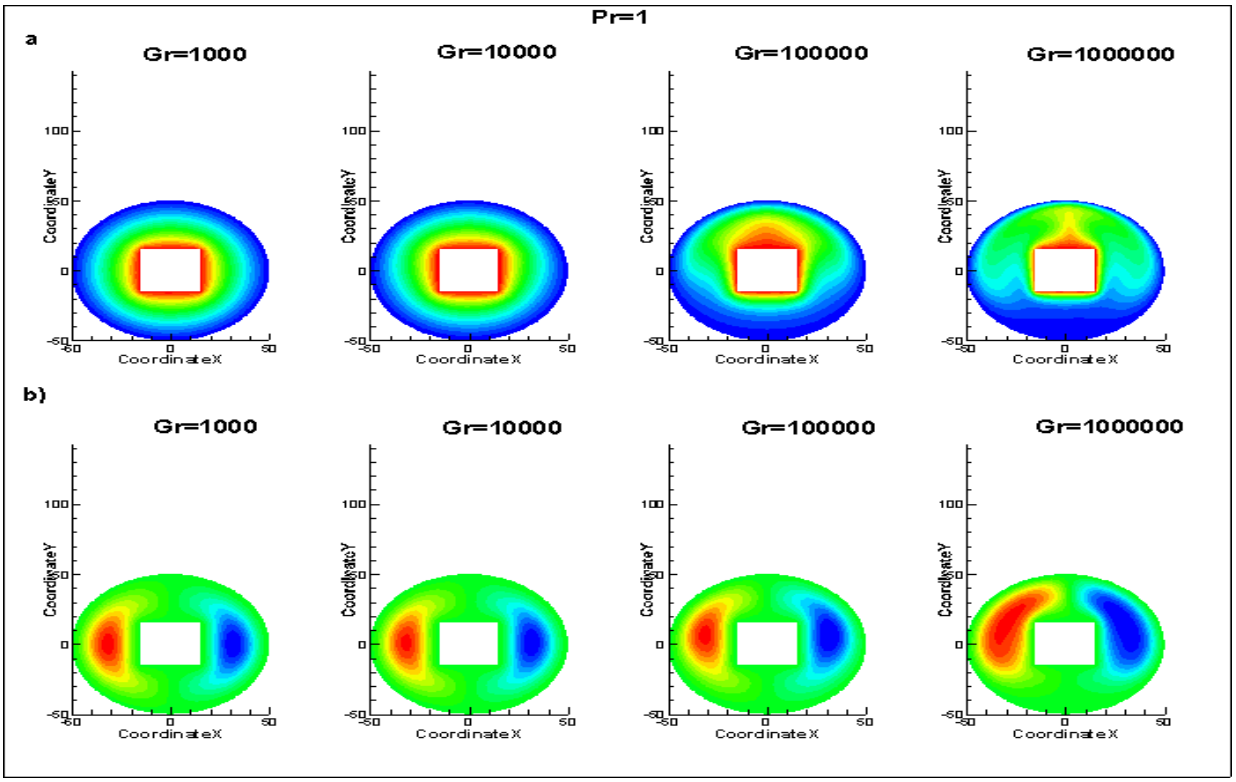

Fig.6.2.9 (A) Temperature profile, (B) Stream Function (Blockage=30%, Pr=100)

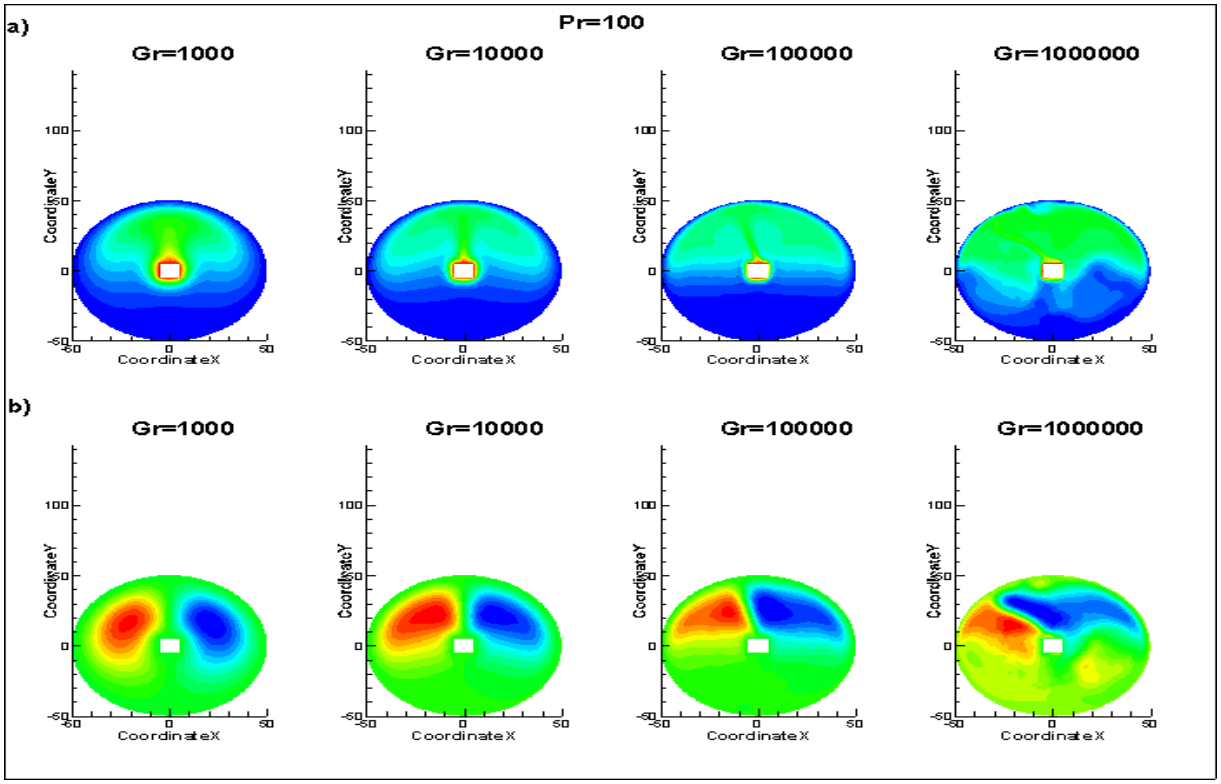

Fig.6.2.10 (A) Temperature profile, (B) Stream Function (Blockage=10%, Pr=100)

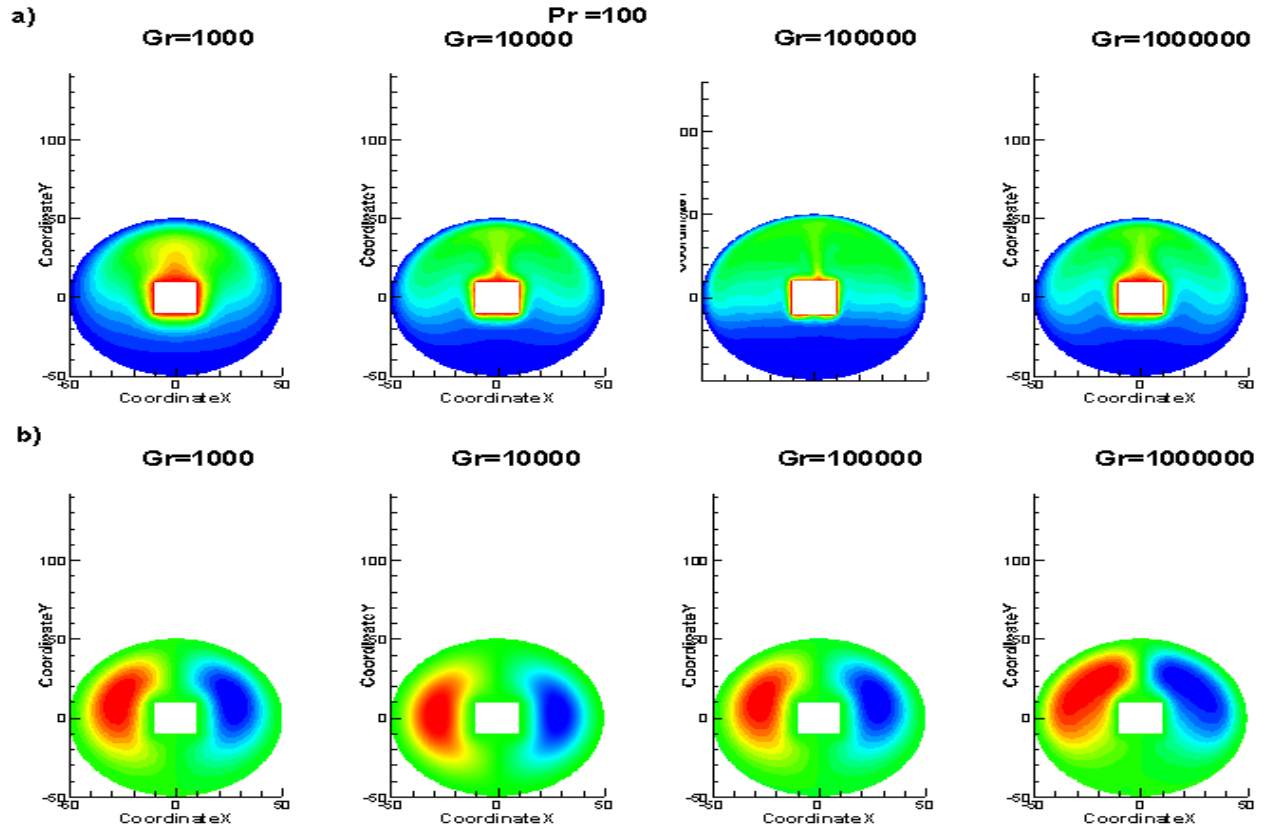

Fig.6.2.11 (A) Temperature profile, (B) Stream Function (Blockage=20%, Pr=100)

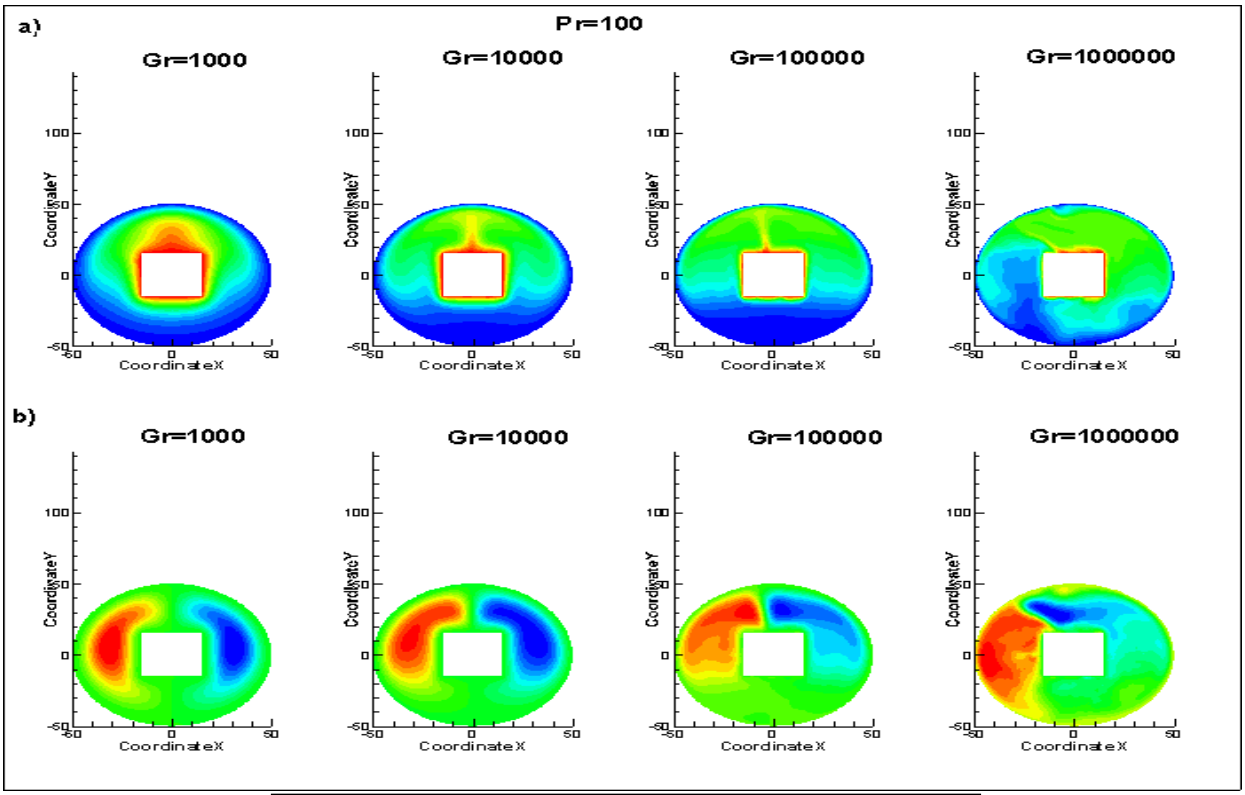

Fig.6.2.12 (A) Temperature profile, (B) Stream Function (Blockage=30%, Pr=100)

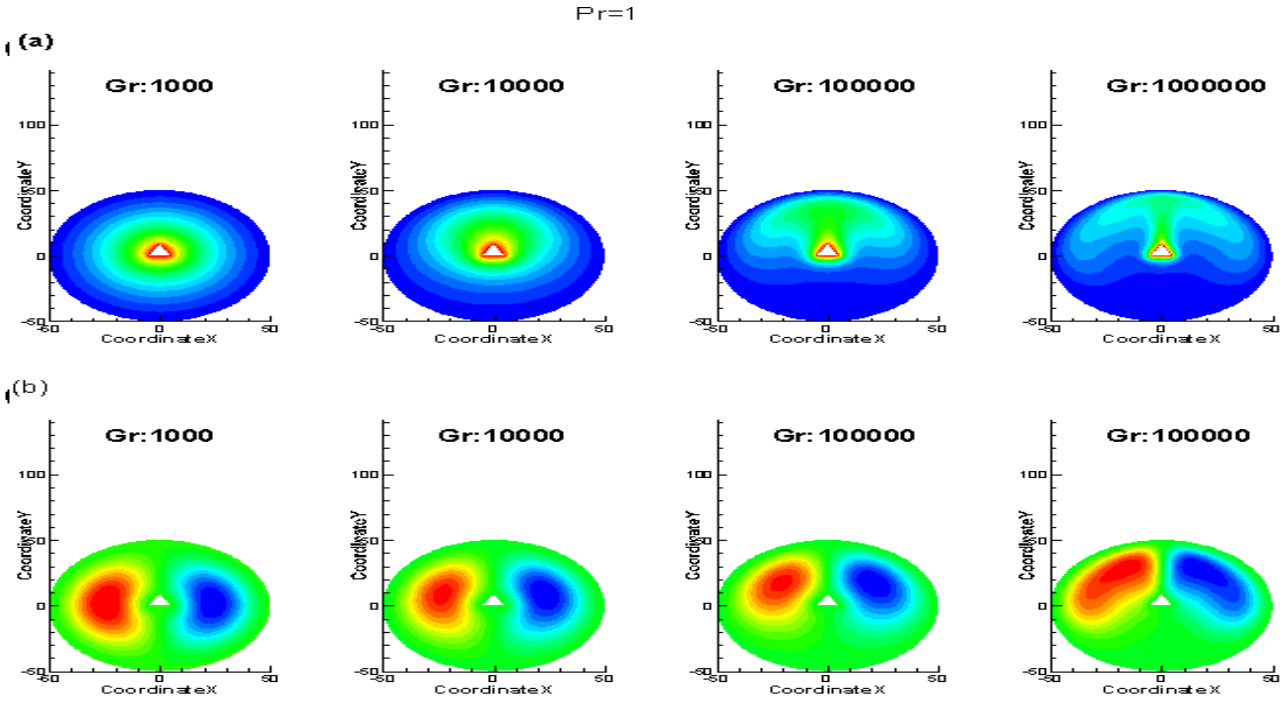

Fig.6.2.13 (A) Temperature profile, (B) Stream Function (Blockage=10%, Pr=1)

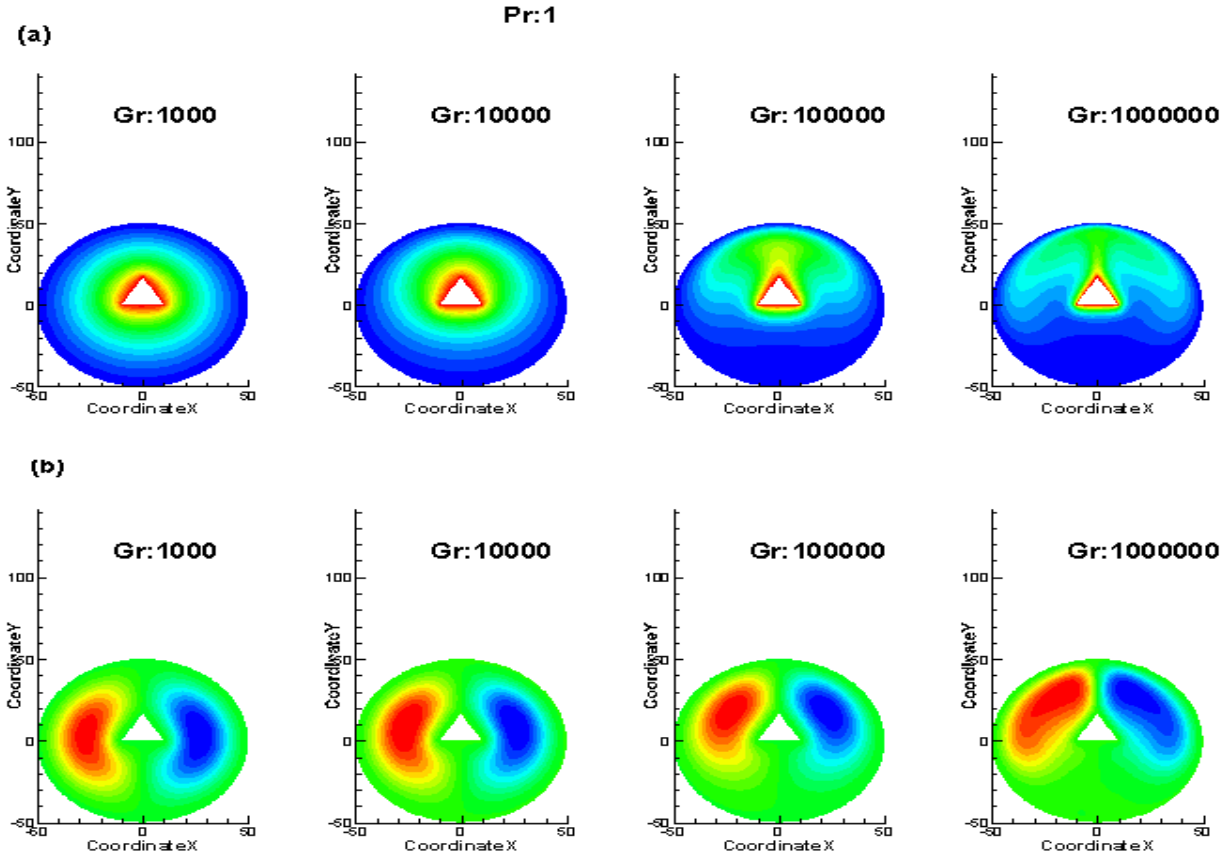

Fig.6.2.14 (A) Temperature profile, (B) Stream Function (Blockage=20%, Pr =1)

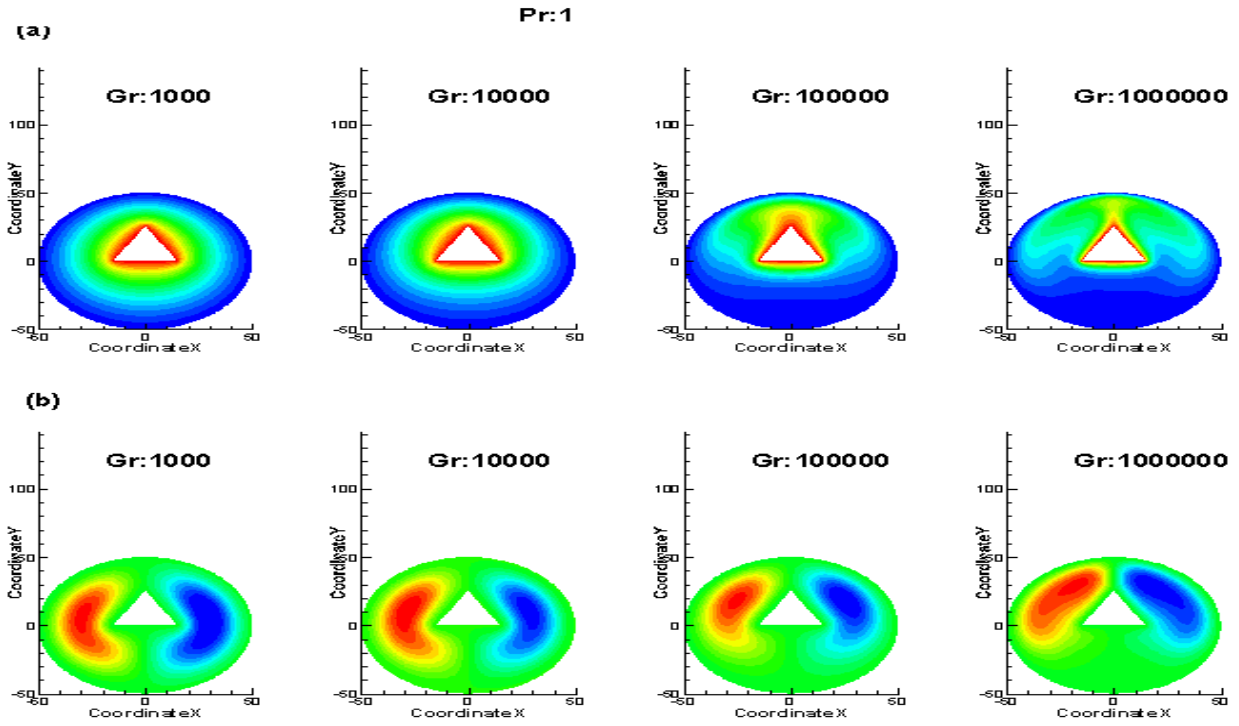

Fig.6.2.15 (A) Temperature profile, (B) Stream Function (Blockage=30%, Pr=1)

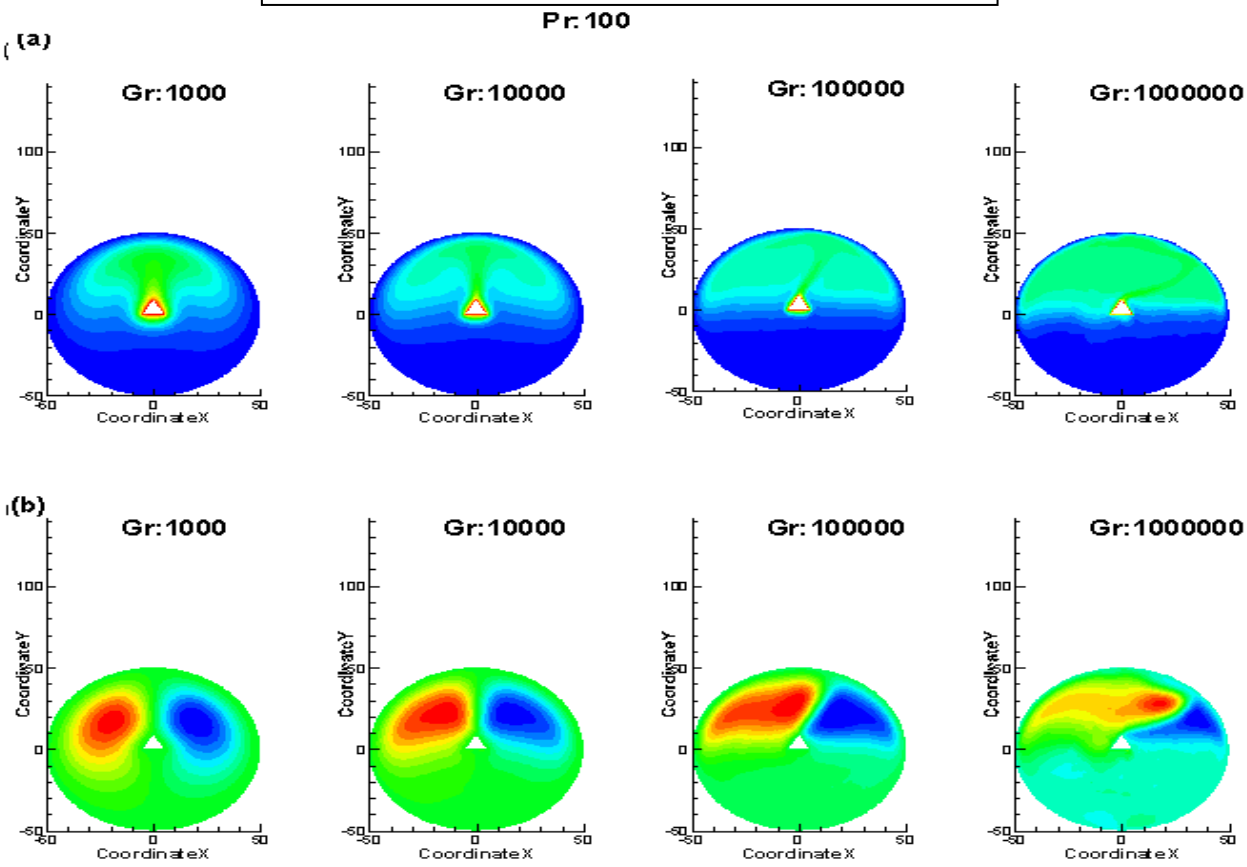

Fig.6.2.16 (A) Temperature profile, (B) Stream Function (Blockage=10%, Pr=100)

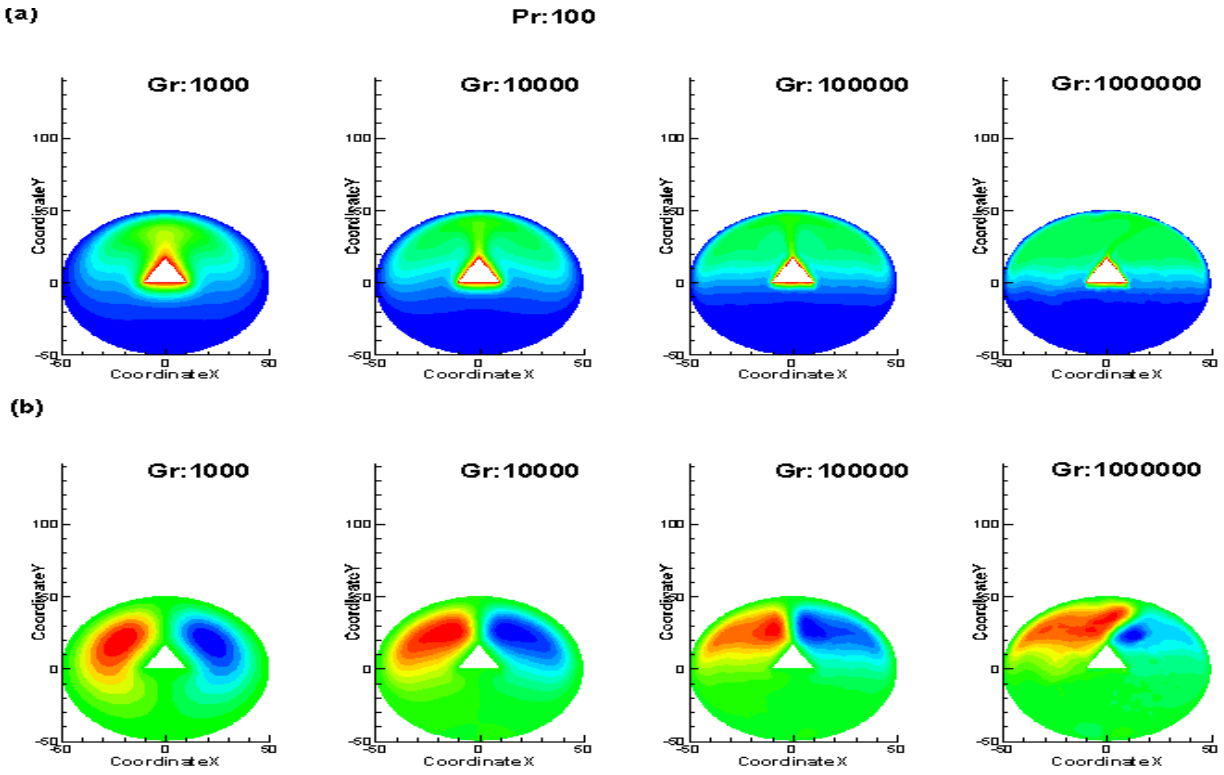

Fig.6.2.17 (A) Temperature profile, (B) Stream Function (Blockage=20%, Pr=100)

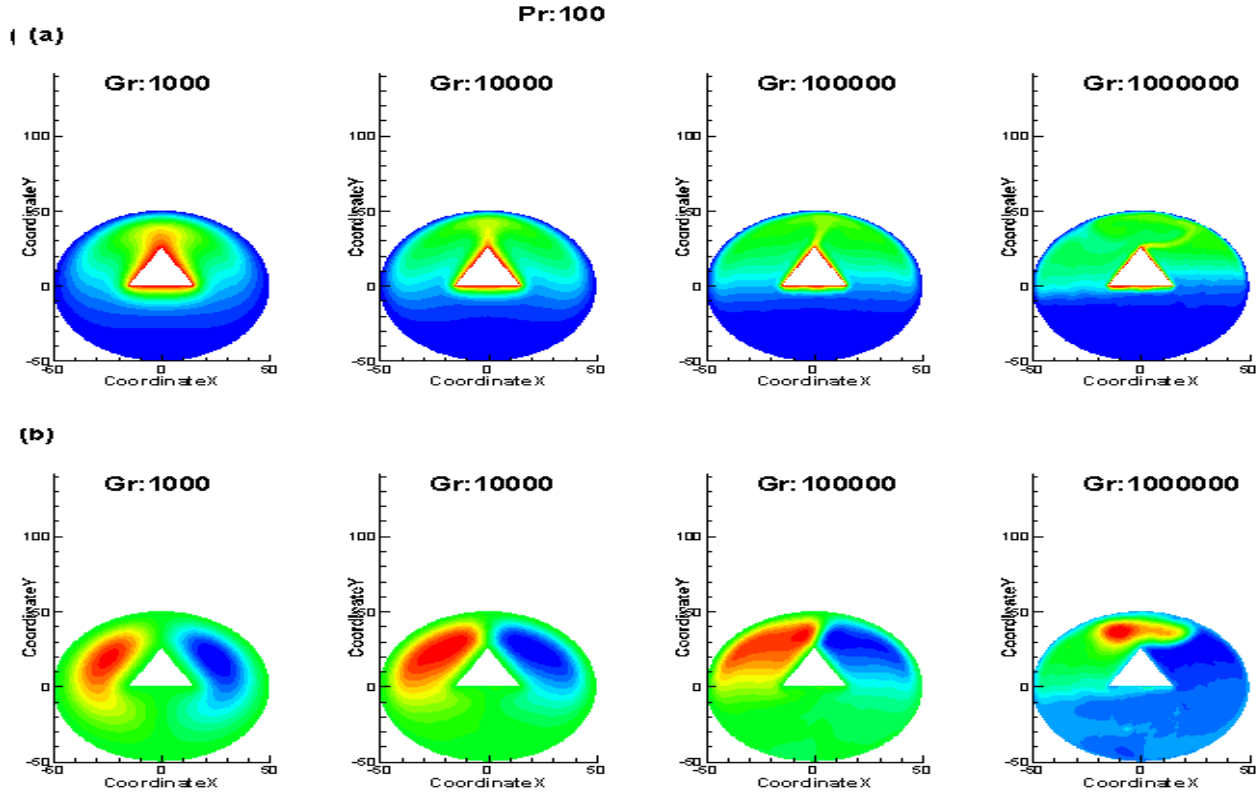

Fig.6.2.18 (A) Temperature profile, (B) Stream Function (Blockage=30%, Pr=100)

Non-Newtonian Fluids Tec plots

N=0.2, Pr=1

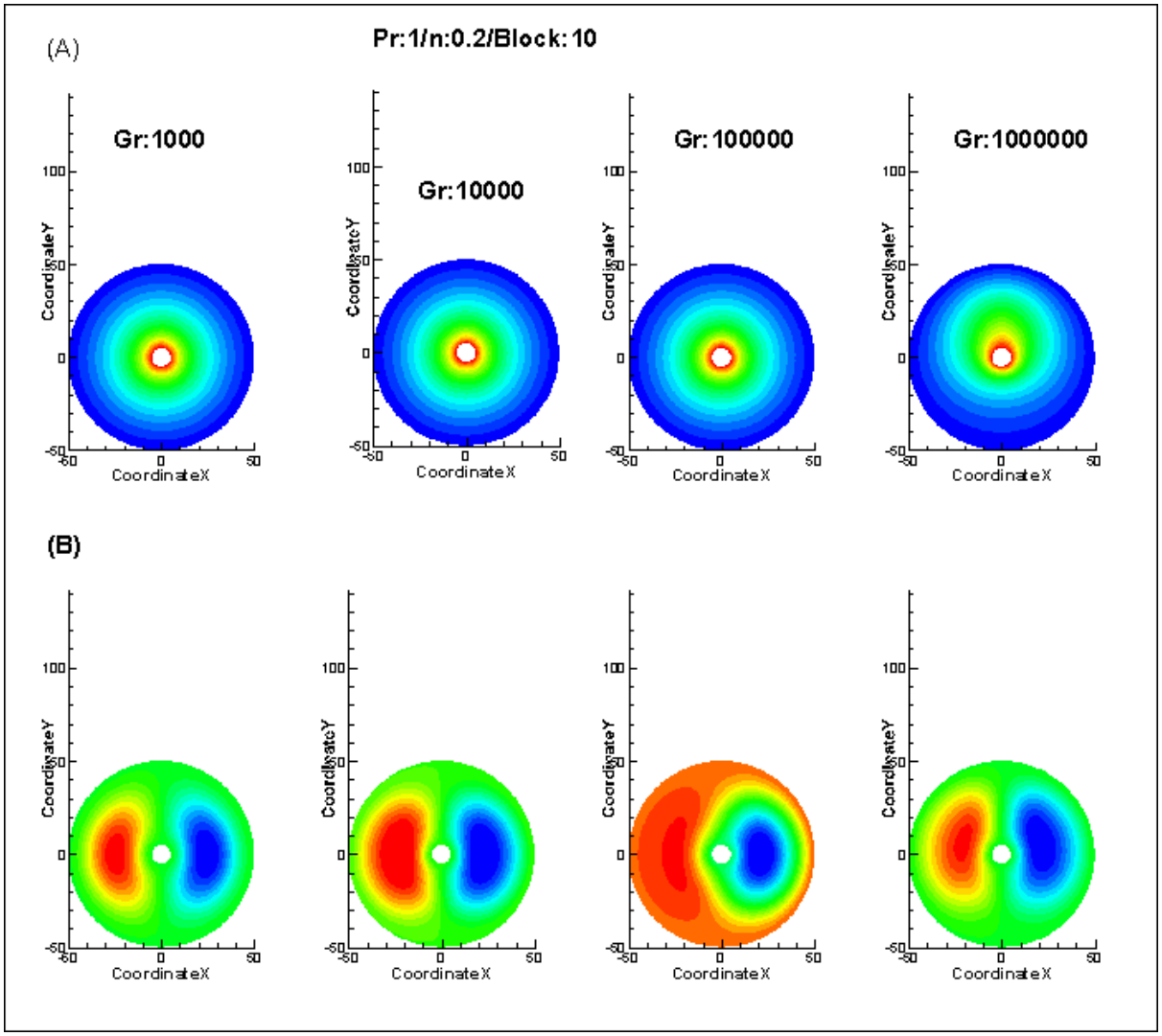

Fig.6.2.19 (A) Temperature profile, (B) Stream Function (Blockage=10%, Pr=1/0.2)

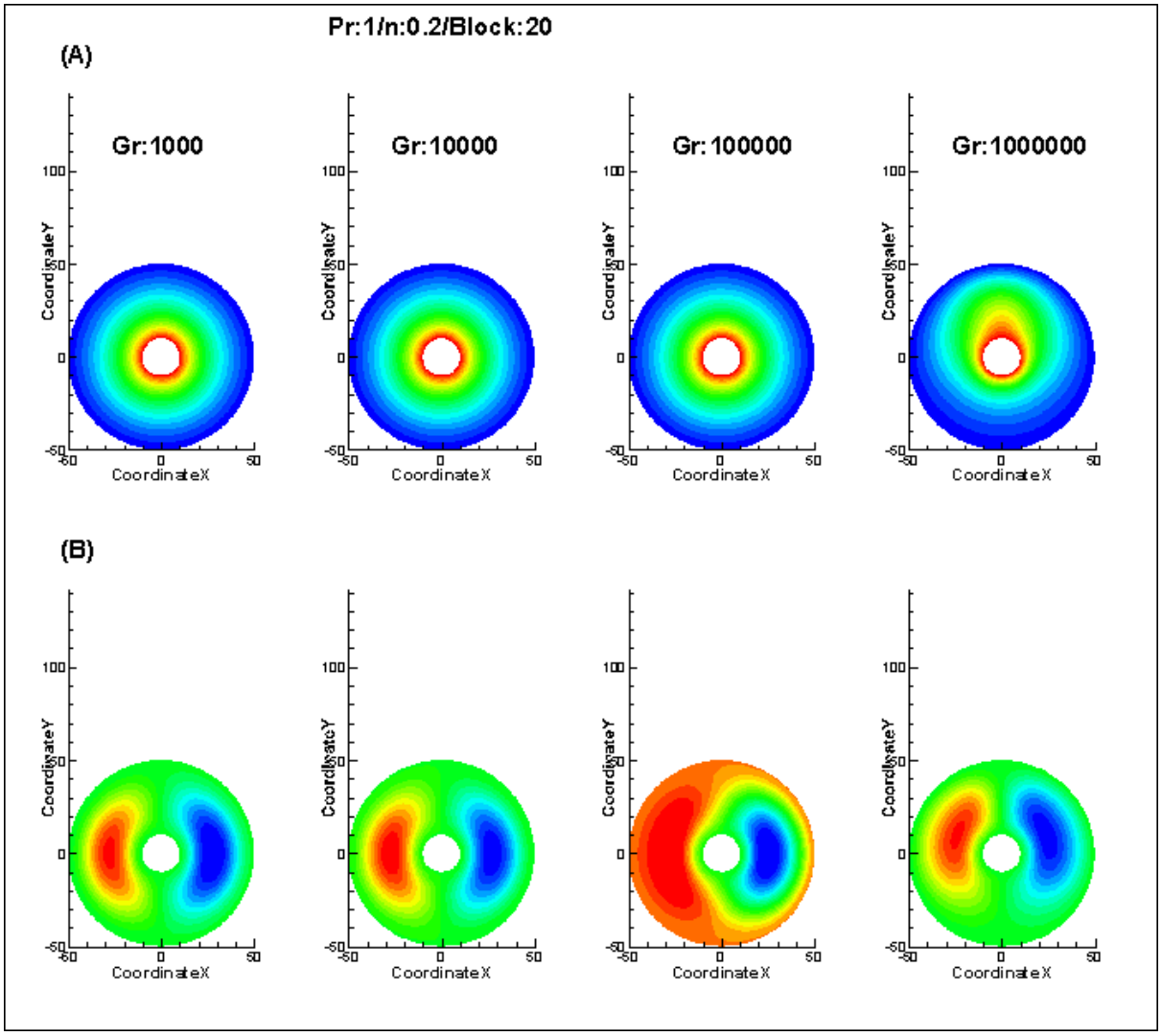

Fig.6.2.20 (A) Temperature profile, (B) Stream Function (Blockage=20%, Pr=1/0.2)

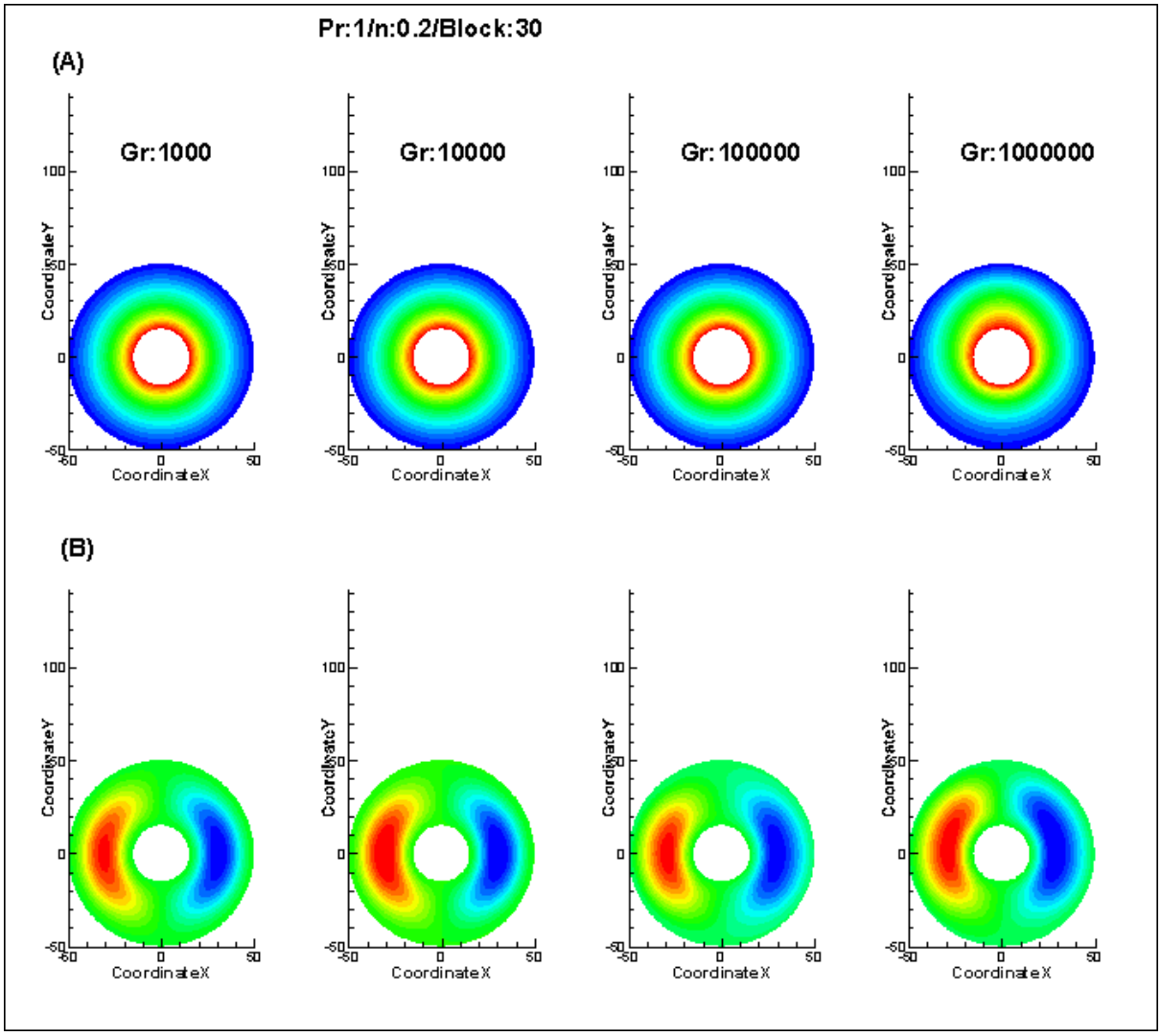

Fig.6.2.21 (A) Temperature profile, (B) Stream Function (Blockage=30%, Pr=1/0.2)

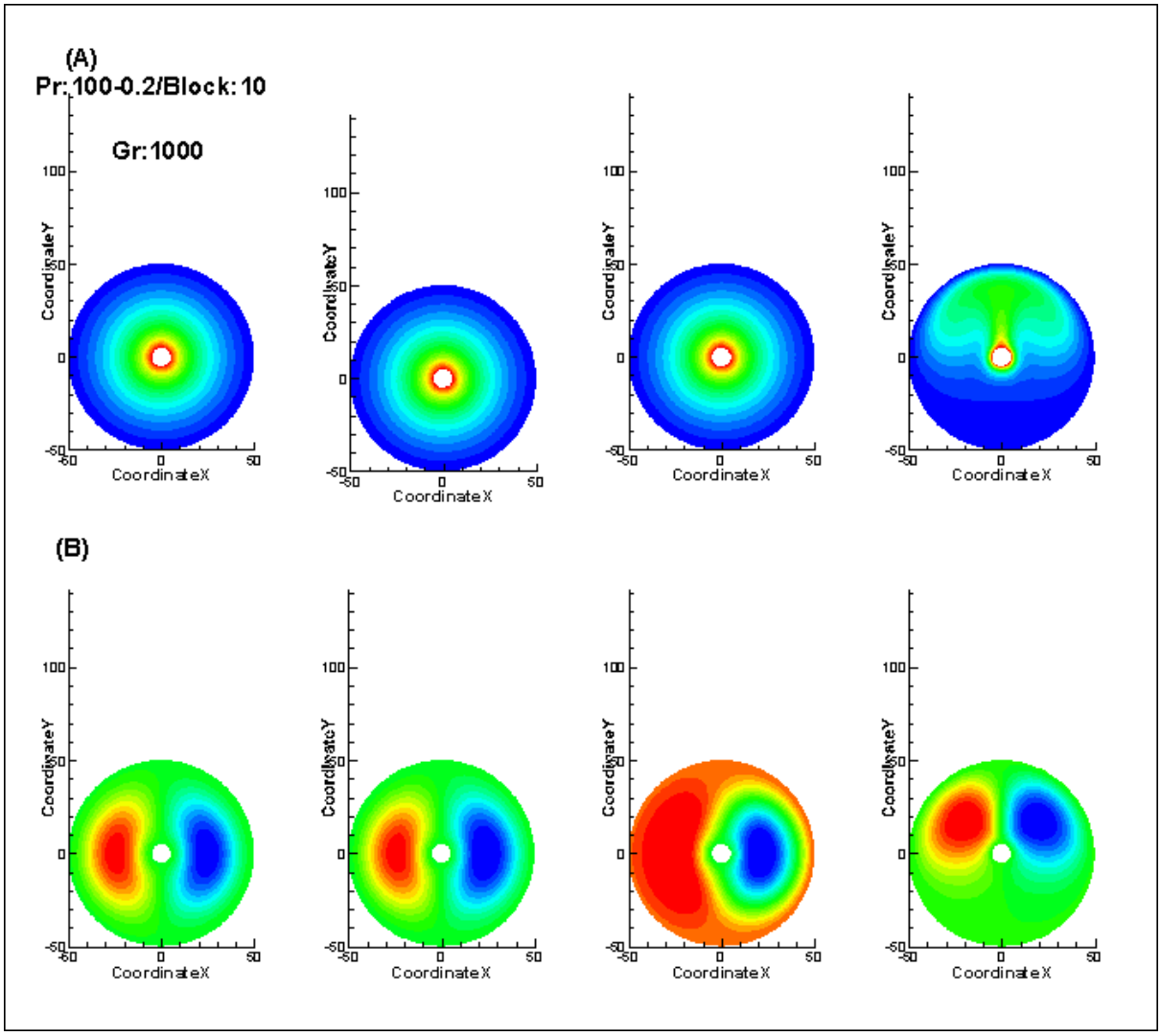

Fig.6.2.22 (A) Temperature profile, (B) Stream Function (Blockage=10%, Pr=100/0.2)

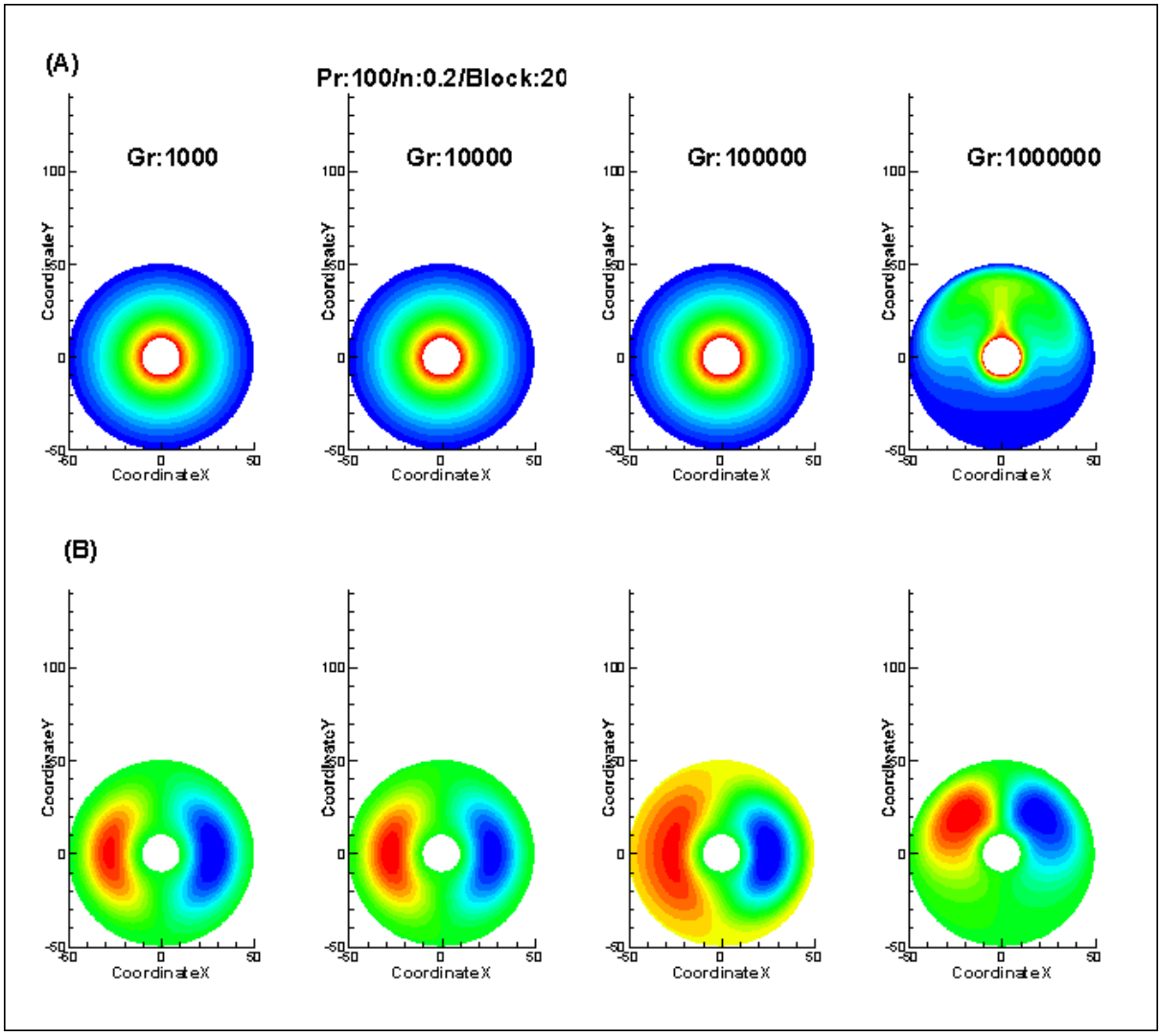

Fig.6.2.23 (A) Temperature profile, (B) Stream Function (Blockage=20%, Pr=100/0.2)

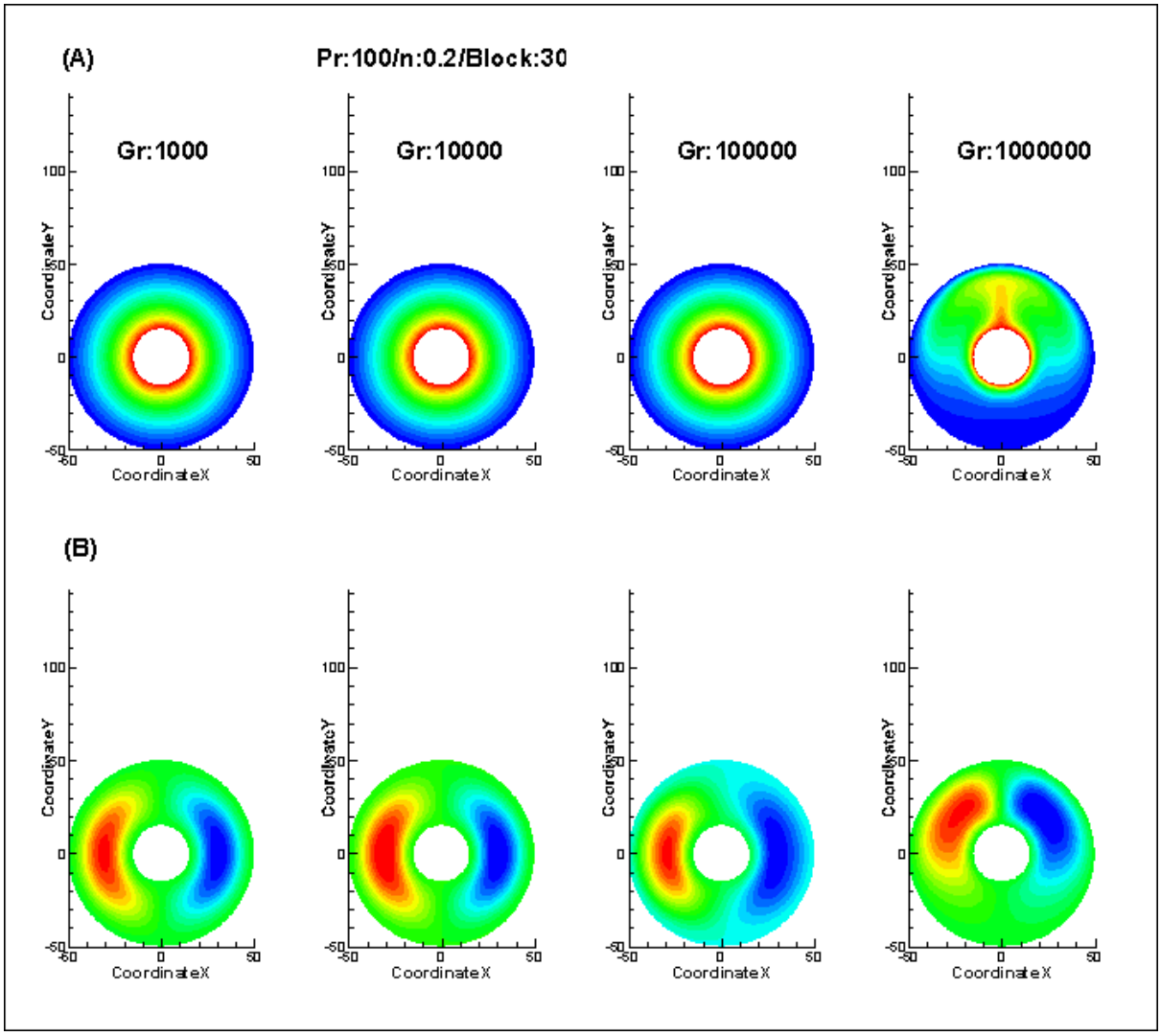

Fig.6.2.24 (A) Temperature profile, (B) Stream Function (Blockage=30%, Pr=100/0.2)

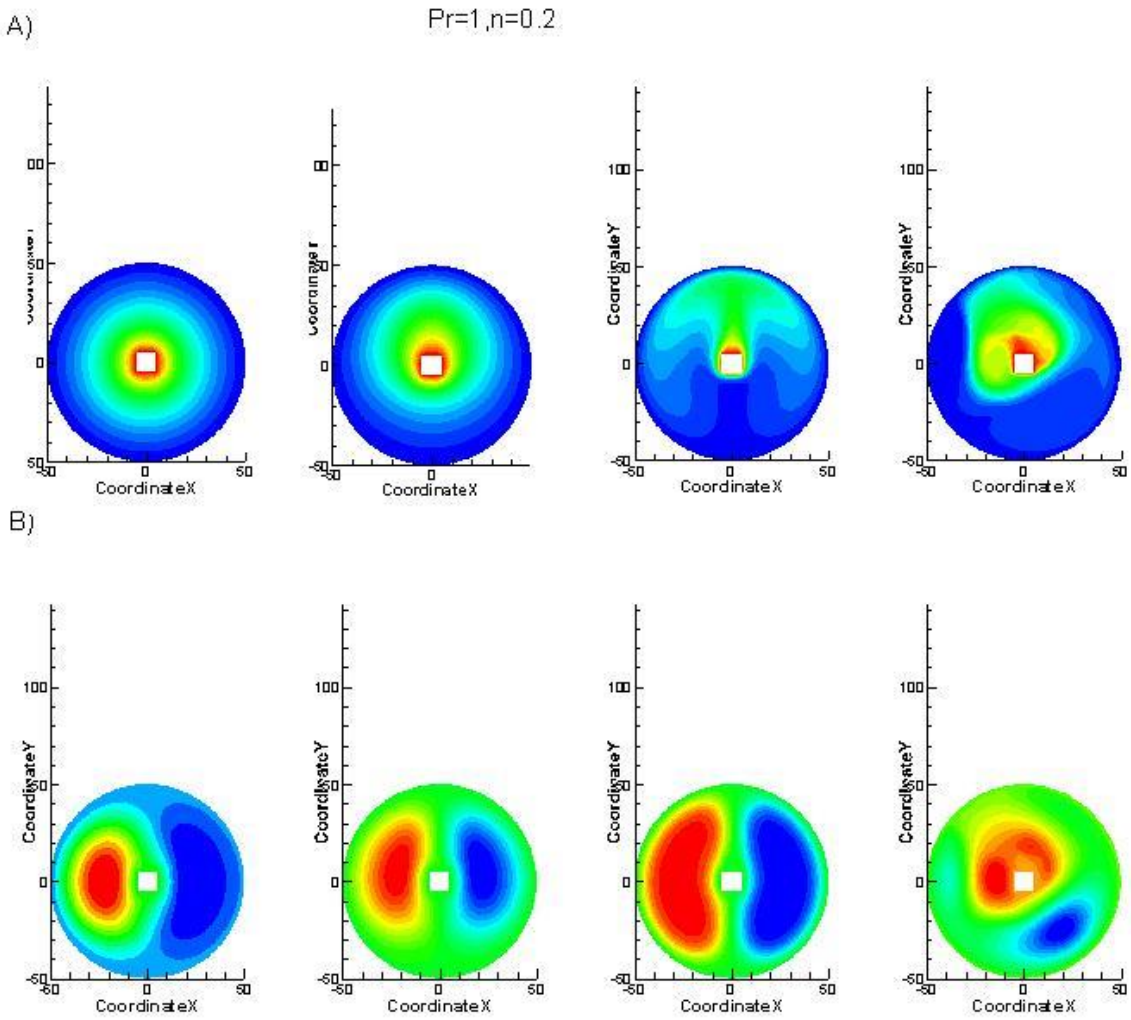

Fig.6.2.25 (A) Temperature profile, (B) Stream Function (Blockage=10%, Pr=1/0.2)

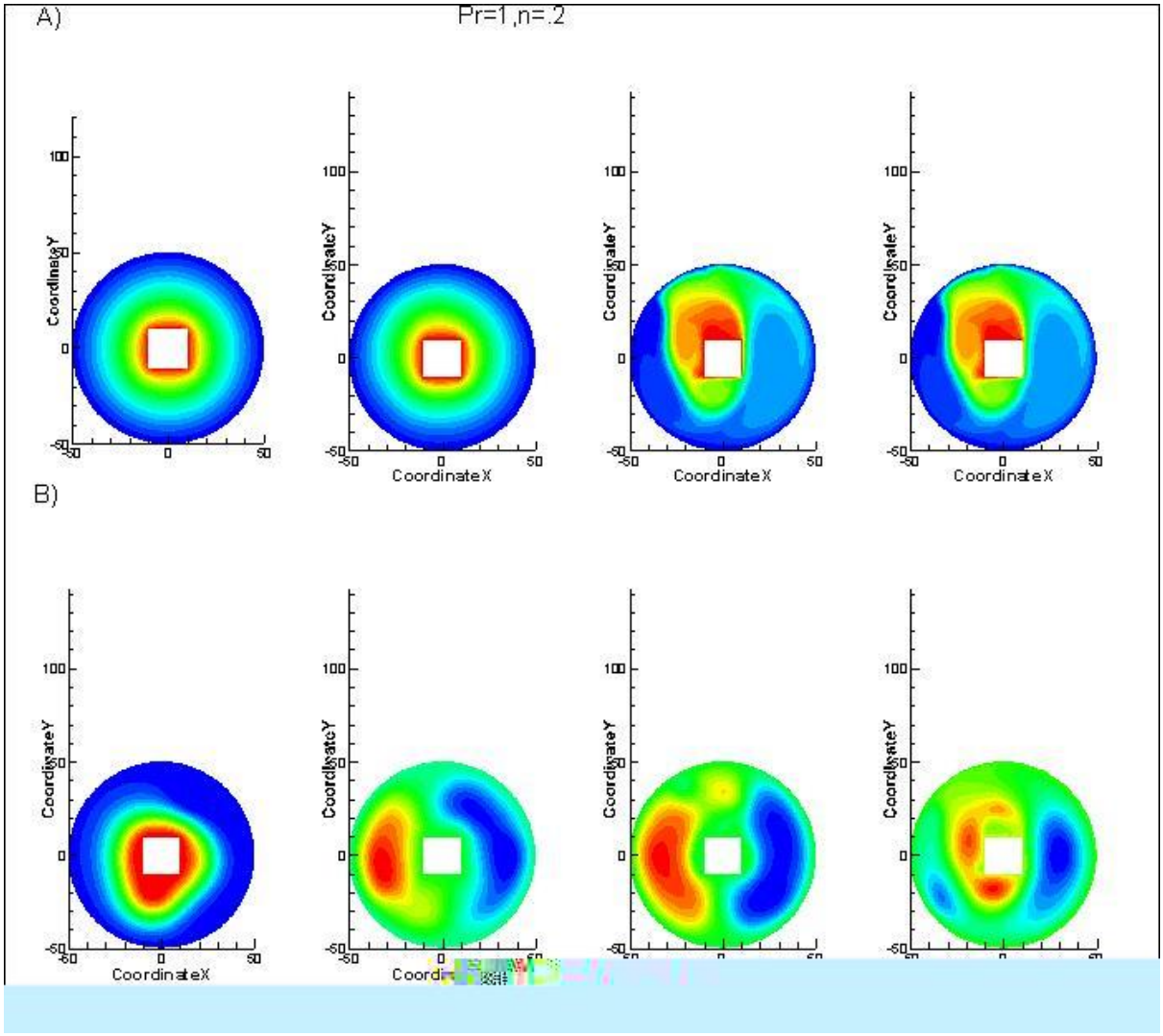

Fig.6.2.26 (A) Temperature profile, (B) Stream Function (Blockage=20%, Pr=1/0.2)

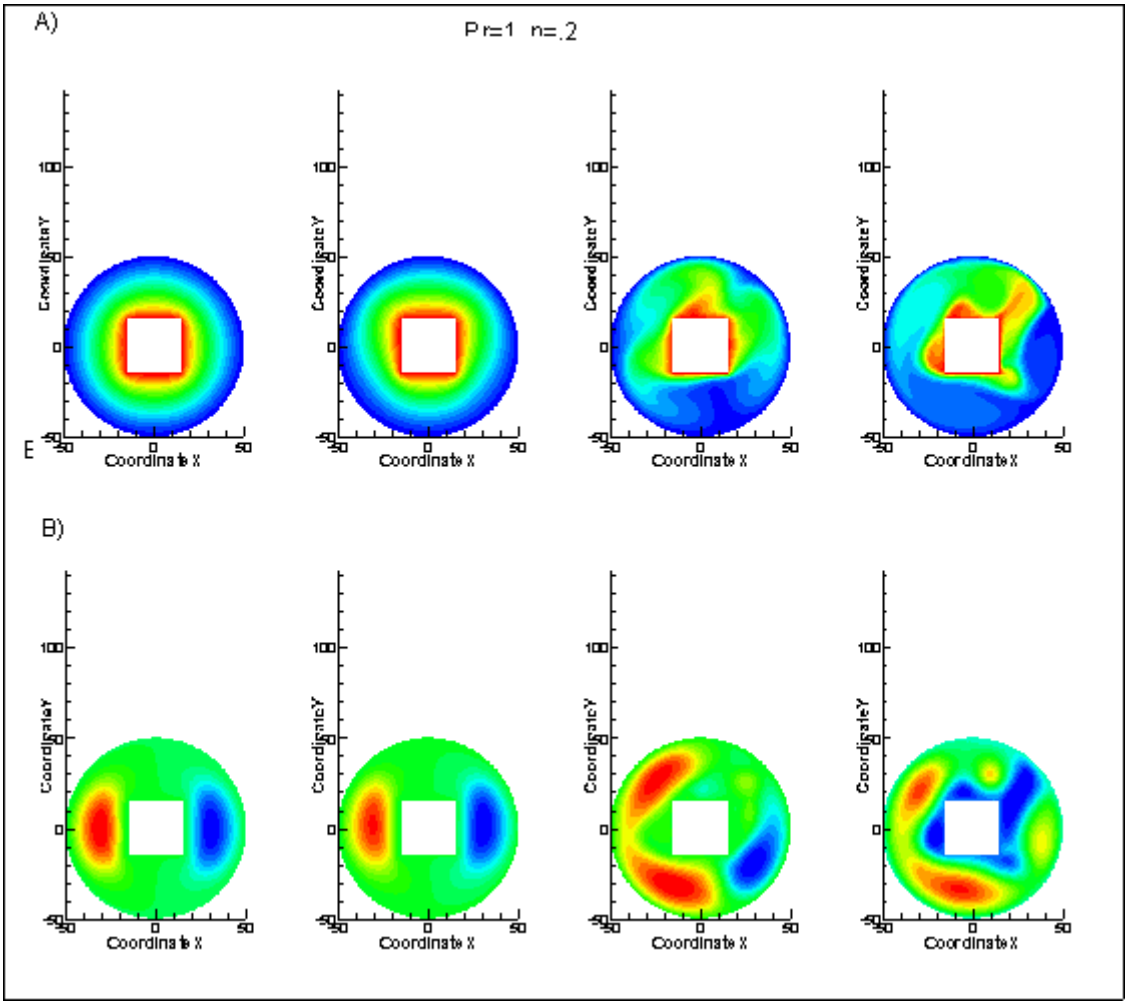

Fig.6.2.27 (A) Temperature profile, (B) Stream Function (Blockage=30%, Pr=1/0.2)

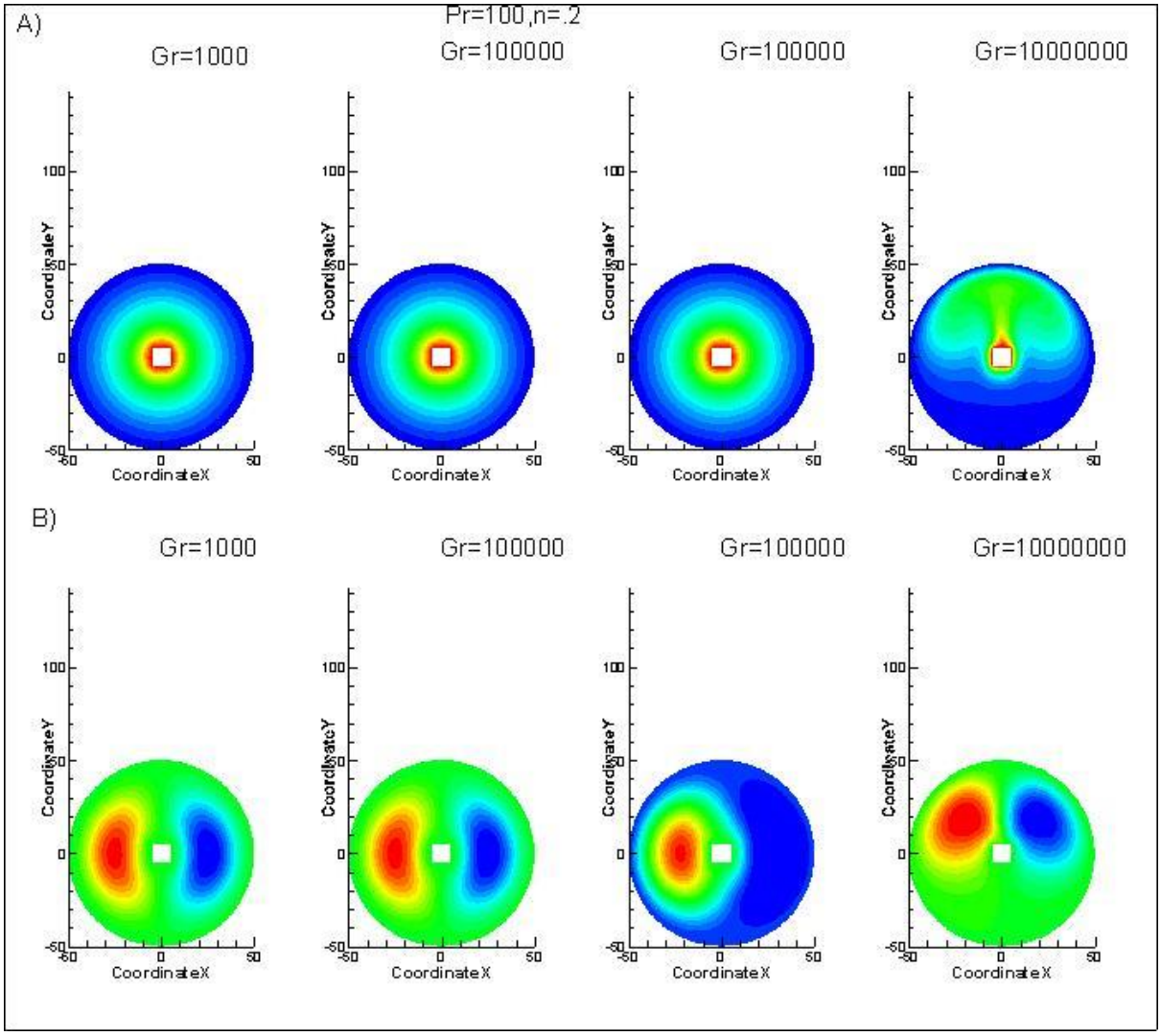

Fig.6.2.28 (A) Temperature profile, (B) Stream Function (Blockage=10%, Pr=100/0.2)

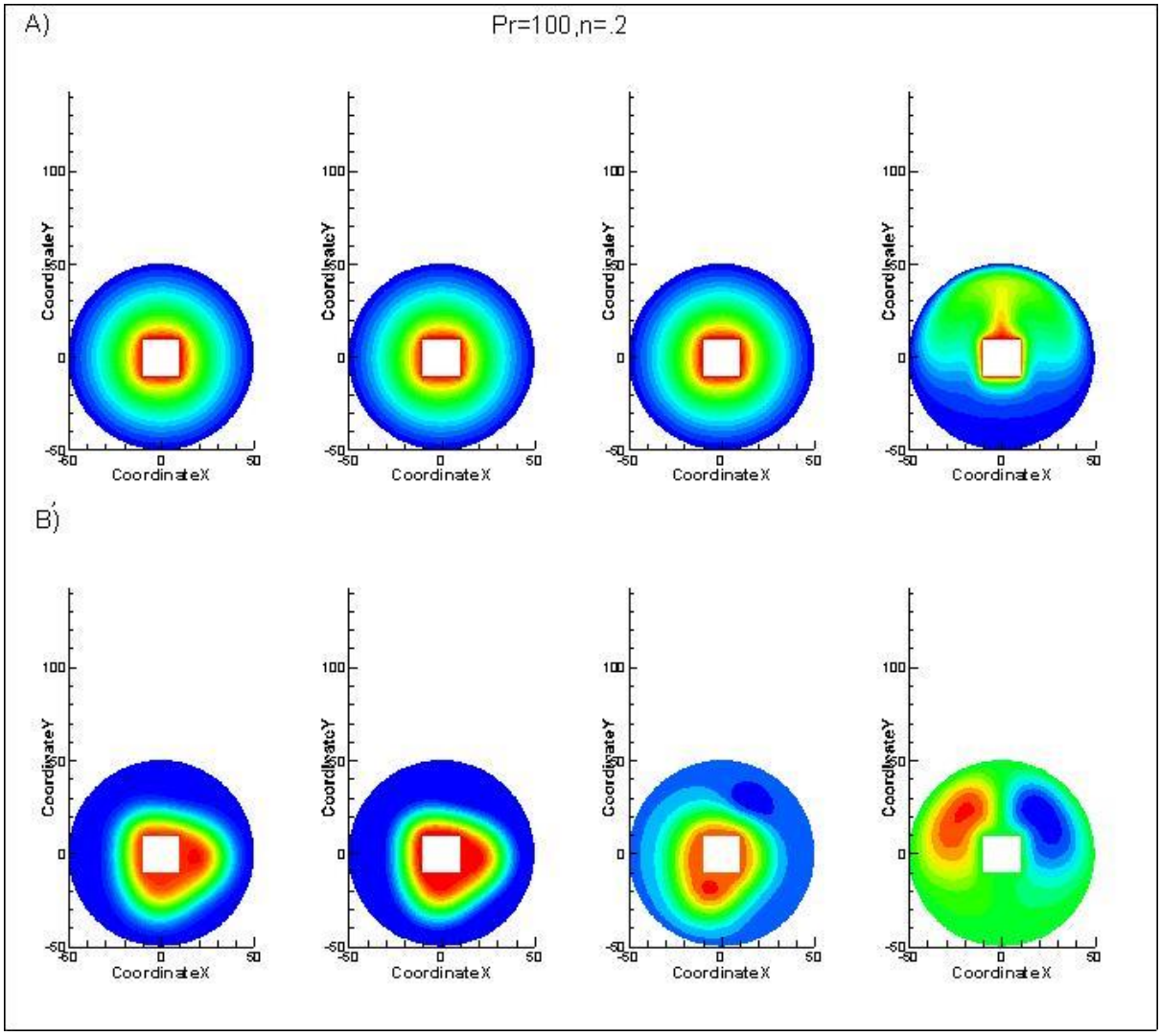

Fig.6.2.29 (A) Temperature profile, (B) Stream Function (Blockage=20%, Pr=100/0.2)

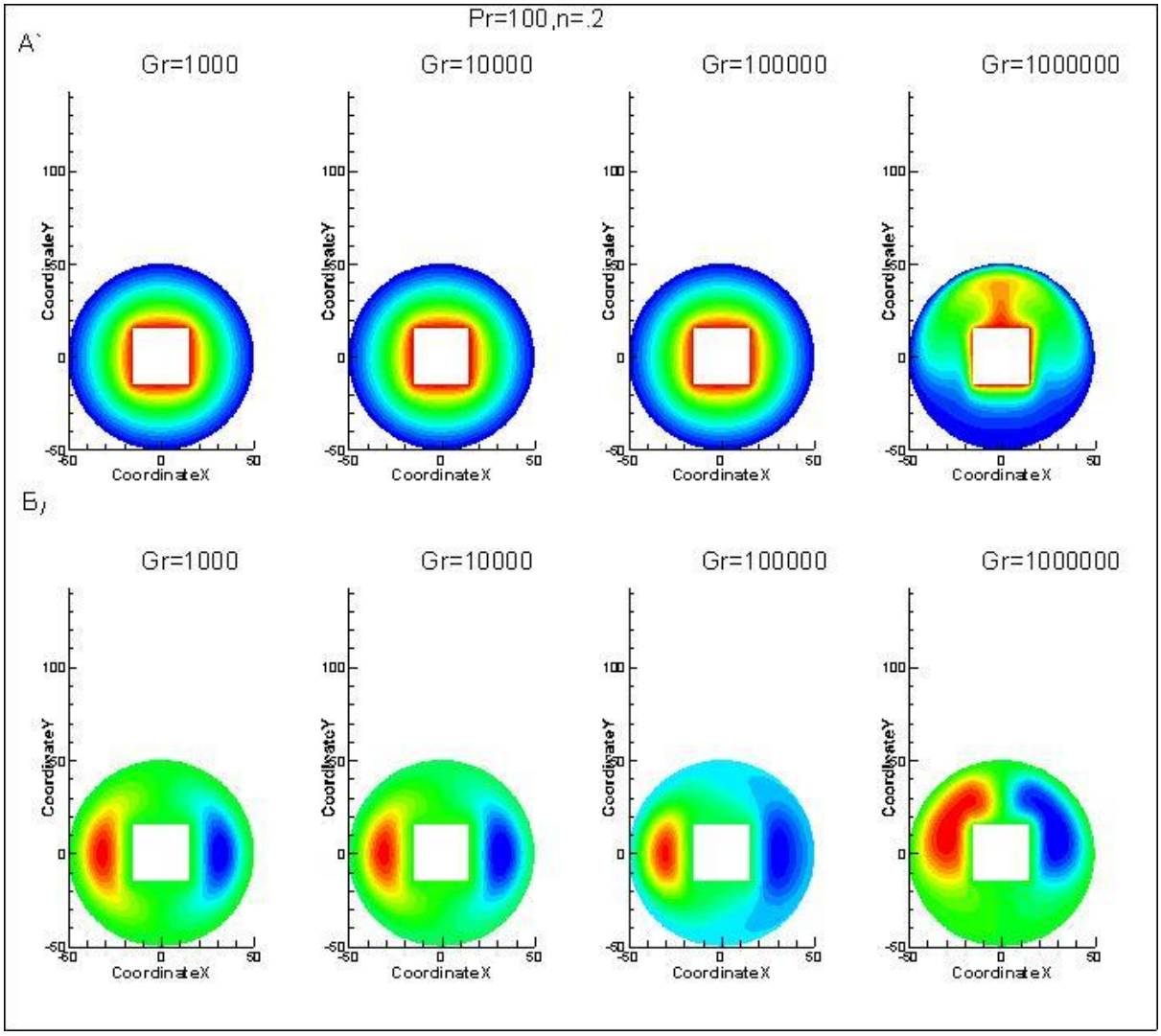

Fig.6.2.30 (A) Temperature profile, (B) Stream Function (Blockage=30%, Pr=100/0.2)

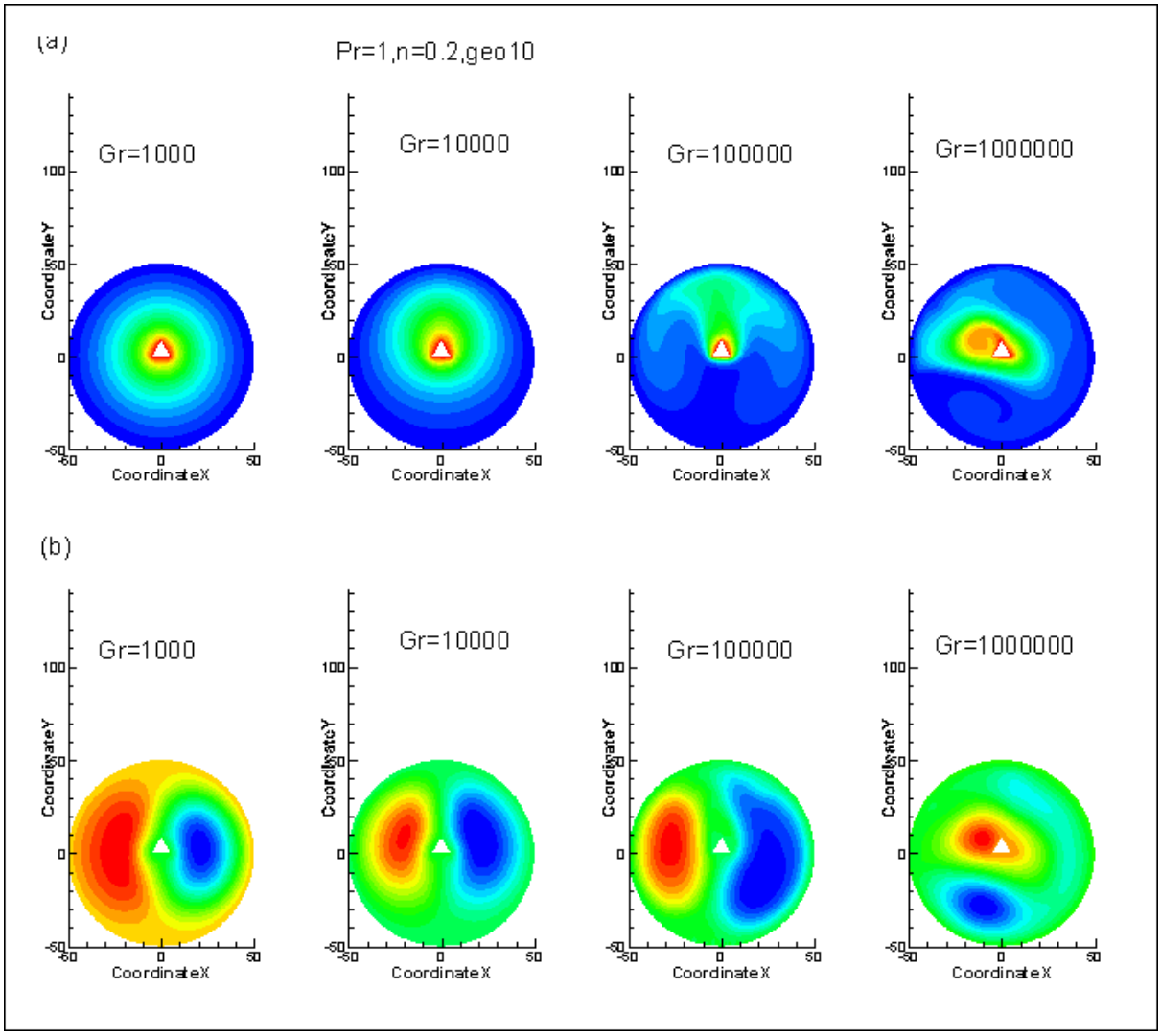

Fig.6.2.31 (A) Temperature profile, (B) Stream Function (Blockage=10%, Pr=1/0.2)

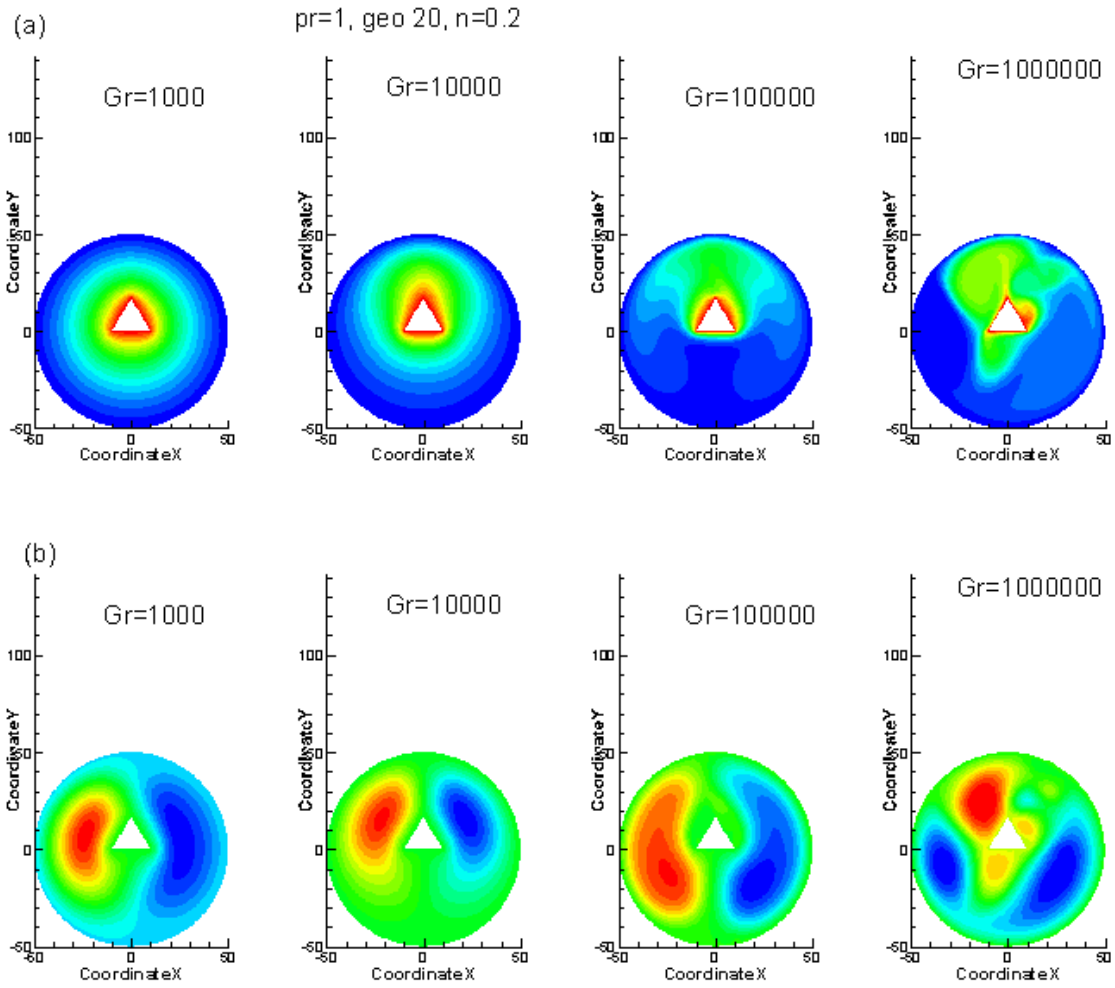

Fig.6.2.32 (A) Temperature profile, (B) Stream Function (Blockage=20%, Pr=1/0.2)

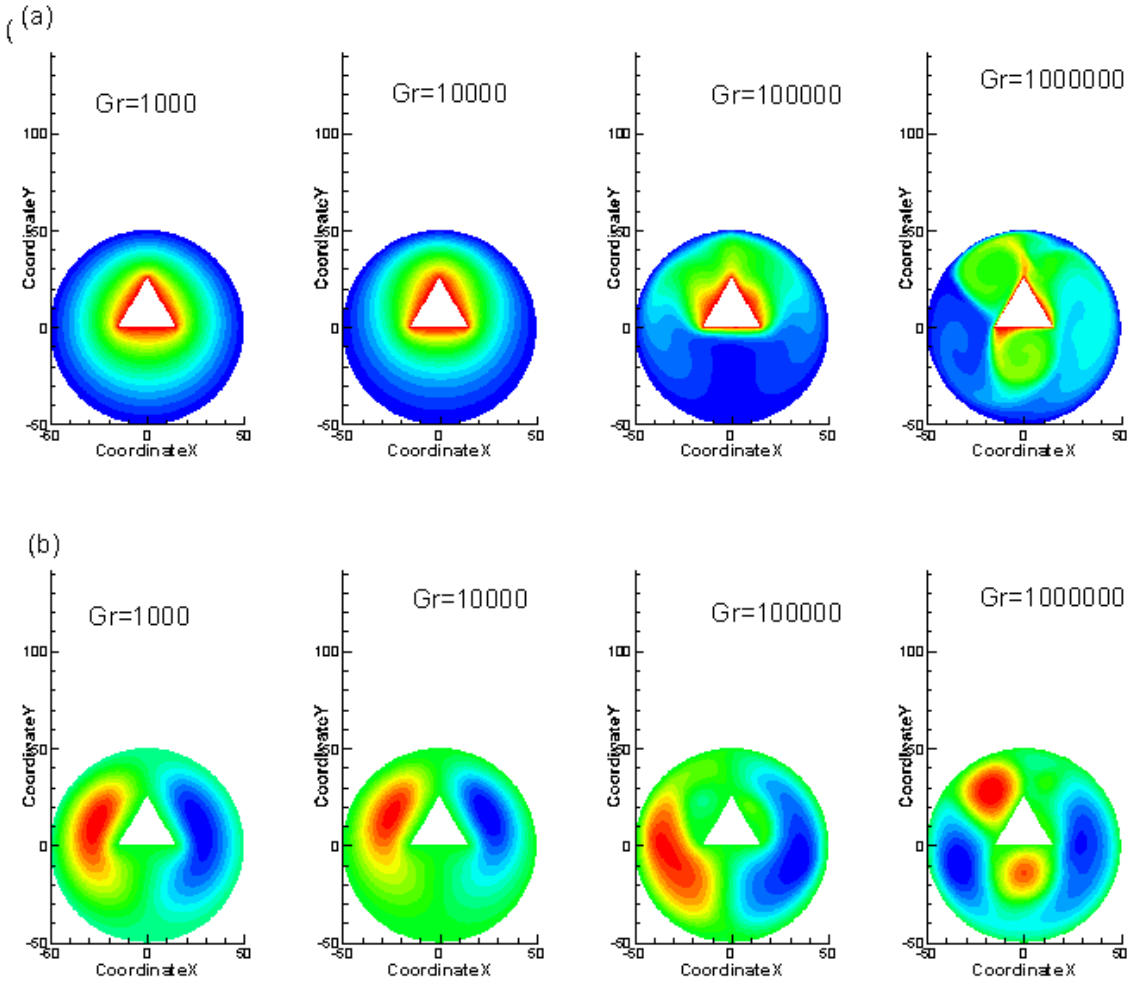

Fig.6.2.33 (A) Temperature profile, (B) Stream Function (Blockage=30%, Pr=1/0.2)

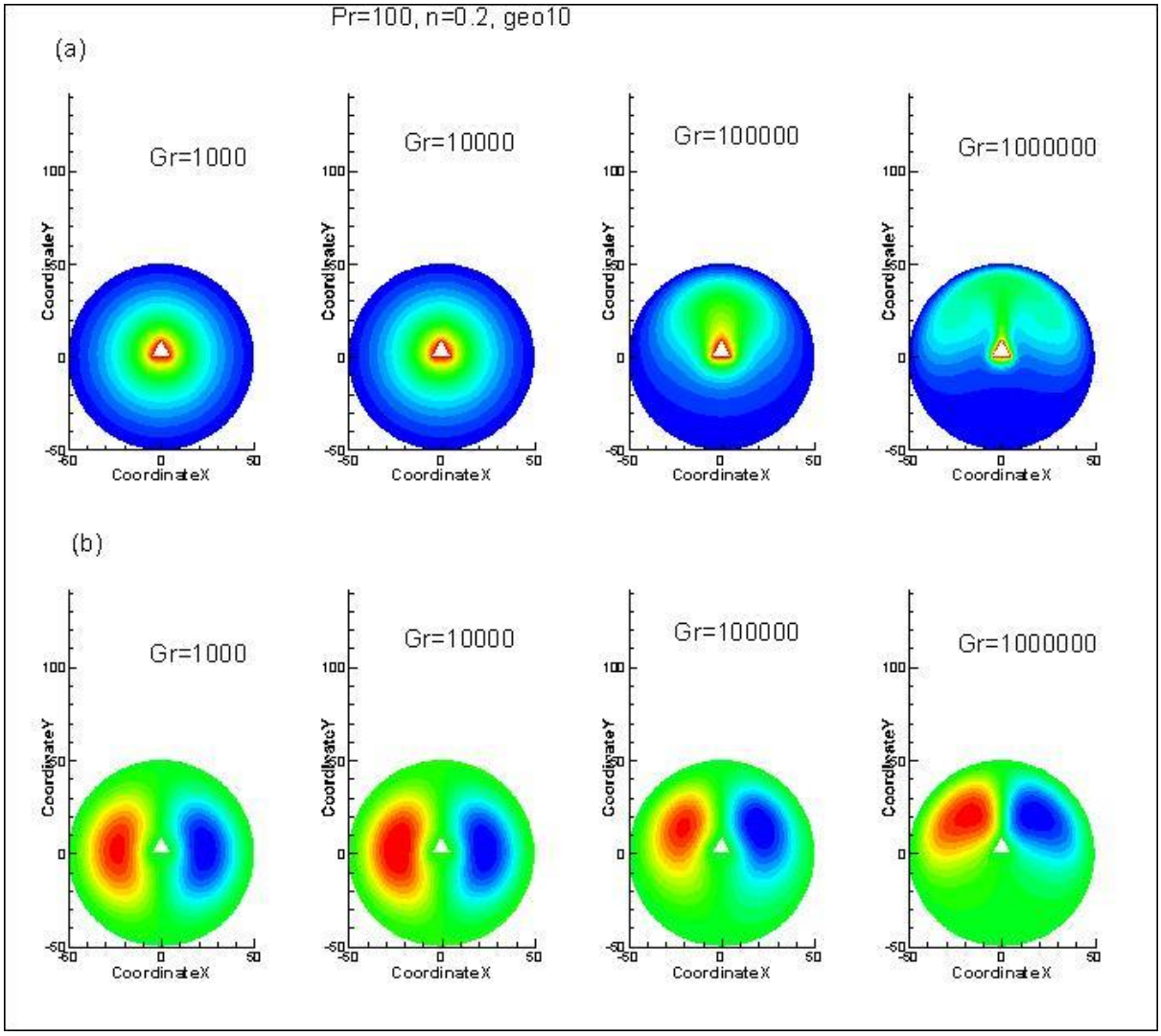

Fig.6.2.34 (A) Temperature profile, (B) Stream Function (Blockage=10%, Pr=100/0.2)

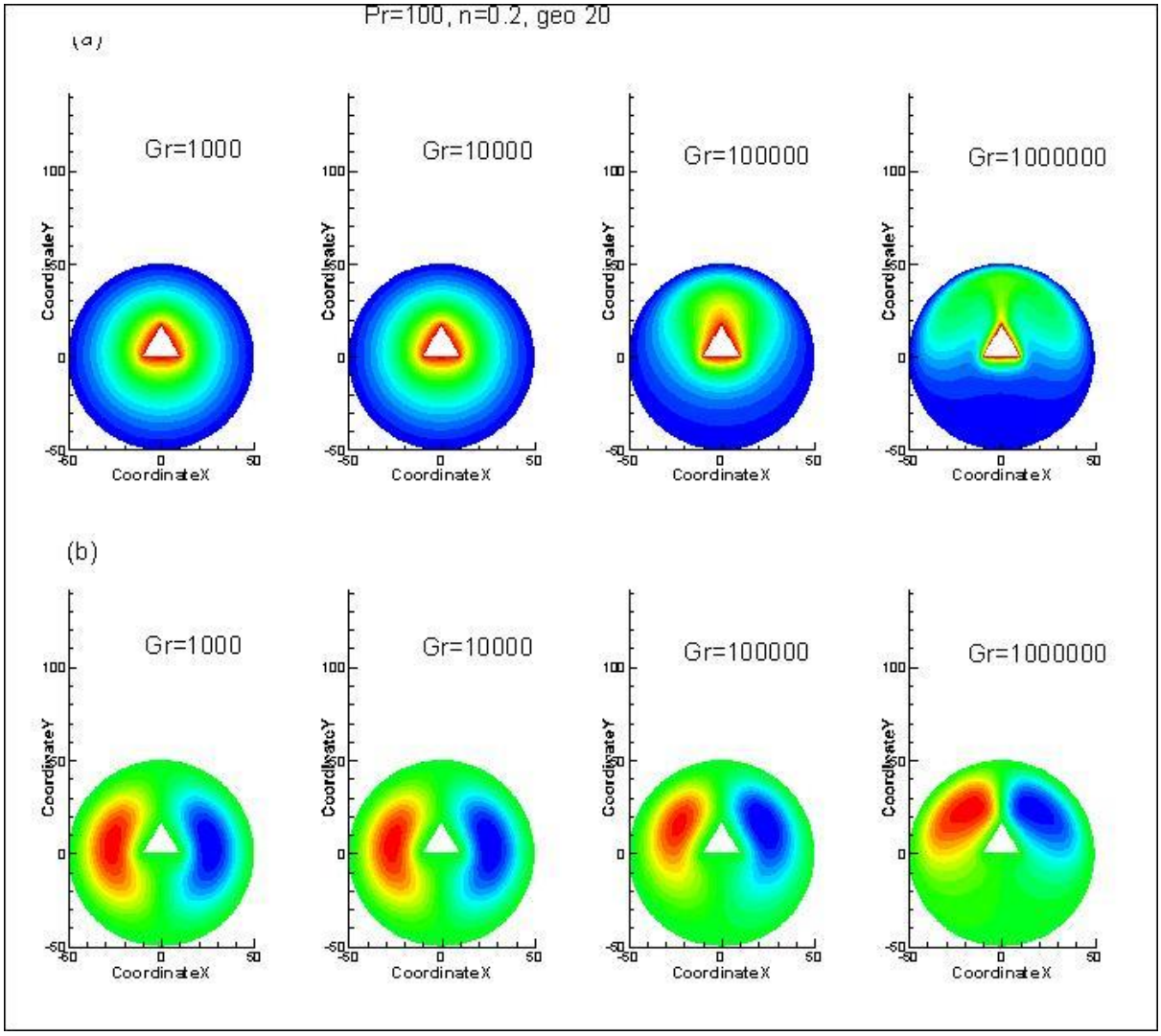

Fig.6.2.35 (A) Temperature profile, (B) Stream Function (Blockage=20%, Pr=100/0.2)

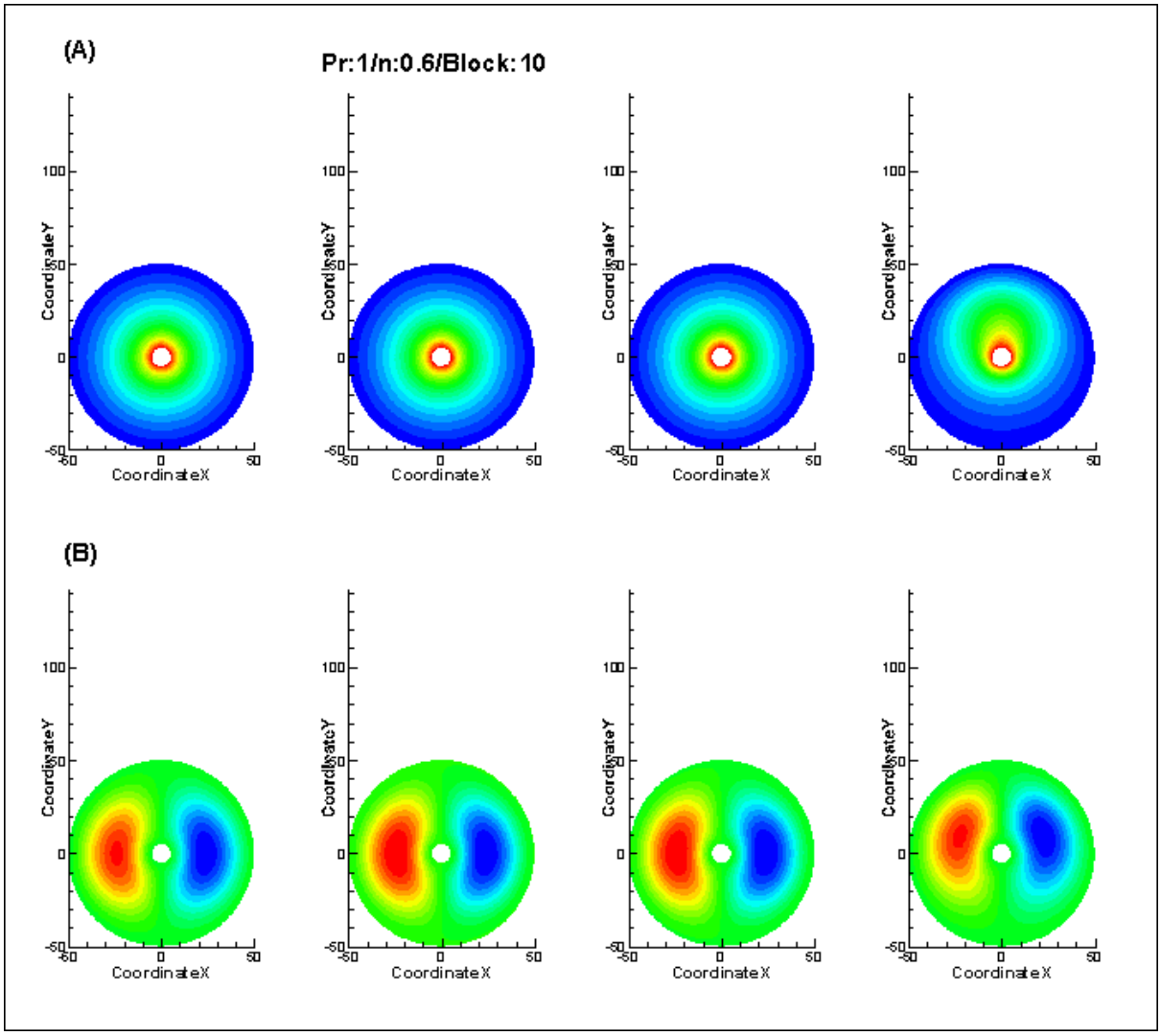

Fig.6.2.37 (A) Temperature profile, (B) Stream Function (Blockage=10%, Pr=1/0.6)

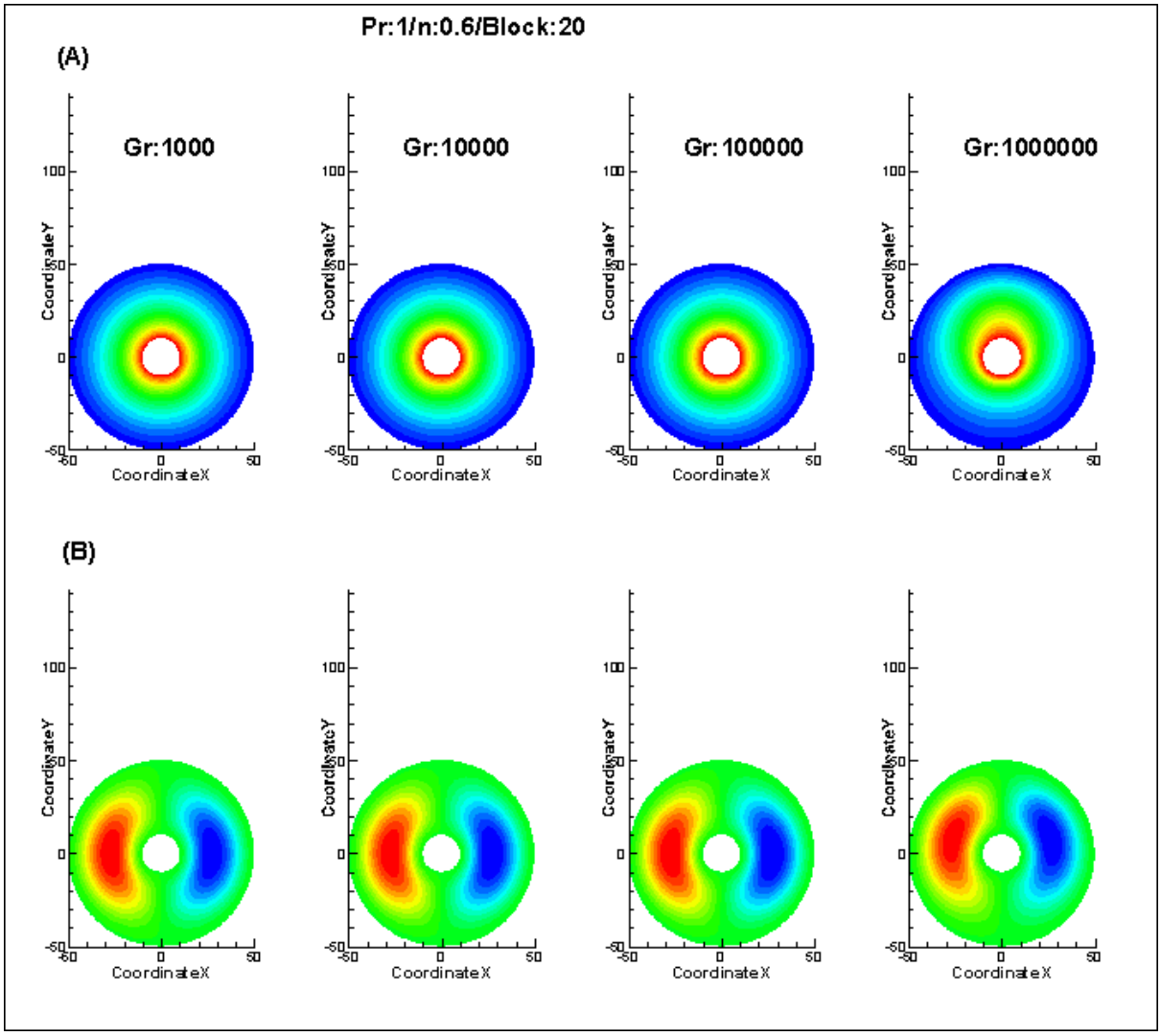

Fig.6.2.38 (A) Temperature profile, (B) Stream Function (Blockage=20%, Pr=1/0.6)

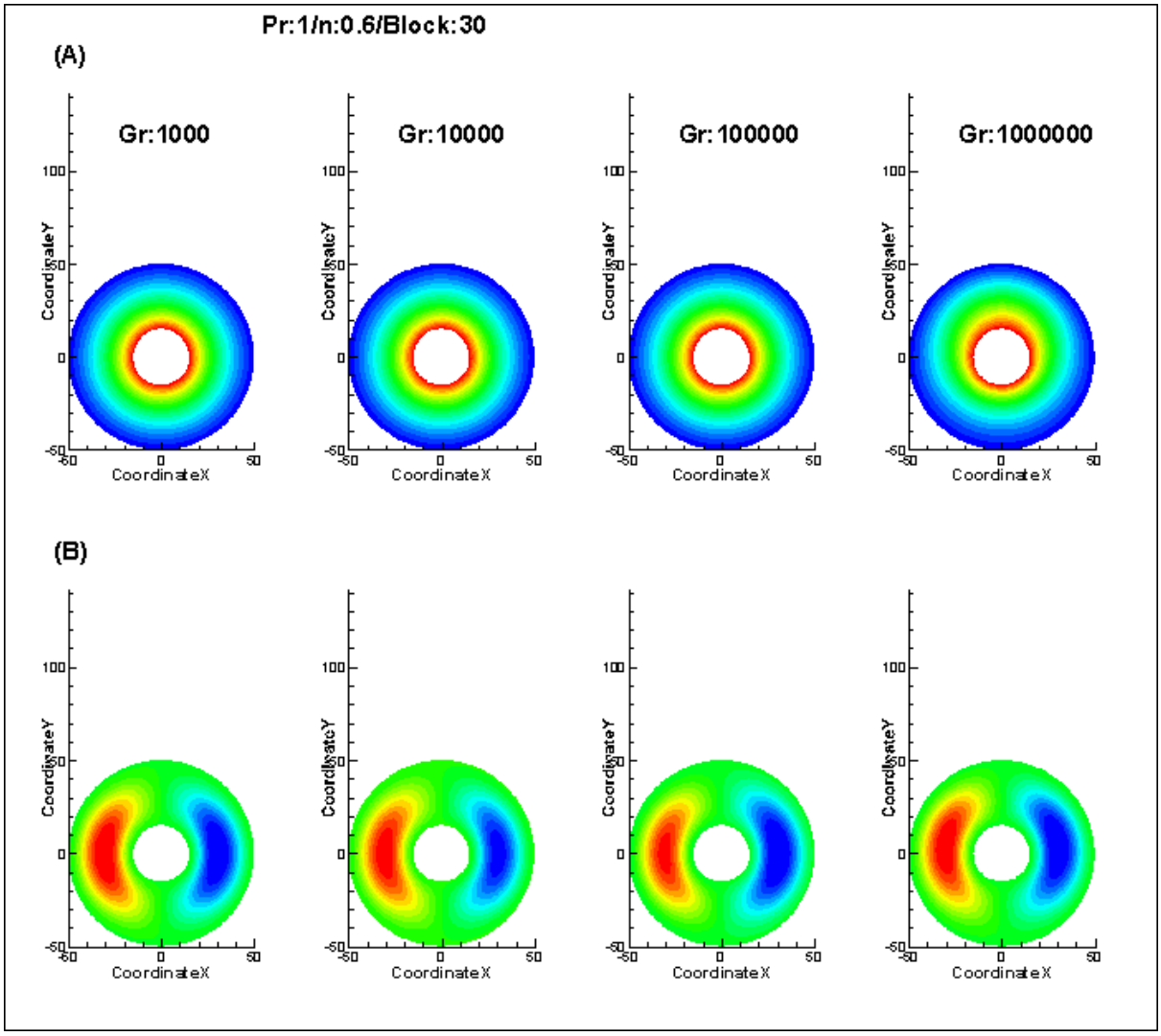

Fig.6.2.39 (A) Temperature profile, (B) Stream Function (Blockage=30%, Pr=1/0.6)

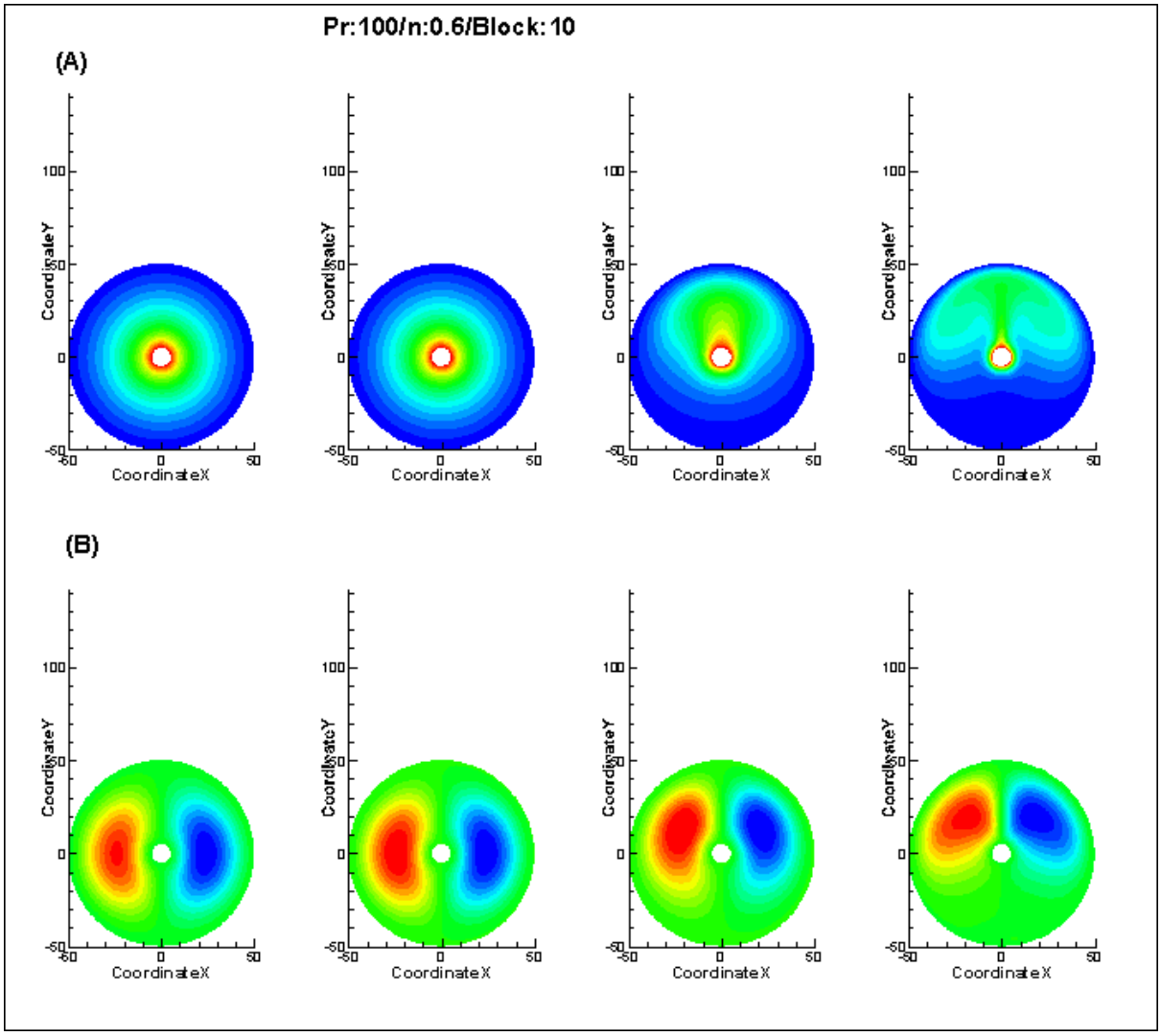

Fig.6.2.40 (A) Temperature profile, (B) Stream Function (Blockage=10%, Pr=100/0.6)

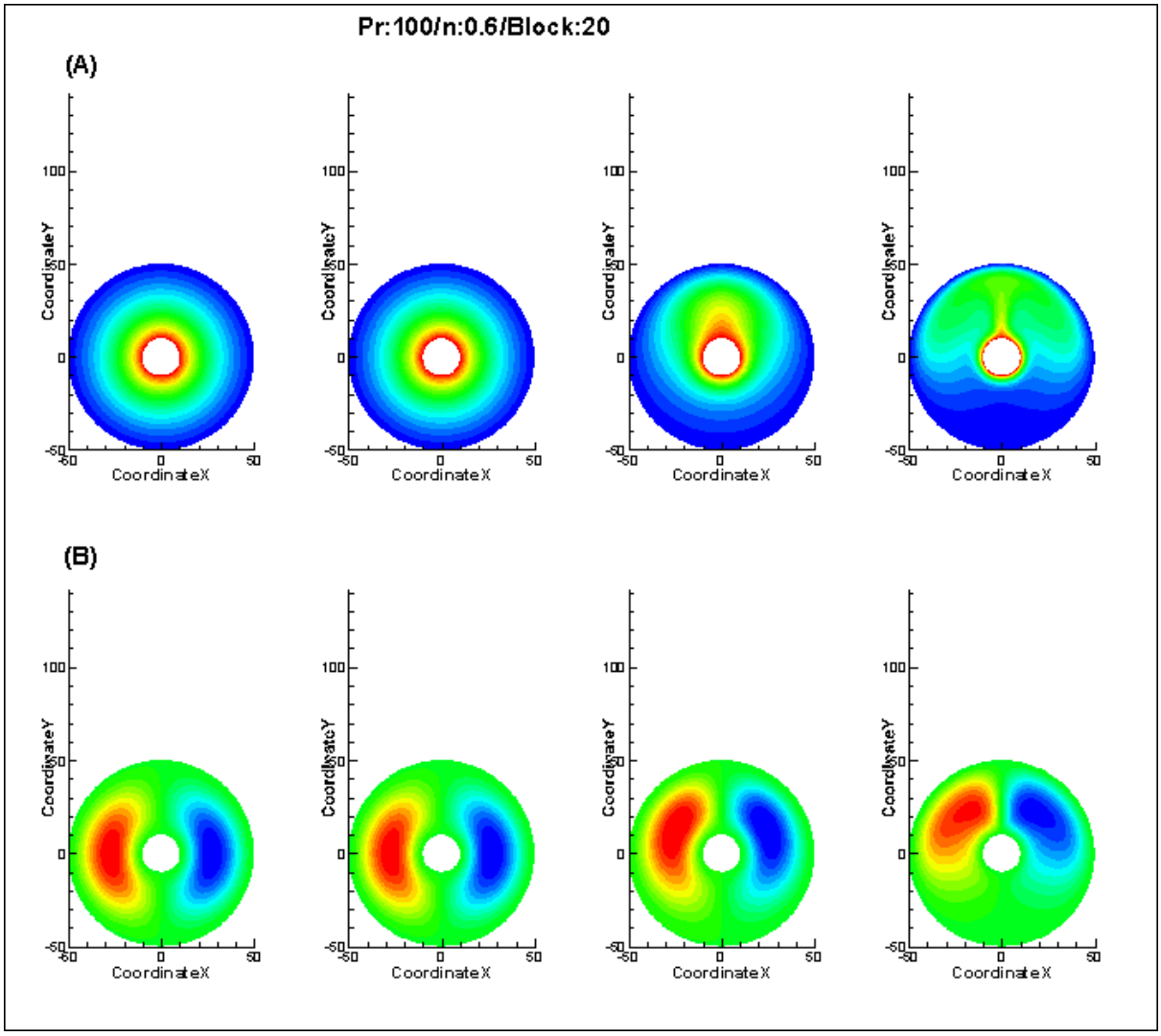

Fig.6.2.41 (A) Temperature profile, (B) Stream Function (Blockage=20%, Pr=100/0.6)

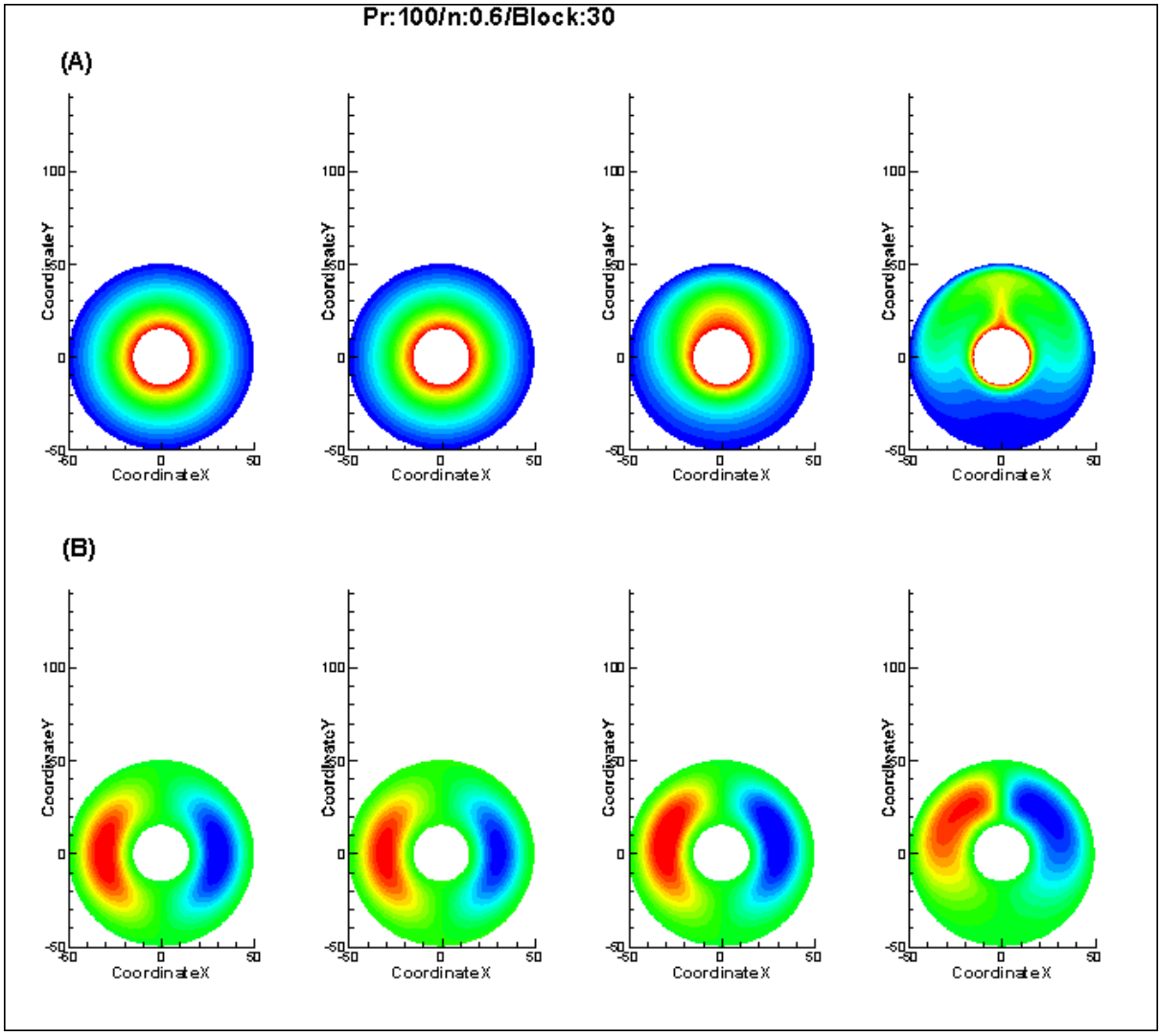

Fig.6.2.42 (A) Temperature profile, (B) Stream Function (Blockage=30%, Pr=100/0.6)

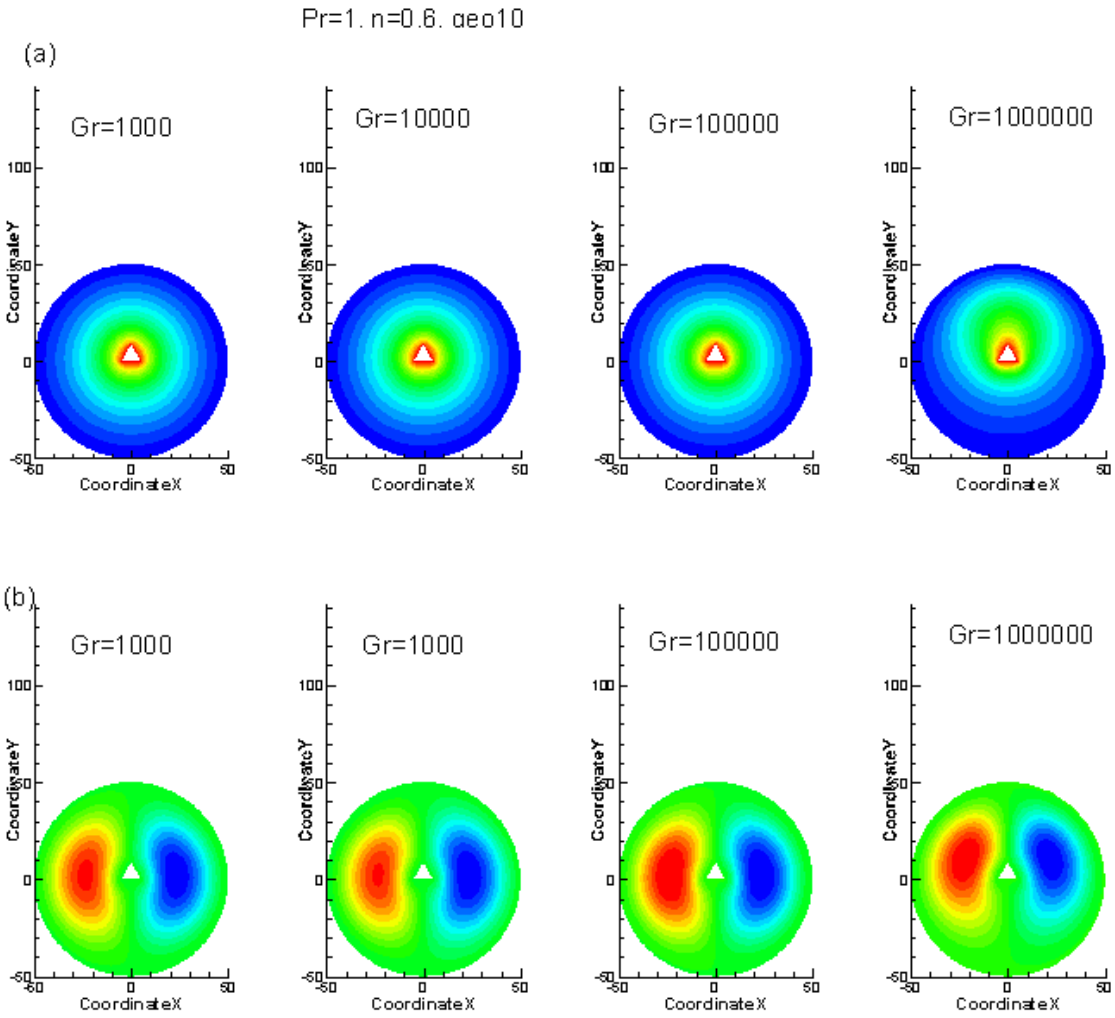

Fig.6.2.43 (A) Temperature profile, (B) Stream Function (Blockage=10%, Pr=1/0.6)

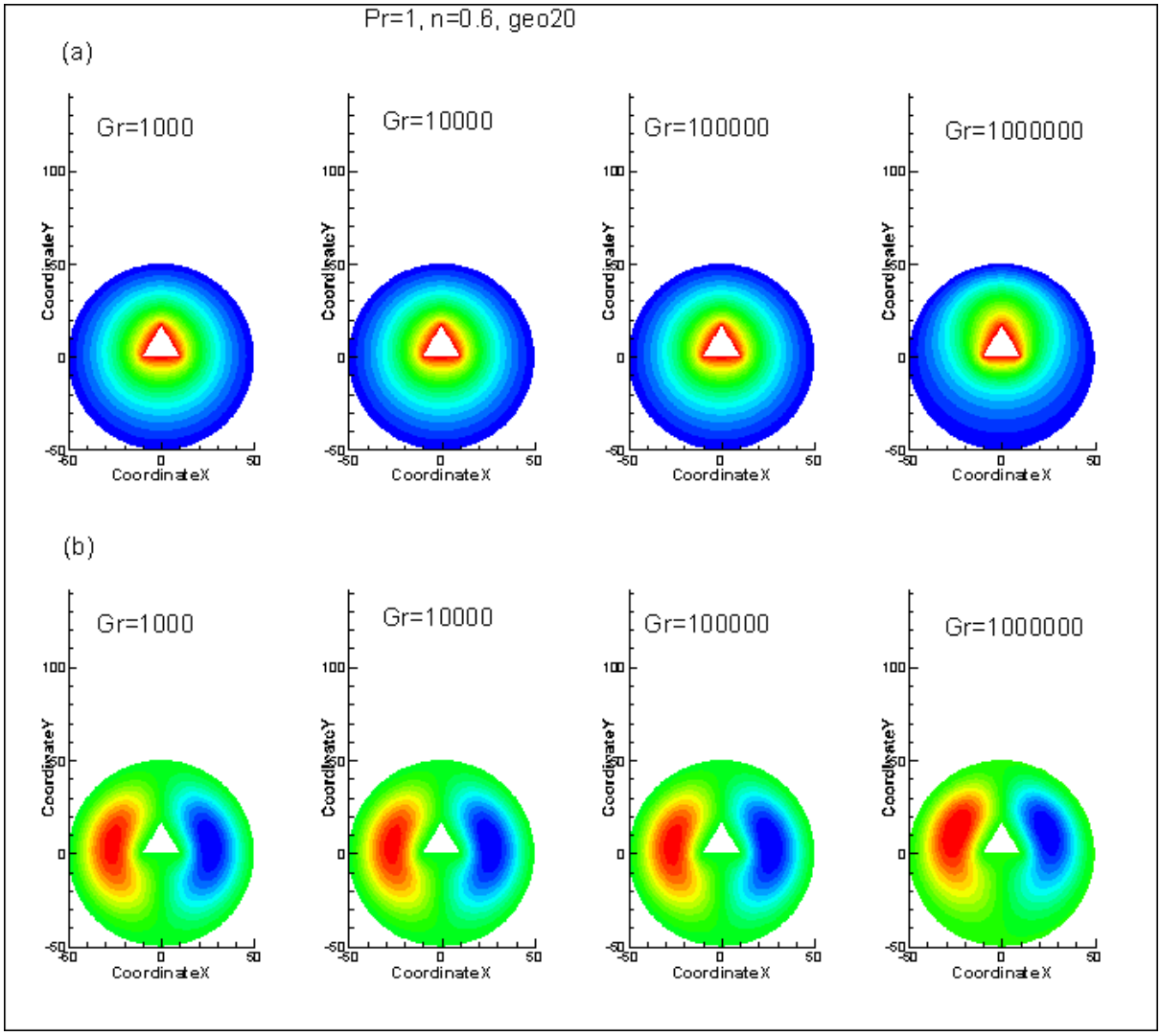

Fig.6.2.44 (A) Temperature profile, (B) Stream Function (Blockage=20%, Pr=1/0.6)

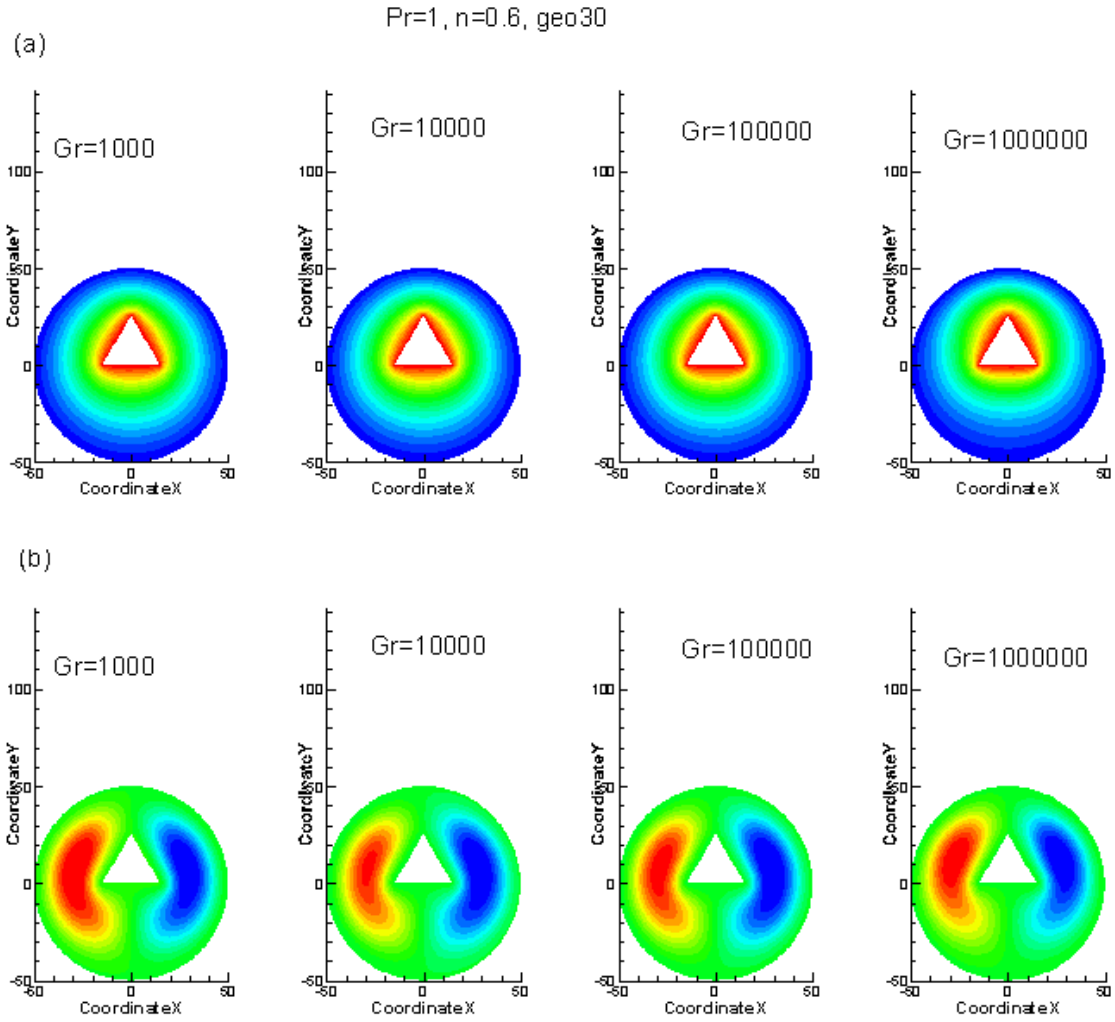

Fig.6.2.45 (A) Temperature profile, (B) Stream Function (Blockage=30%, Pr=1/0.6)

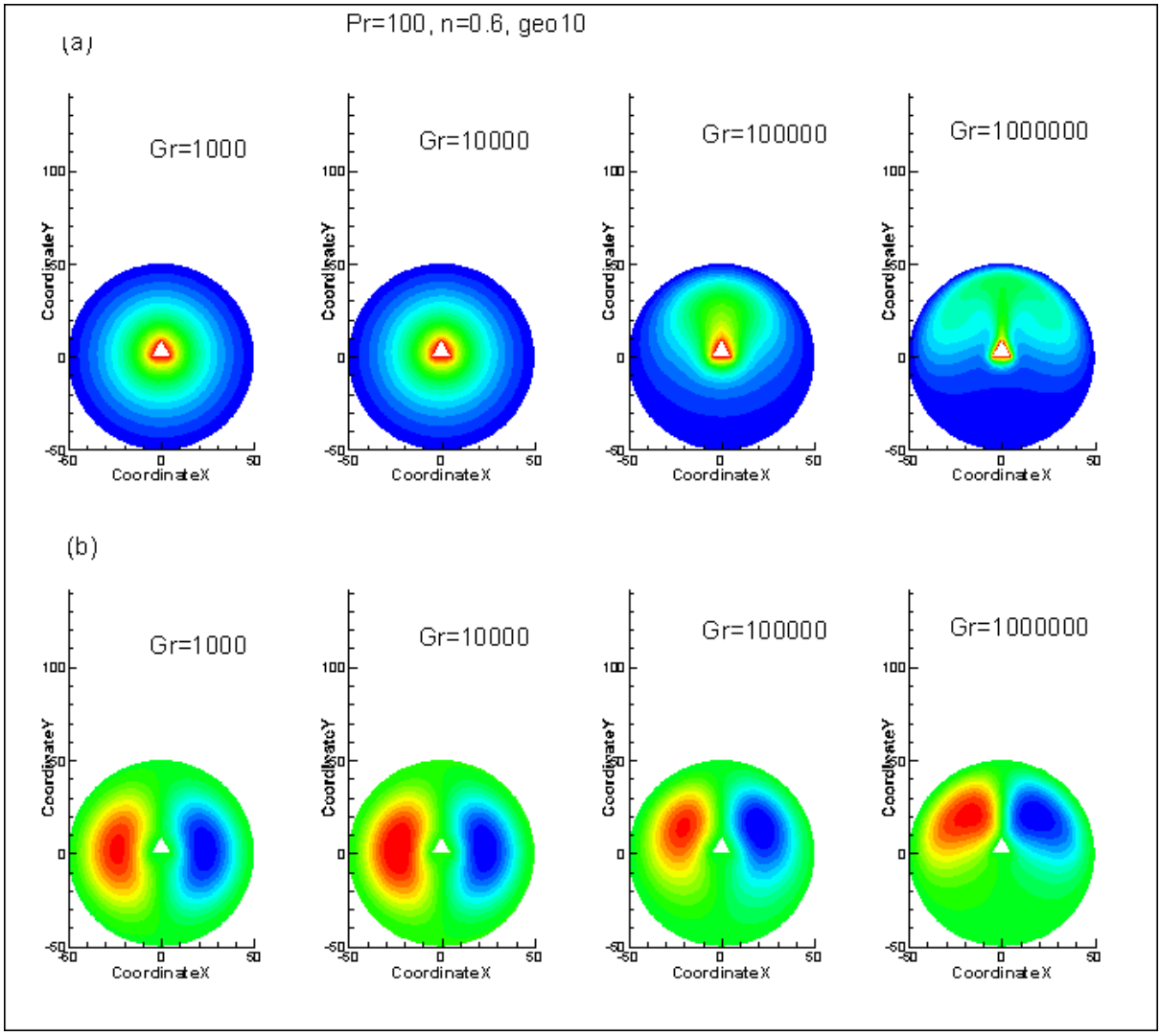

Fig.6.2.46 (A) Temperature profile, (B) Stream Function (Blockage=10%, Pr=100/0.6)

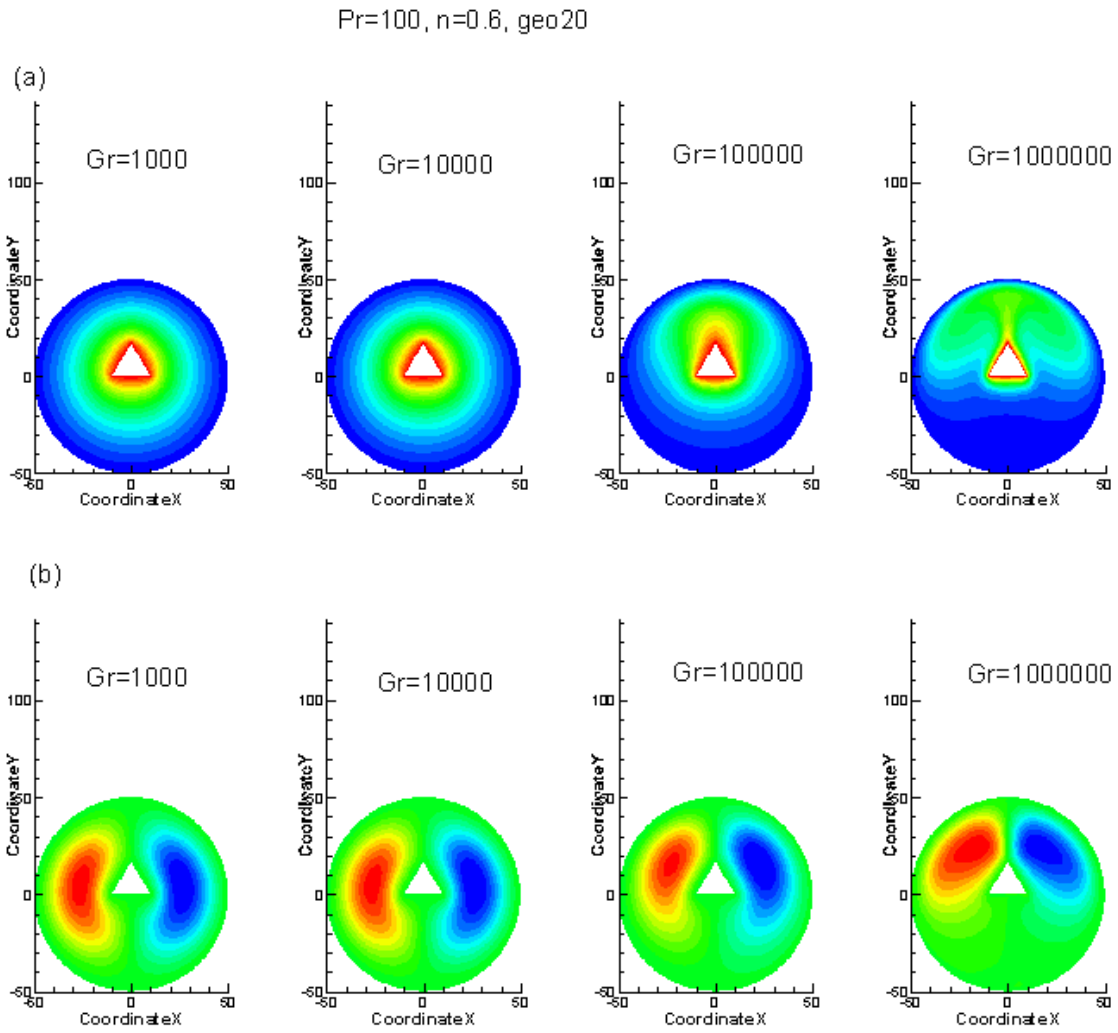

Fig.6.2.47 (A) Temperature profile, (B) Stream Function (Blockage=20%, Pr=100/0.6)

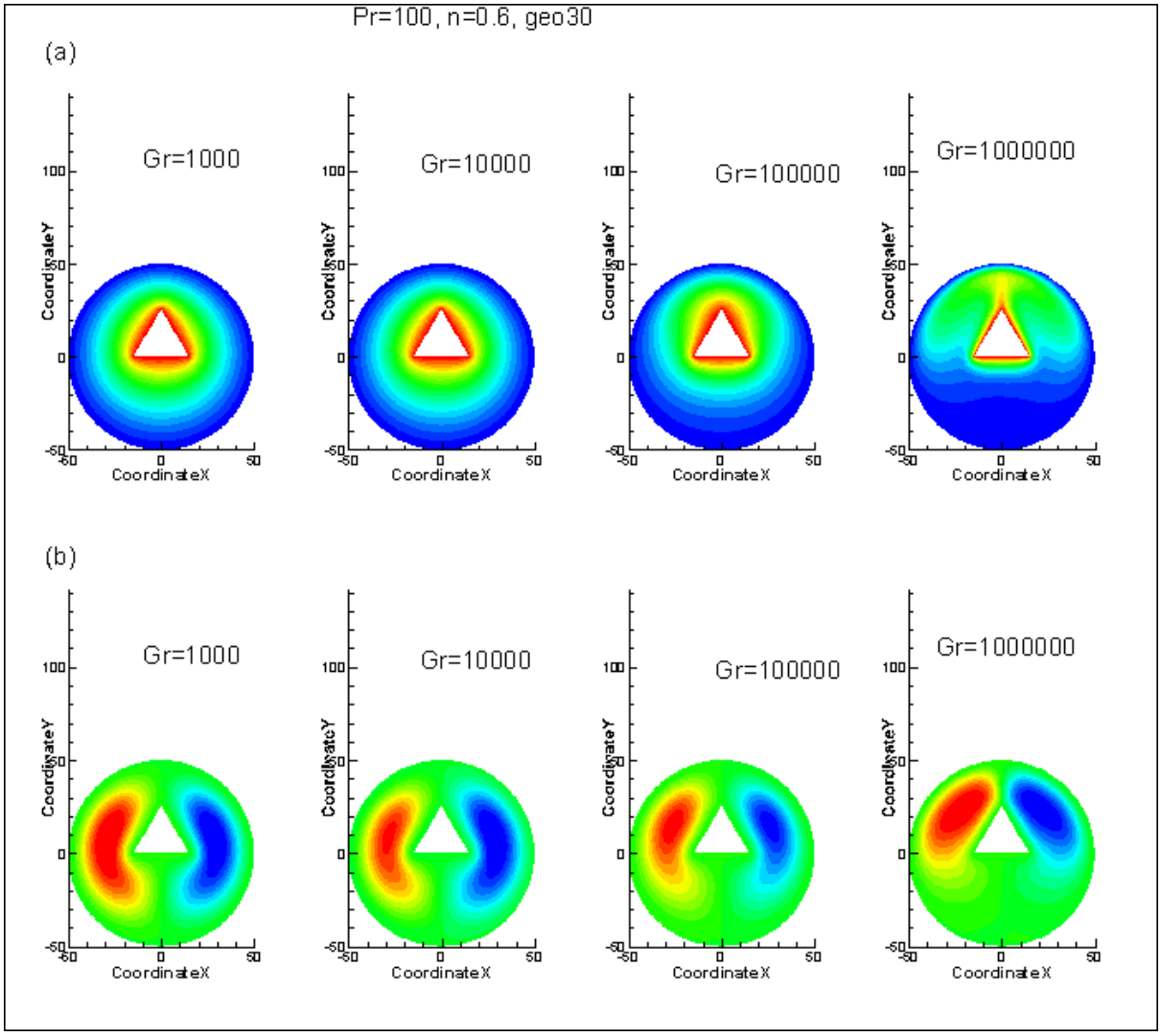

Fig.6.2.48 (A) Temperature profile, (B) Stream Function (Blockage=30%, Pr=100/0.6)

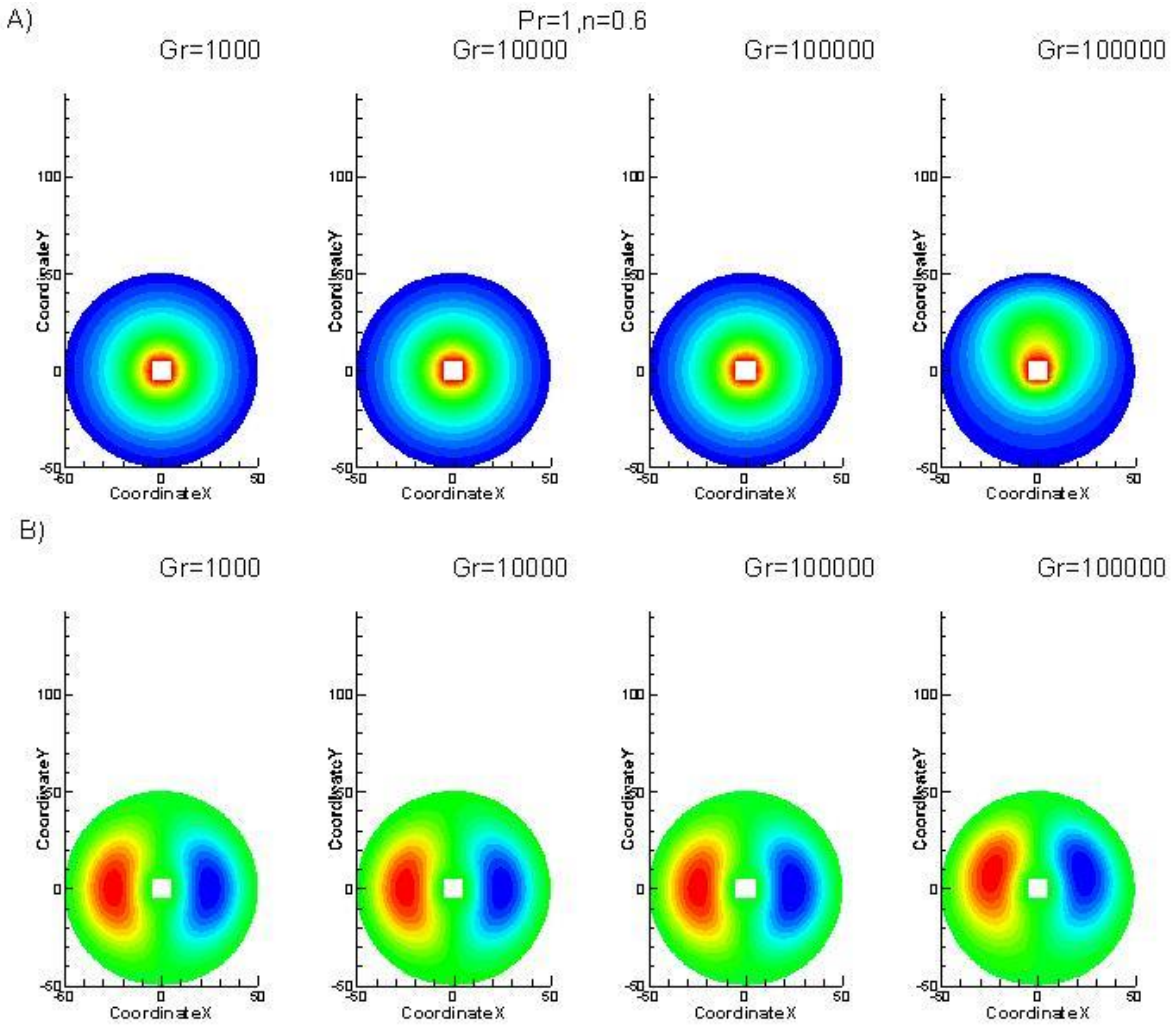

Fig.6.2.49 (A) Temperature profile, (B) Stream Function (Blockage=10%, Pr=1/0.6)

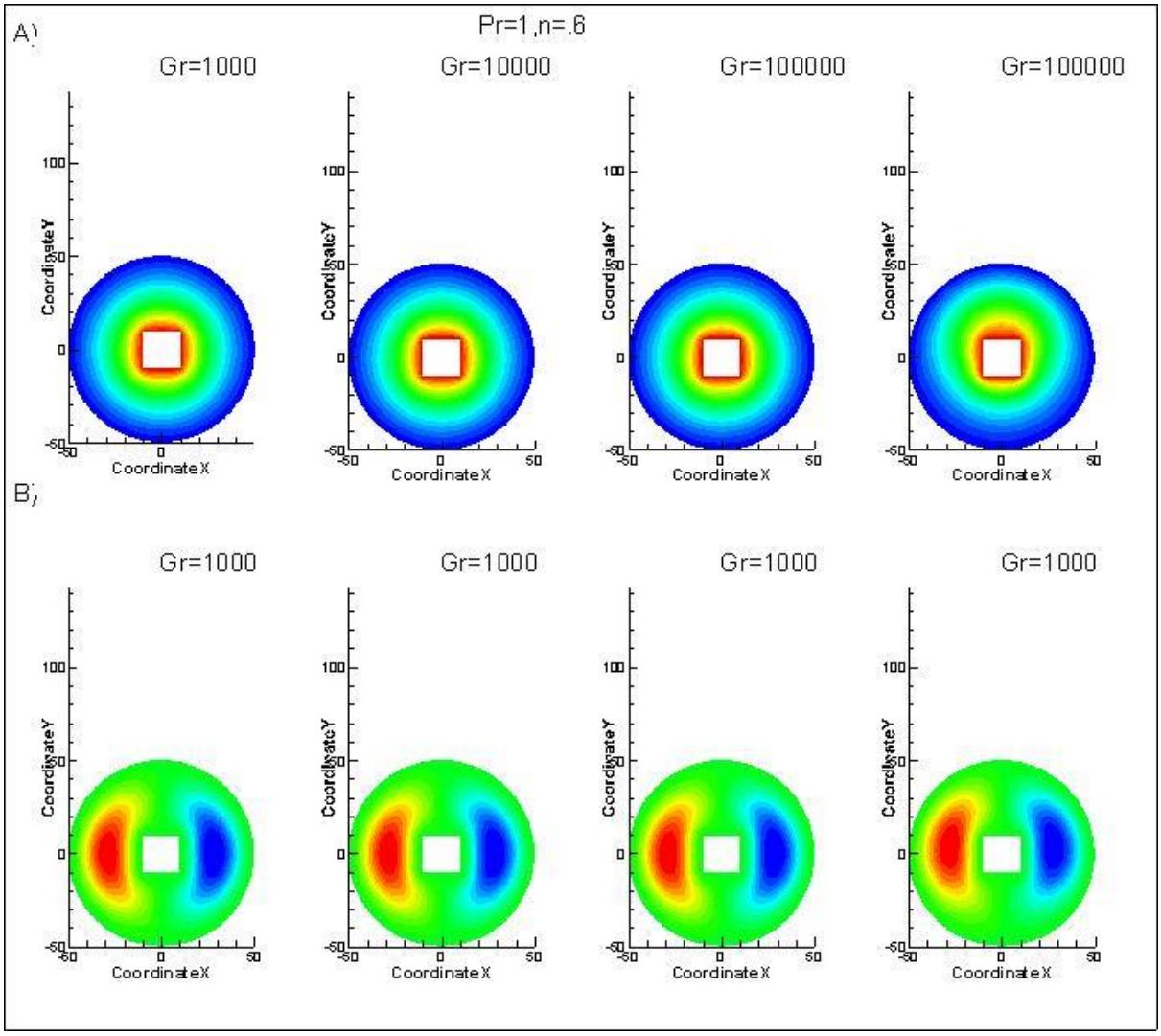

Fig.6.2.50 (A) Temperature profile, (B) Stream Function (Blockage=20%, Pr=1/0.6)

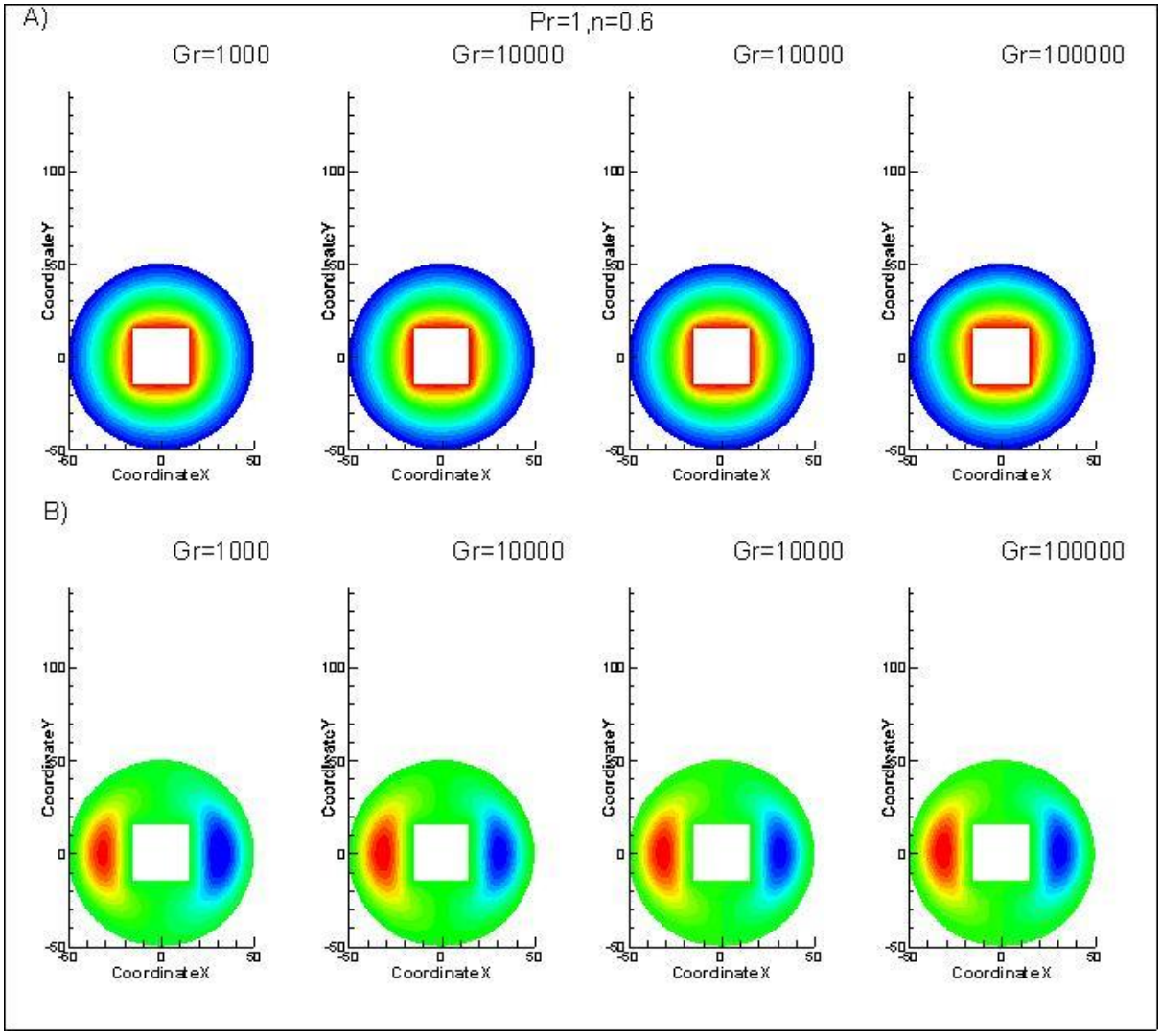

Fig.6.2.51 (A) Temperature profile, (B) Stream Function (Blockage=30%, Pr=1/0.6)

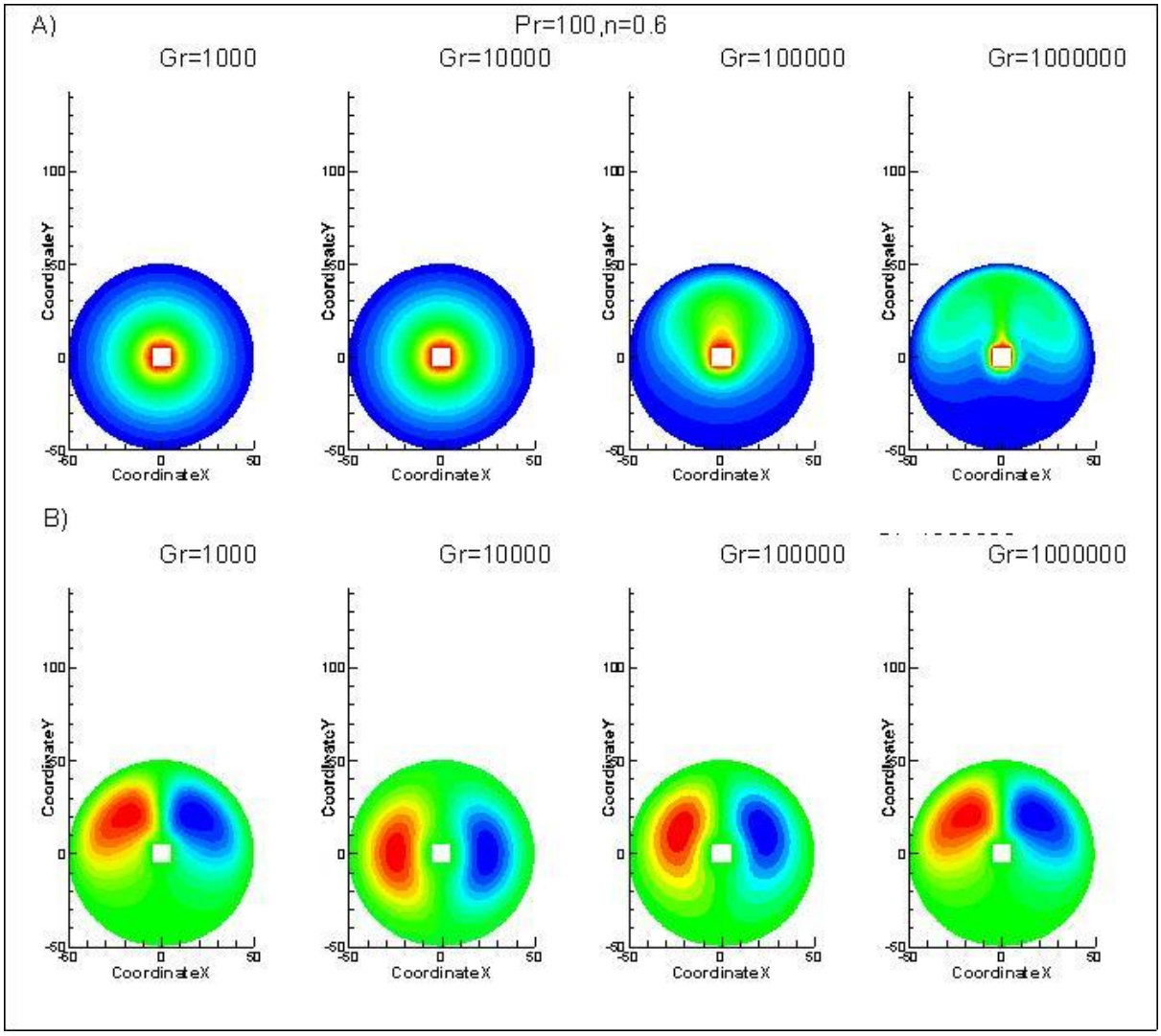

Fig.6.2.52 (A) Temperature profile, (B) Stream Function (Blockage=10%, Pr=100/0.6)

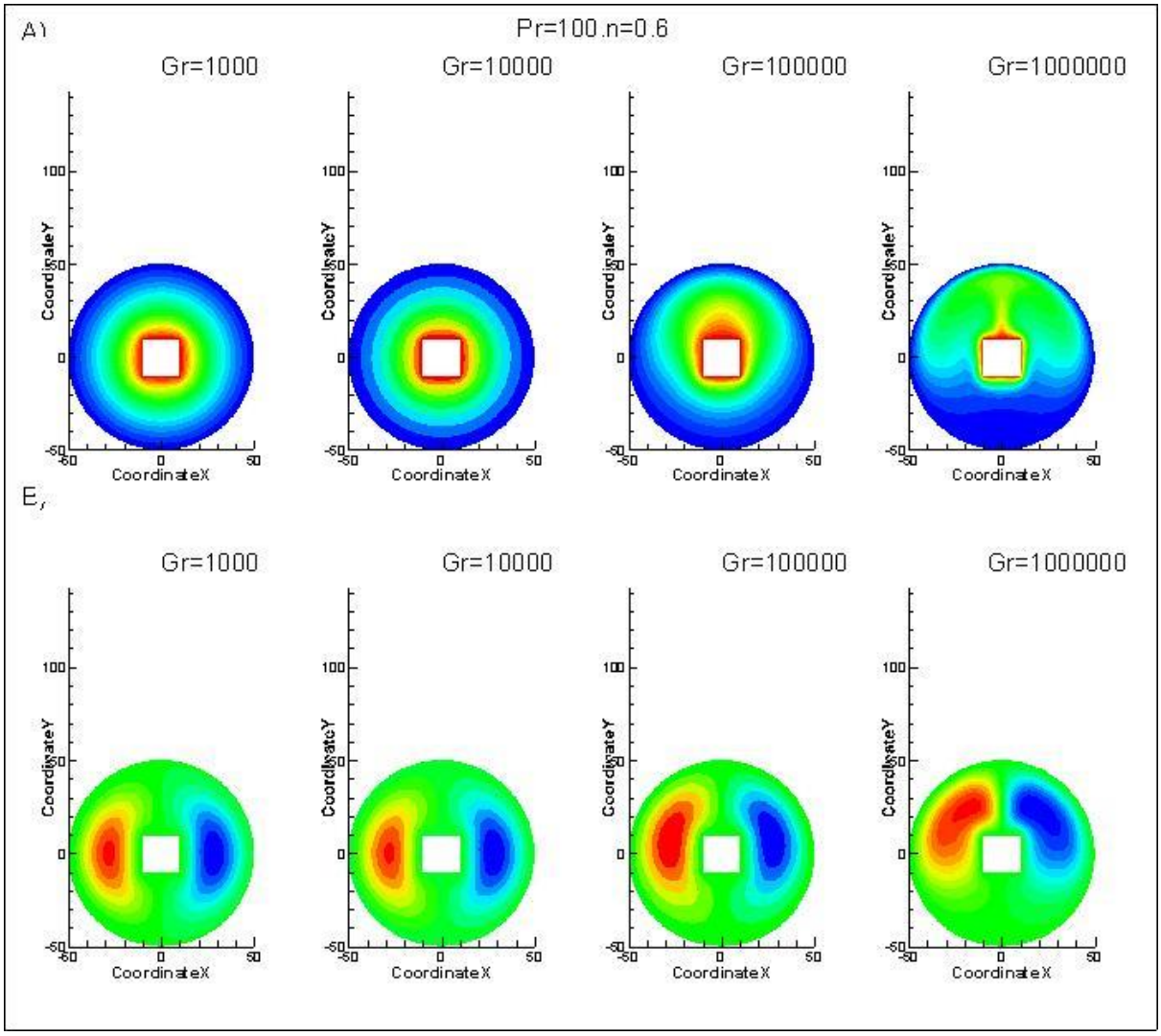

Fig.6.2.53 (A) Temperature profile, (B) Stream Function (Blockage=20%, Pr=100/0.6)

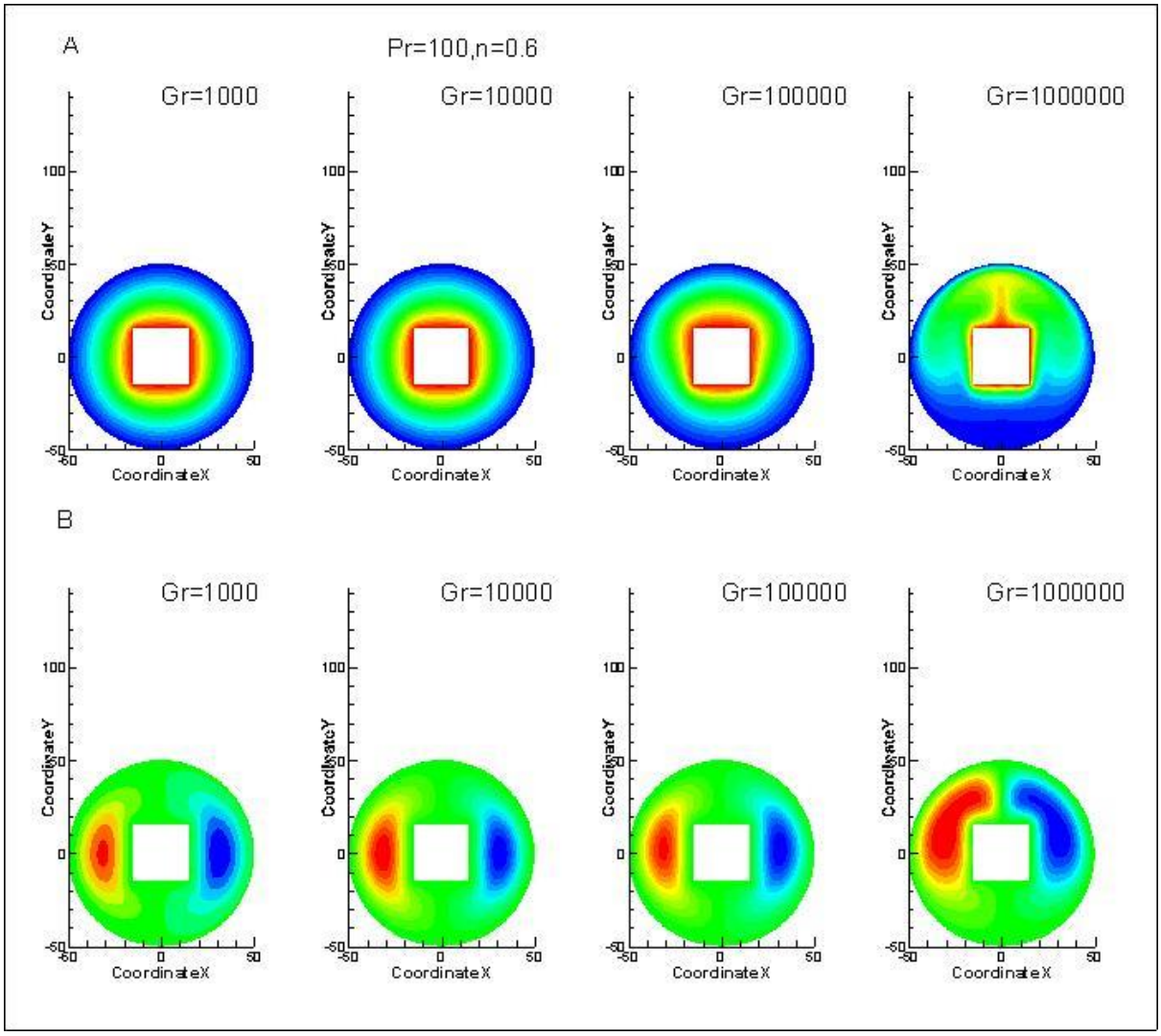

Fig.6.2.54 (A) Temperature profile, (B) Stream Function (Blockage=30%, Pr=100/0.6)

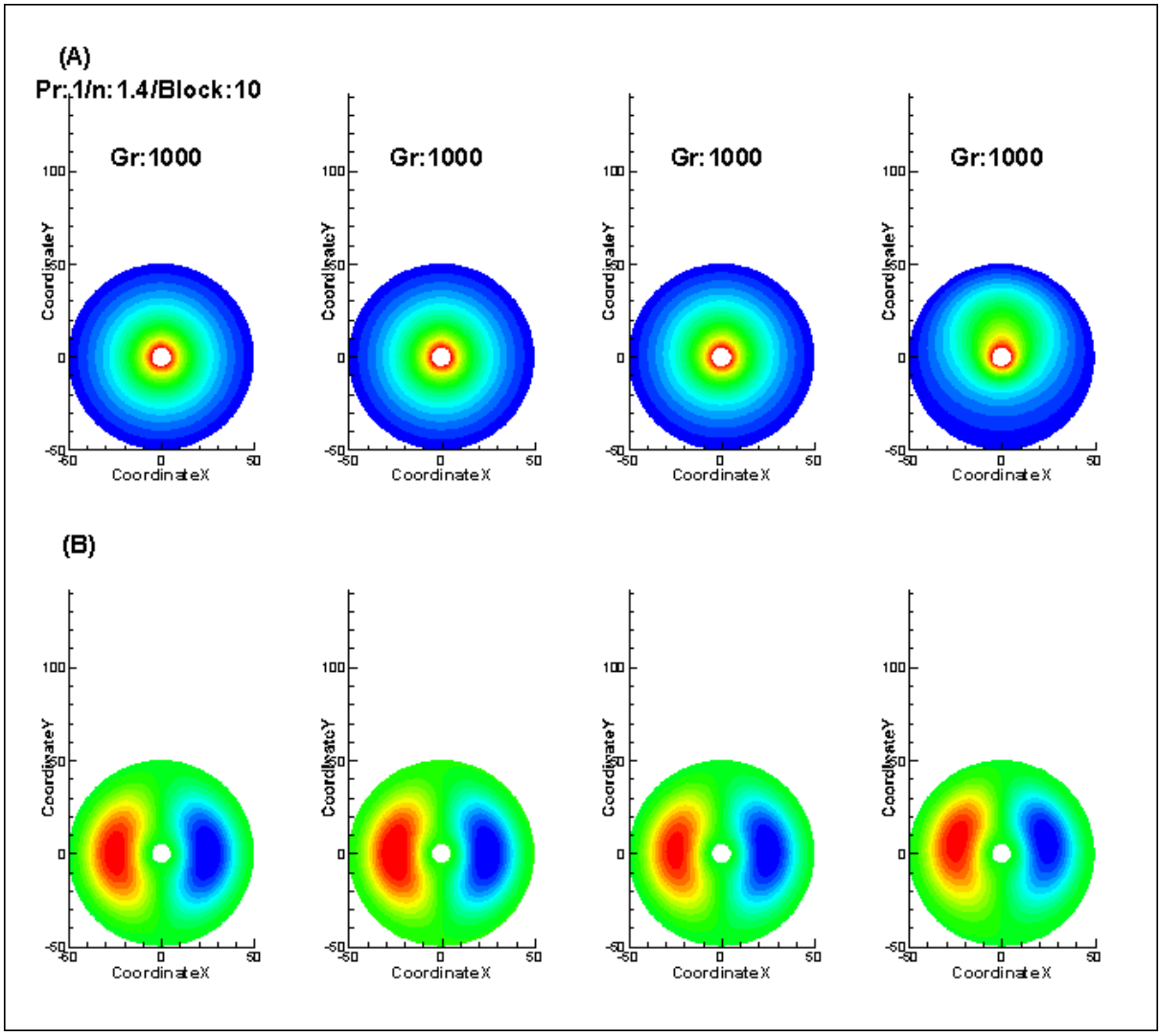

Fig.6.2.55 (A) Temperature profile, (B) Stream Function (Blockage=10%, Pr=1/1.4)

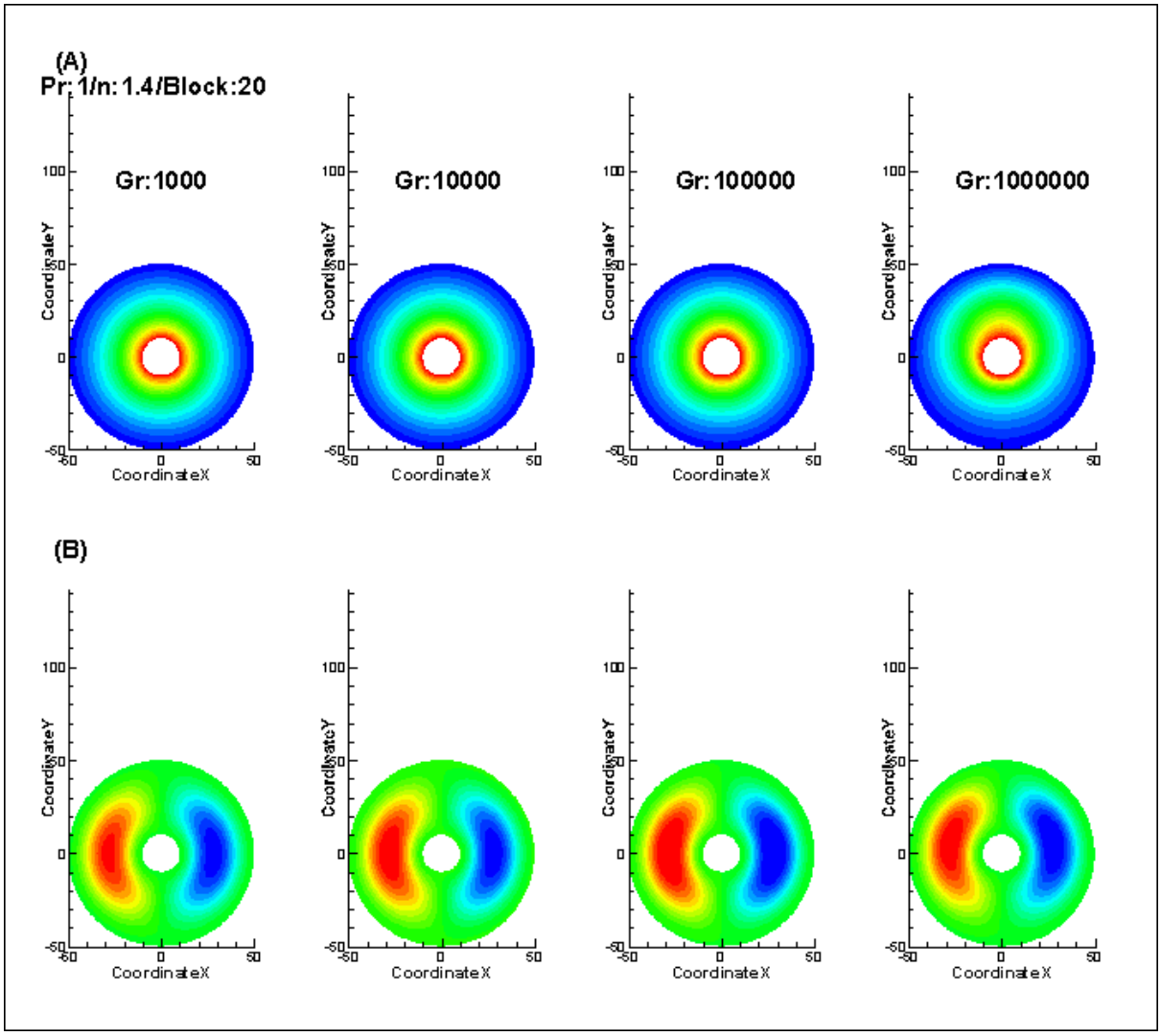

Fig.6.2.56 (A) Temperature profile, (B) Stream Function (Blockage=20%, Pr=1/1.4)

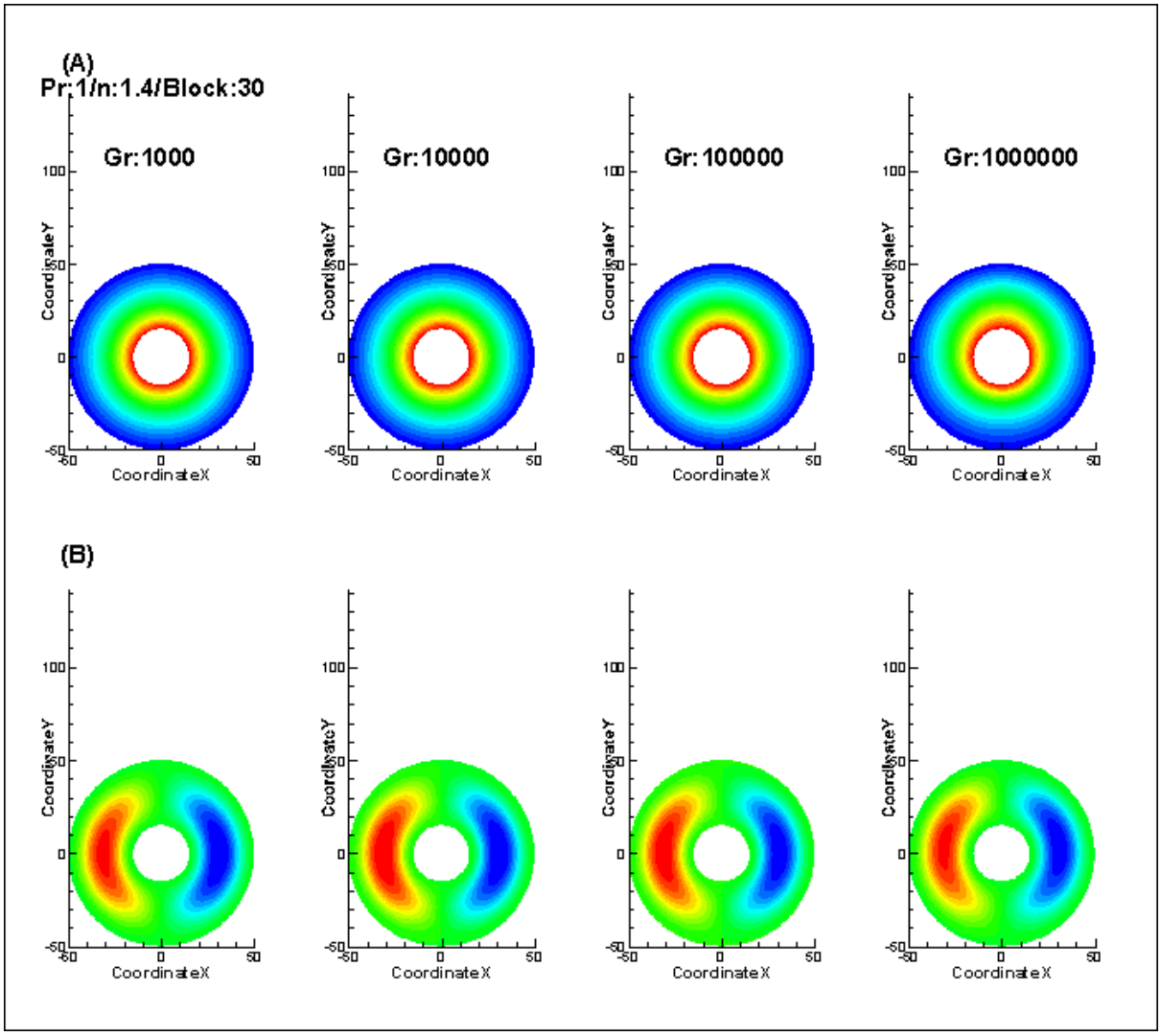

Fig.6.2.57 (A) Temperature profile, (B) Stream Function (Blockage=30%, Pr=1/1.4)

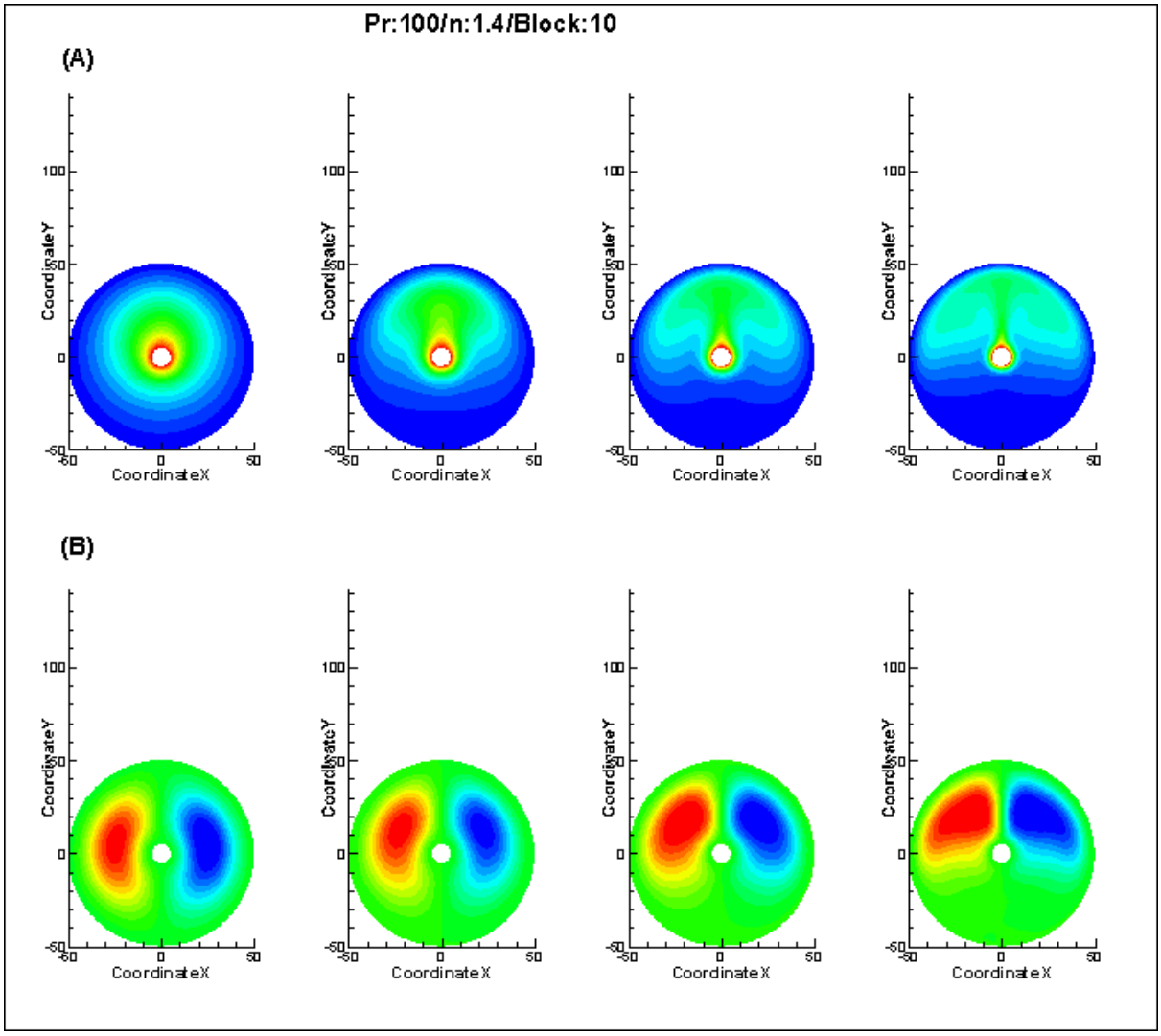

Fig.6.2.58 (A) Temperature profile, (B) Stream Function (Blockage=10%, Pr=100/1.4)

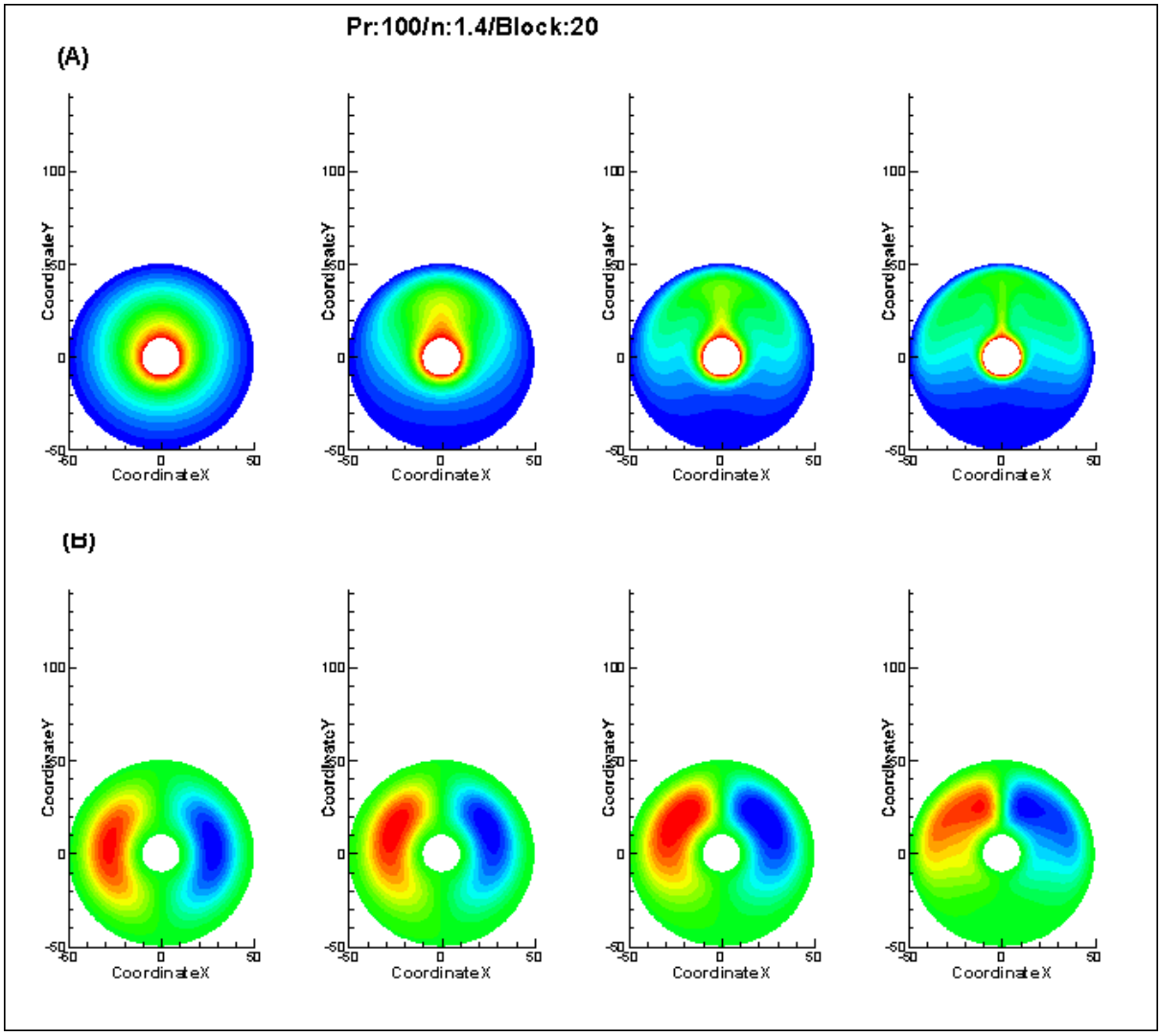

Fig.6.2.59 (A) Temperature profile, (B) Stream Function (Blockage=20%, Pr=100/1.4)

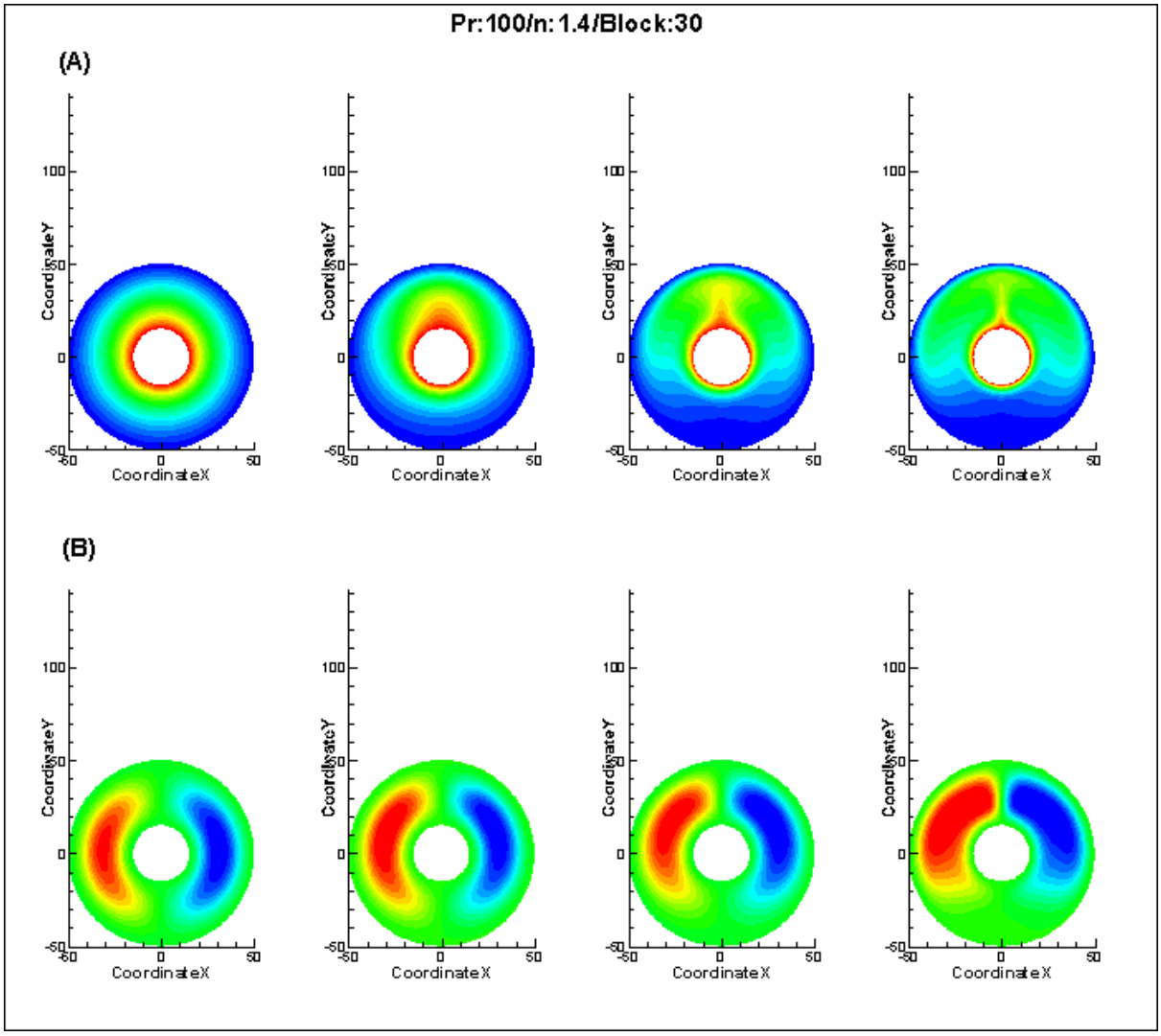

Fig.6.2.60 (A) Temperature profile, (B) Stream Function (Blockage=30%, Pr=100/1.4)

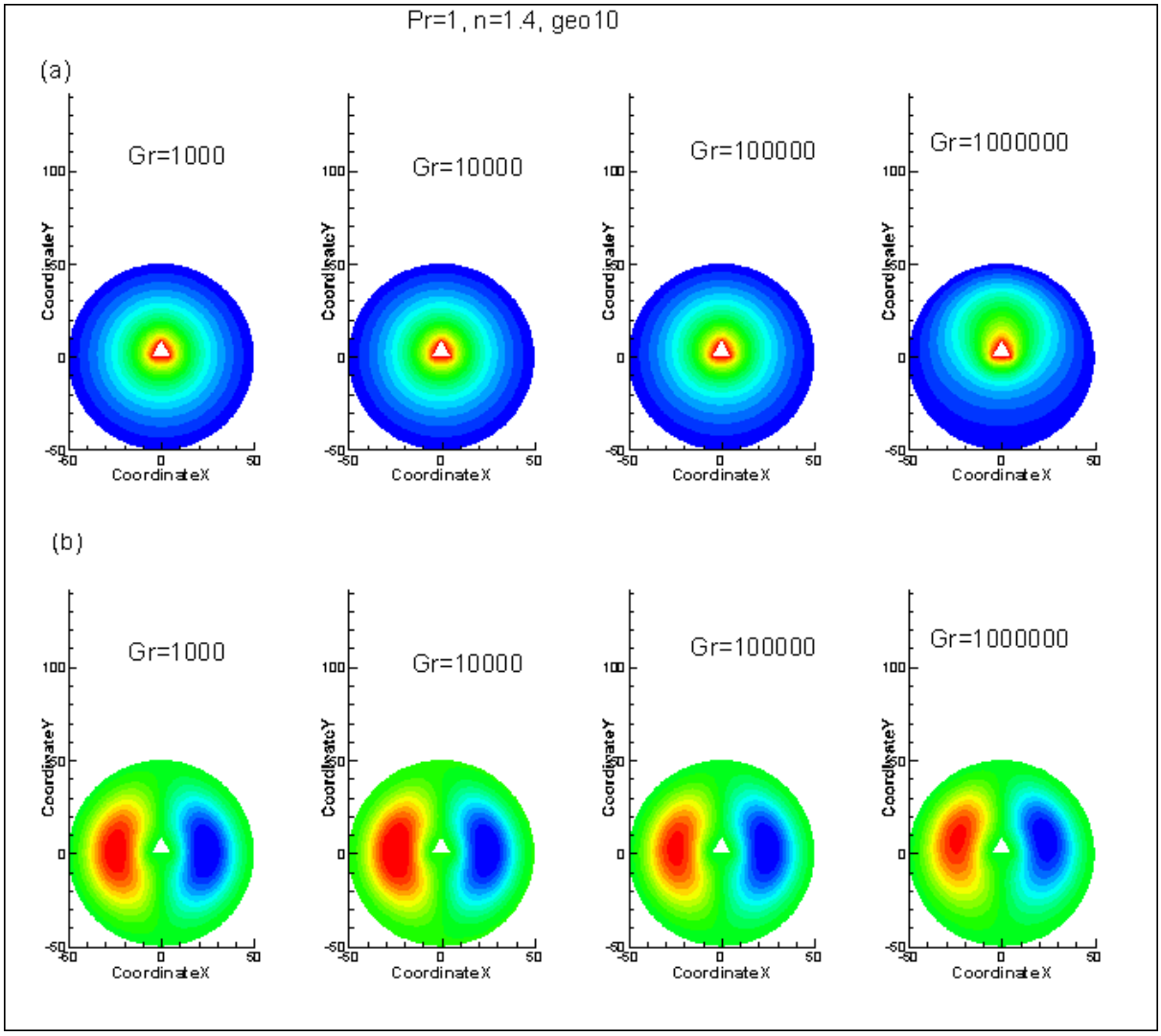

Fig.6.2.61 (A) Temperature profile, (B) Stream Function (Blockage=10%, Pr=1/1.4)

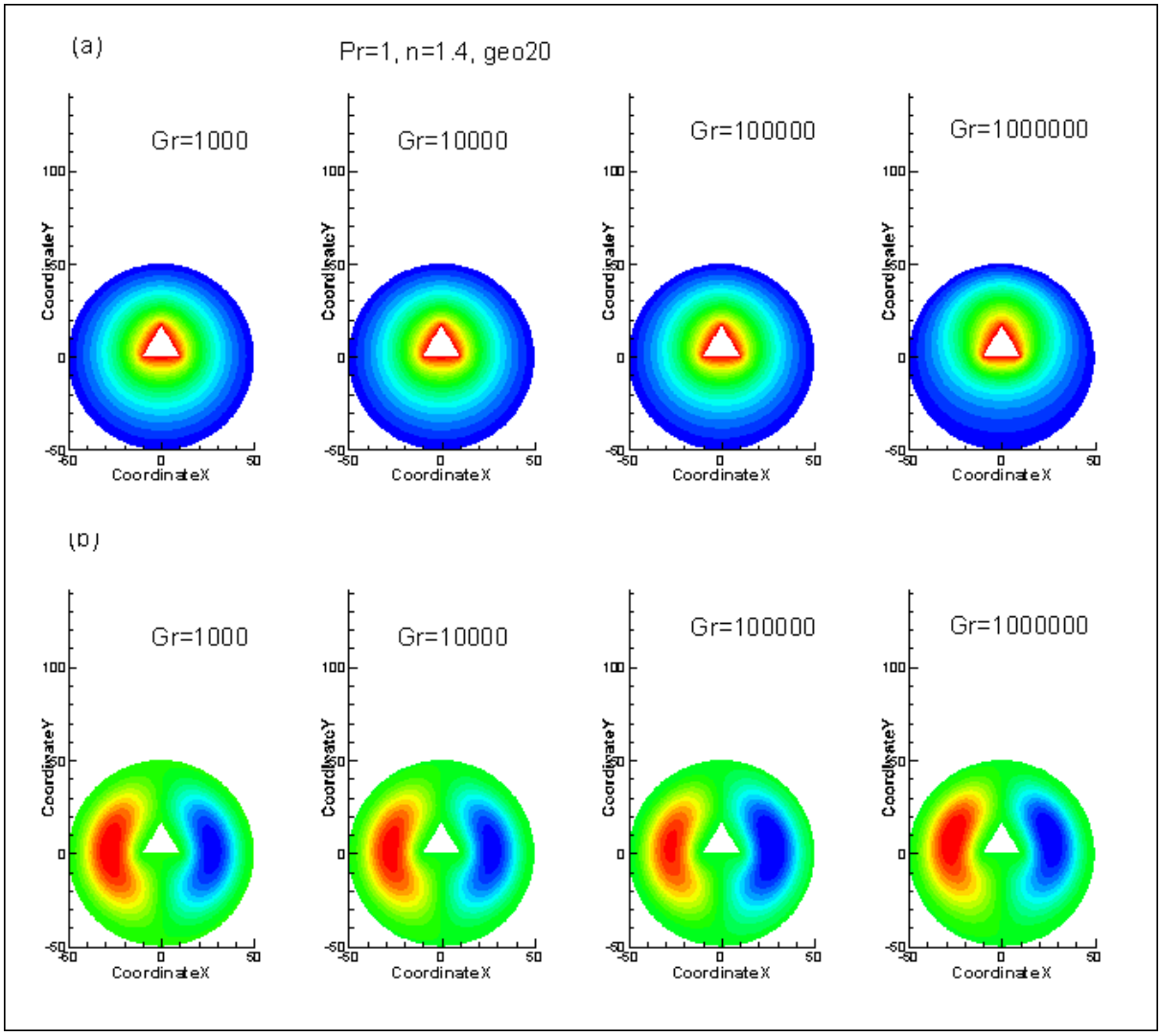

Fig.6.2.62 (A) Temperature profile, (B) Stream Function (Blockage=20%, Pr=1/1.4)

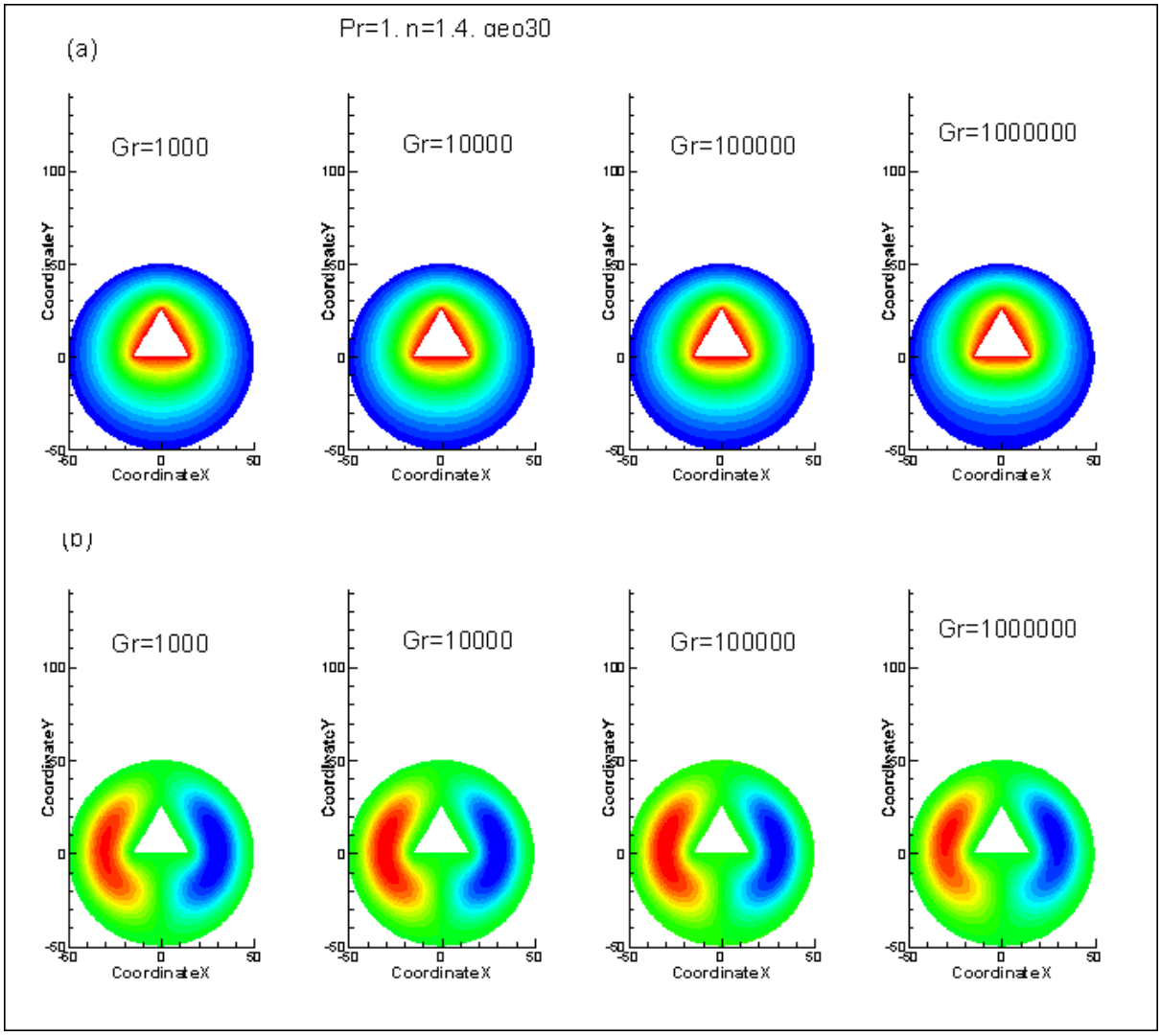

Fig.6.2.63 (A) Temperature profile, (B) Stream Function (Blockage=30%, Pr=1/1.4)

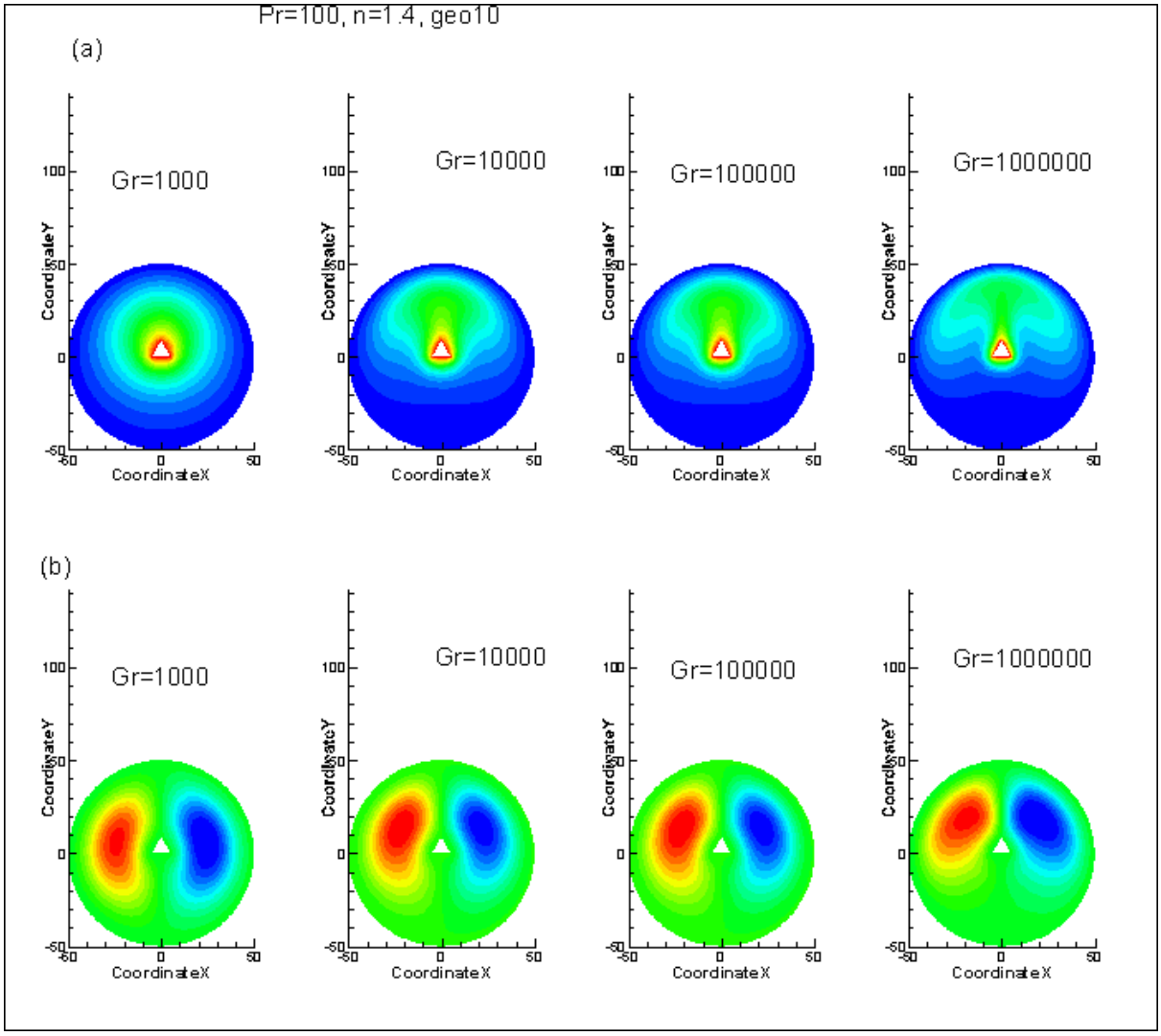

Fig.6.2.64 (A) Temperature profile, (B) Stream Function (Blockage=10%, Pr=100/1.4)

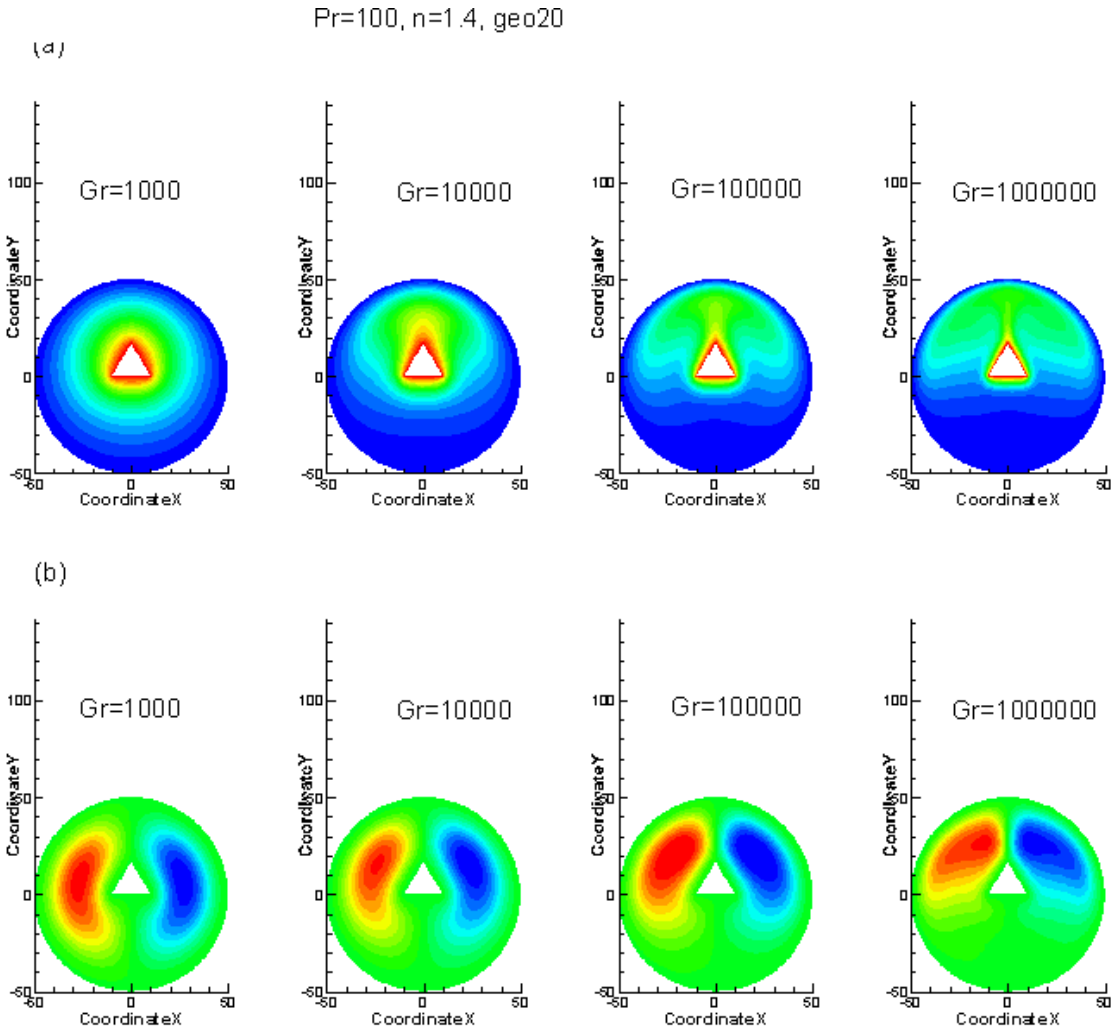

Fig.6.2.65 (A) Temperature profile, (B) Stream Function (Blockage=20%, Pr=100/1.4)

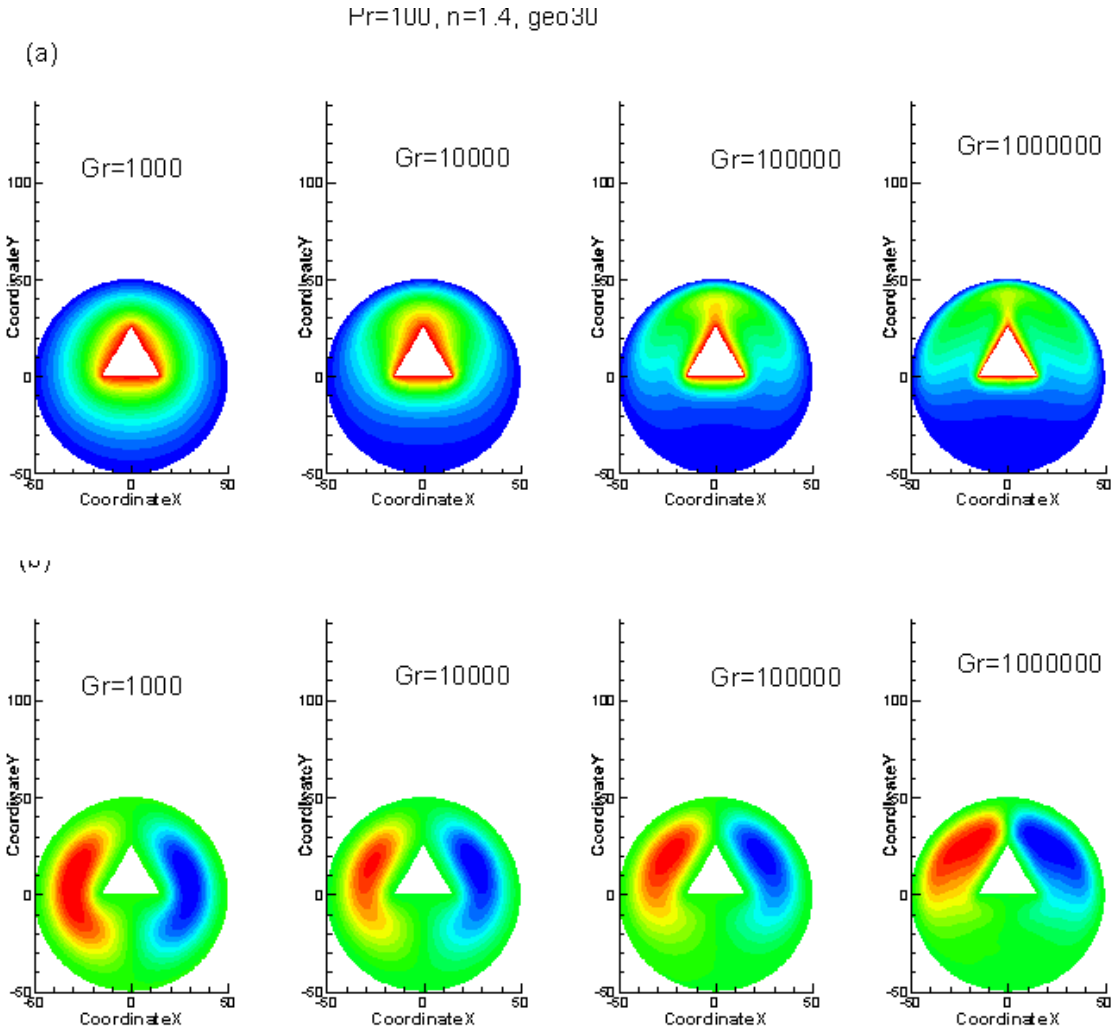

Fig.6.2.66 (A) Temperature profile, (B) Stream Function (Blockage=30%, Pr=100/1.4)

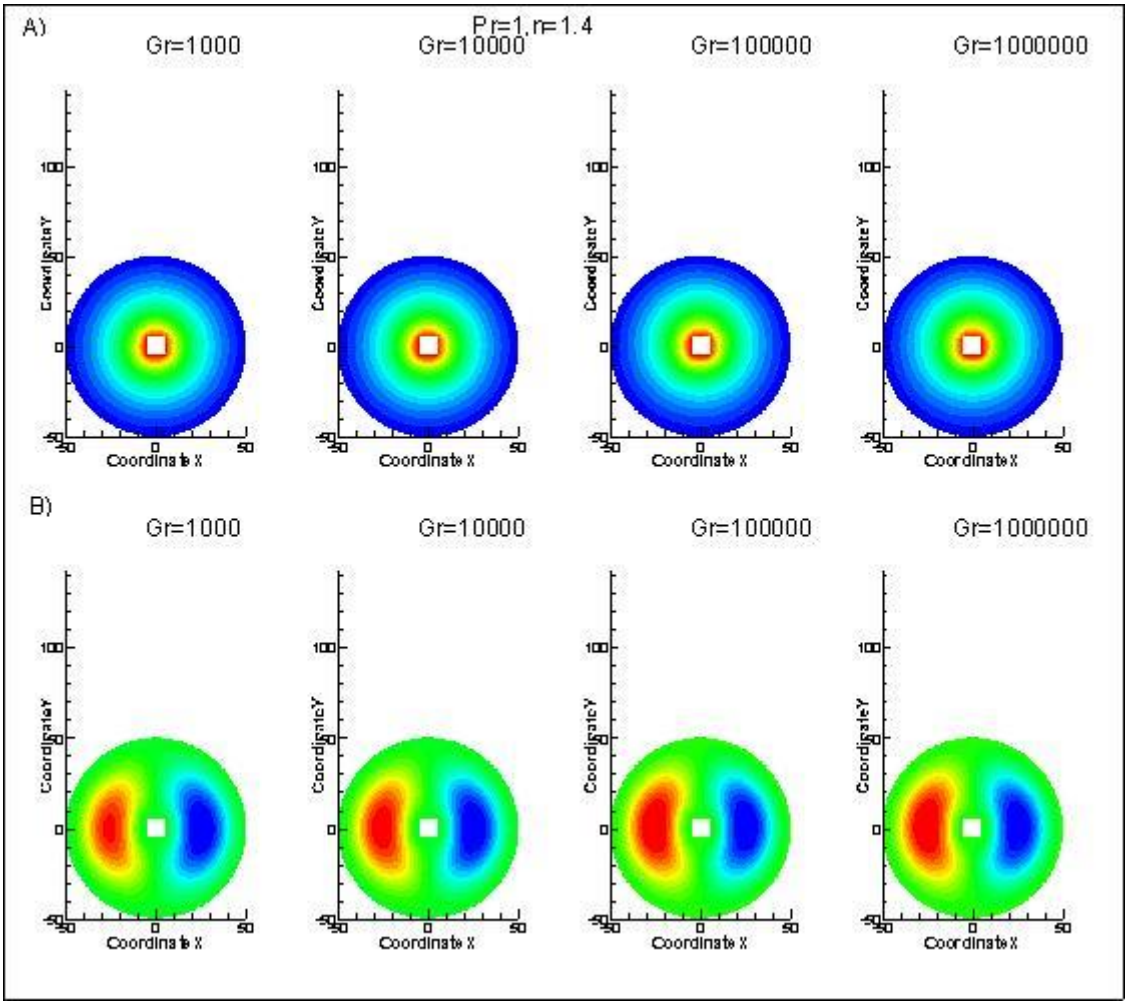

Fig.6.2.67 (A) Temperature profile, (B) Stream Function (Blockage=10%, Pr=1/1.4)

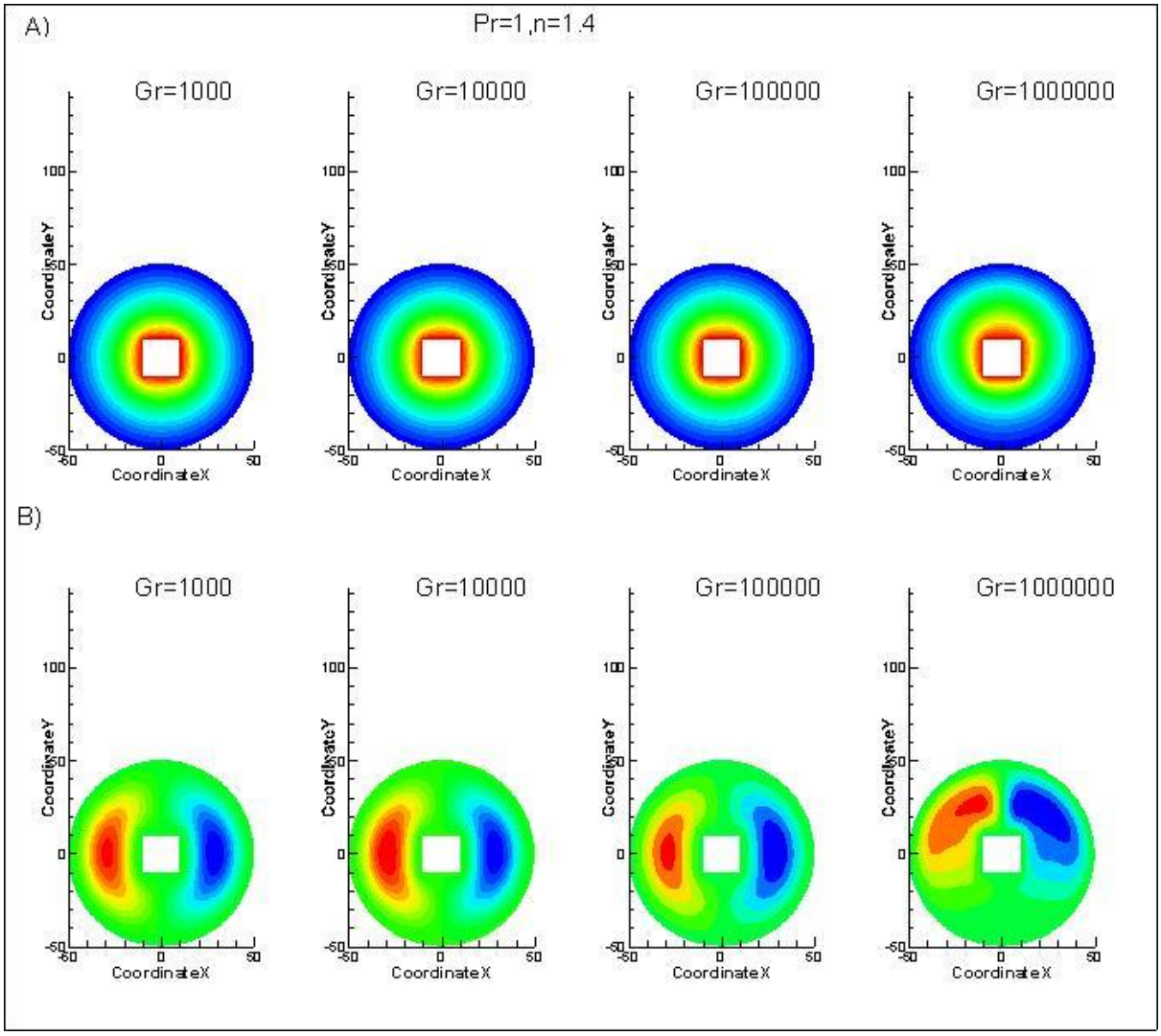

Fig.6.2.68 (A) Temperature profile, (B) Stream Function (Blockage=20%, Pr=1/1.4)

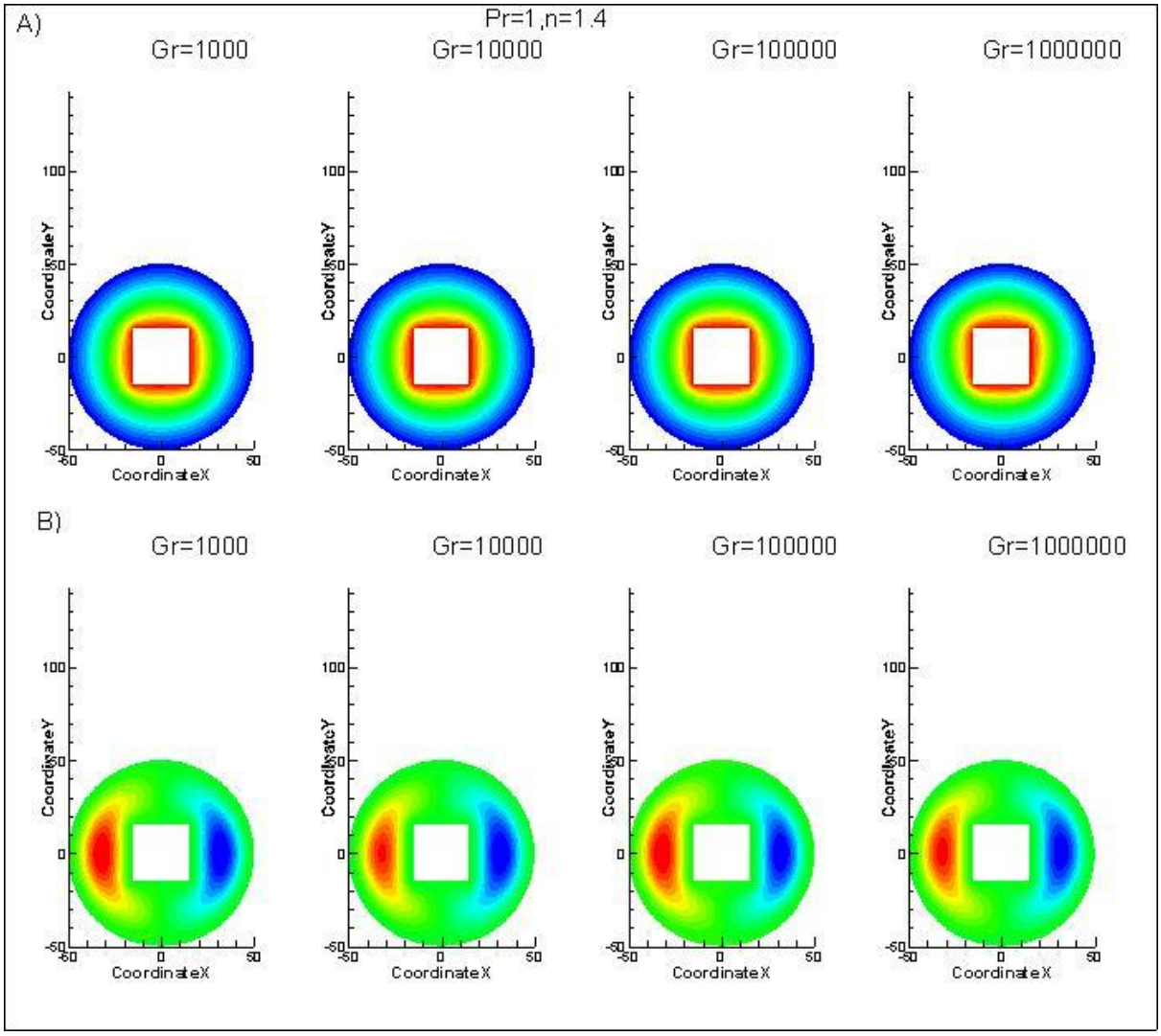

Fig.6.2.69 (A) Temperature profile, (B) Stream Function (Blockage=30%, Pr=1/1.4)

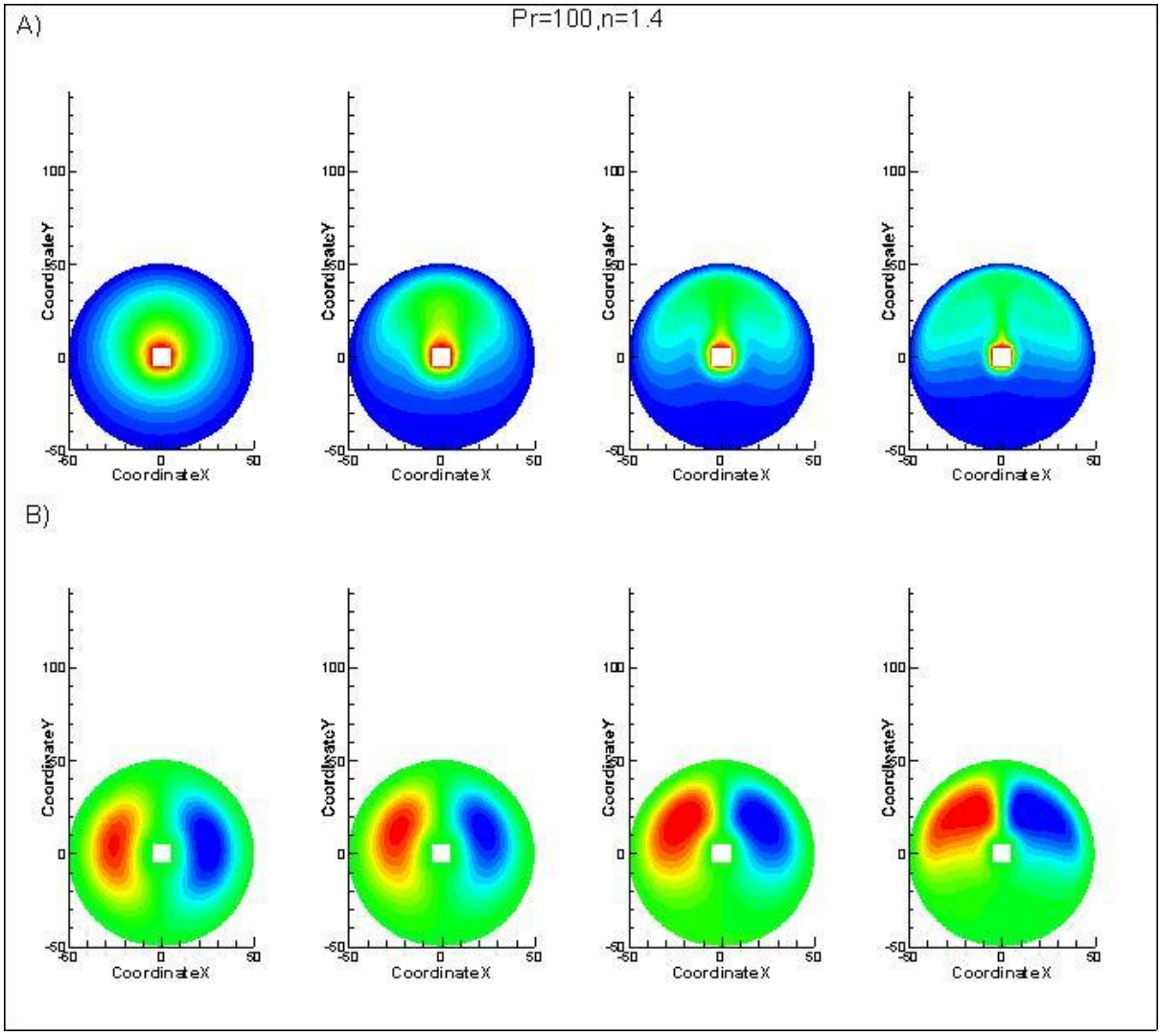

Fig.6.2.70 (A) Temperature profile, (B) Stream Function (Blockage=10%, Pr=100/1.4)

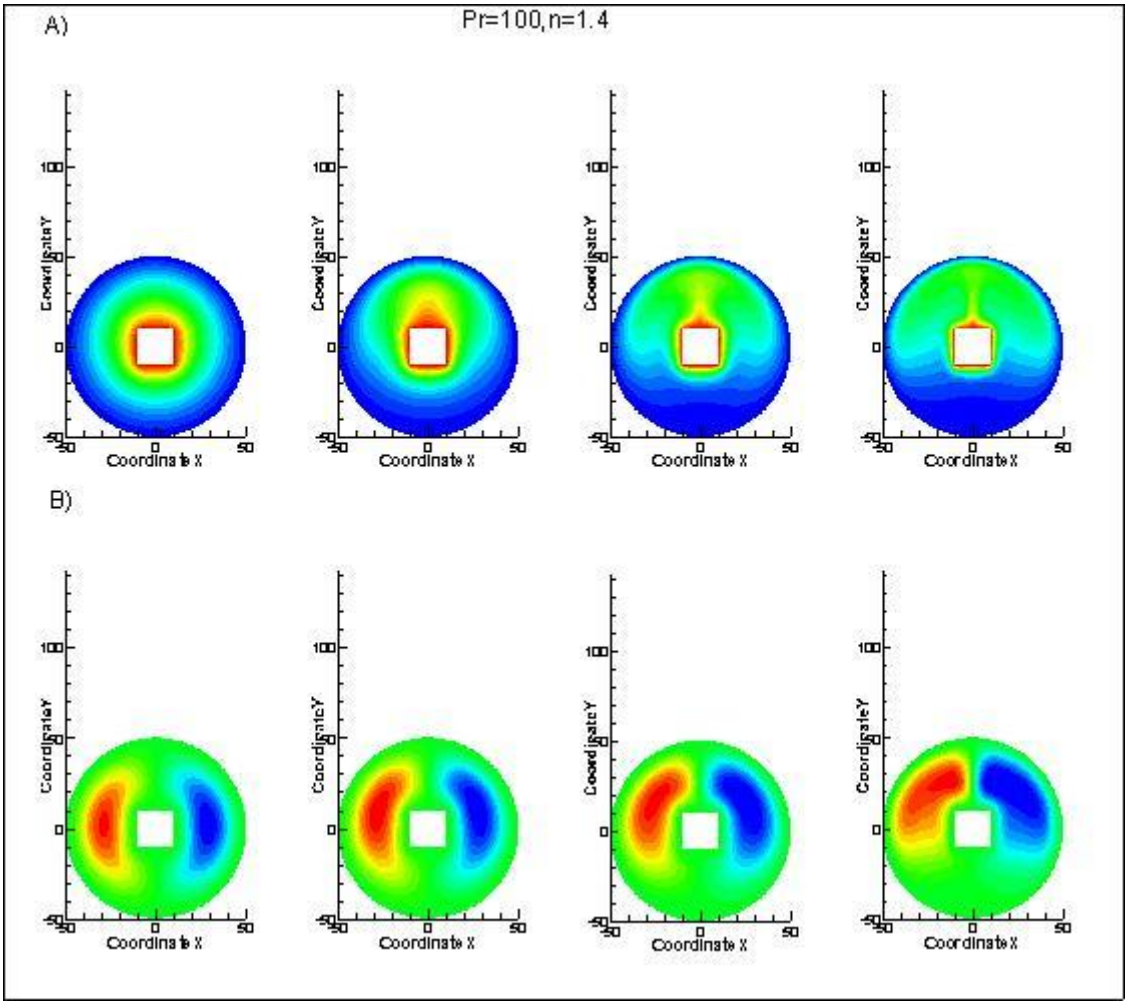

Fig.6.2.71 (A) Temperature profile, (B) Stream Function (Blockage=20%, Pr=100/1.4)

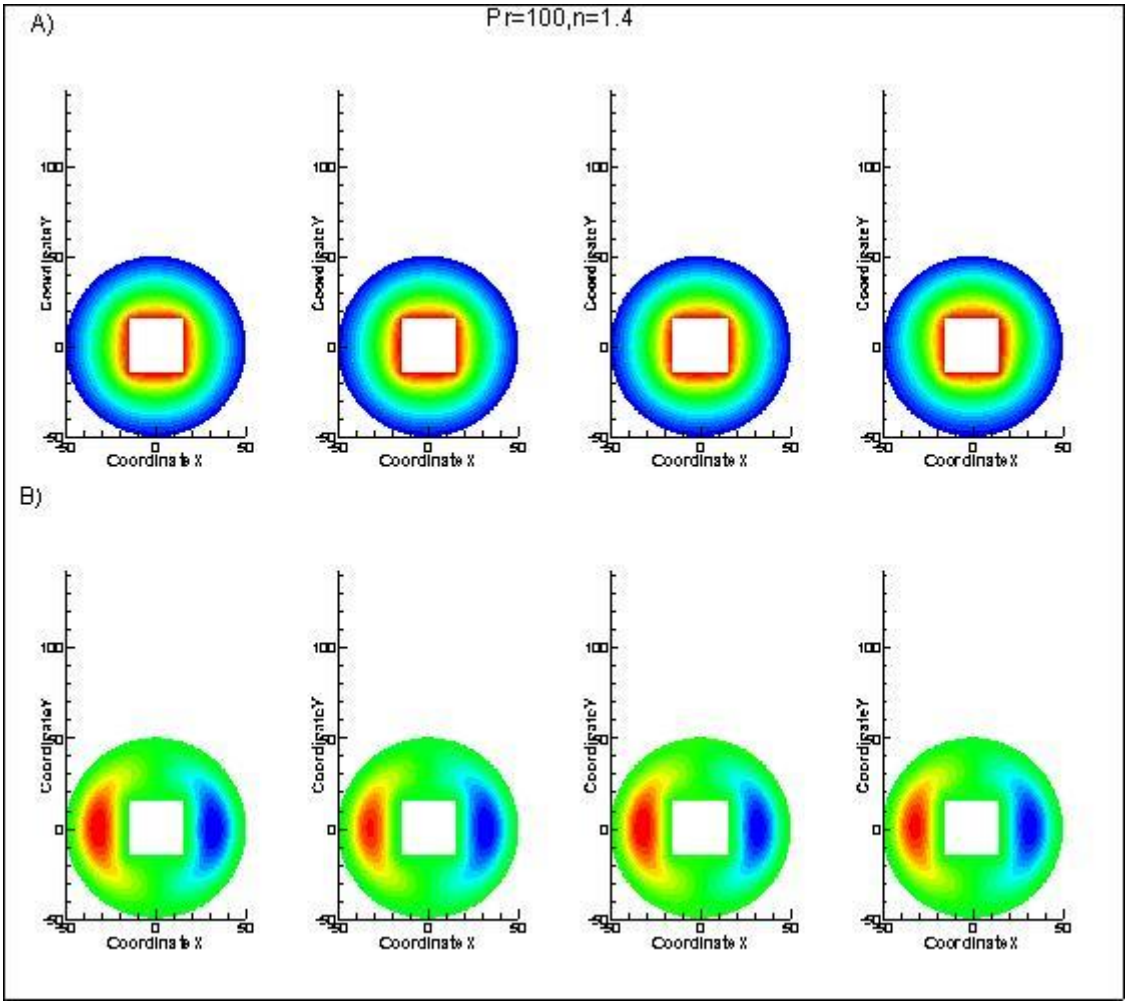

Fig.6.2.72 (A) Temperature profile, (B) Stream Function (Blockage=30%, Pr=100/1.4)

CHAPTER 7

CONCLUSION

Co-axial Cylinders

- ✓ It can be clearly seen that for Grashoff number of 10^3, and Prandtl number=1, irrespective of blockage the dominant form of heat transfer is conduction but as Grashoff number increases from $10^4 to\ 10^6$ the plume starts to form and convection starts to dominate. For Prandtl number =100, the effect of convection seems to dominate.
- ✓ By noticing streamlines and isotherms, the central vortex or eddy formed moves up because of buoyancy effect when Pandtl number is increased from 1-100, it becomes more and more pronounced as we move from Grashoff number from$10^3 to 10^6$.
- ✓ By noticing streamlines and isotherms, In 10% blockage of co-axial cylinders (Pr=1) for Grashoff number of 10^3, there seems to be no effect of buoyancy but as Grashoff increased to 10^4, we see some plume rising upward it becomes more and more pronounced as we increase Grashoff number to 10^6, also for Grashoff number of 10^3 & 10^4 the outer cylinder temperature is undisturbed but as Grashoff number increases from $10^5\ to\ 10^6$, the outer temperature seems to get disturbed due to high natural convection.
- ✓ In 20% blockage of co-axial cylinder (Pr=1) for Grashoff number of 10^3 we don't see any buoyancy effect but for Grashoff number of 10^4 the buoyancy effect is very strong and it increases as we move on increasing Grashoff number, the same goes for thermal boundary layer i.e. for Grashoff number of 10^3 the thermal boundary layer of hot cylinder (inside one) is small and it does not disturb the outer cylinder temperature but on increasing Grashoff number the inside body's thermal boundary layer increases and it disturbs the outer temperature.
- ✓ In 30% blockage of co-axial cylinder (Pr=1) for Grashoff number of 10^3 and 10^4 we don't see any buoyancy driven flow but by increasing Grashoff number, there seems to be effect of buoyancy, the same goes for thermal boundary layer.
- ✓ By noticing above plots, we can clearly see effect of buoyancy driven flow is clearly more dependent on Prandtl than on Grashoff number because when Prandtl increases from 10 to 100, irrespective of Grashoff Number Buoyancy driven flow seems to

dominate in each case. Its effect became more pronounced when Grashoff number is increased.

- ✓ When noticing streamlines (Pr=100) on increasing blockage from 10% to 30 %, Eddies become more like air foil than oval shape in lower blockages.

For Cuboid inside Cylinder co-axially

- ✓ By simply looking at isotherms and streamlines for blockage of 10% and Prandtl number of 1, as seen in the co-axial cylinder the convection heat transfer dominate, when Grashoff is more than 10^4. The same goes for boundary layer of hot body i.e. boundary layer does not disturbs the outer temperature at lower Grashoff number due to low natural convection but when Grashoff number become high large thermal boundary layer tends to disturb the outer temperature.
- ✓ For same case but blockage of 20% and 30%, buoyancy driven flow is seen when Grashoff is equal or greater than 10^5. The same observation as mentioned above is seen for this case also. As Grashoff number is increased the oval shaped eddy in stream function curve becomes more like stretched air foil
- ✓ As quoted above, effect of increasing Prandtl number from 10 to 100 on buoyancy driven flow is immense.

For Triangle inside cylinder co-axially

- ✓ The effect of this case is almost the same as mentioned in above two.

Non- Newtonian Fluids Analysis

Triangle inside cylinder

- ✓ As can be seen for image having Pr=1& 100, n=0.2 and for 10% geometry that on subsequent increase in Grashoff number effect of buoyancy is taking place steadily.
- ✓ For 20% blockage geometry and for Prandtl number of 1, it can be seen for Grashoff number of 10^4 and above a good heat transfer by convection is taking place as opposed to the 10 % geometry where a slight increase in convection heat transfer is seen as it increase the Grashoff number.
- ✓ For 30% geometry, the effect is somewhat similar as seen for 10% geometry i.e. on increase in Grashoff number convection starts to dominate; the effect can also be seen on stream function plot.

- ✓ For all blockages i.e. 10%, 20% & 30%, for viscosity index of 0.6 and Prandtl number of 1, it can be seen almost no change in temperature as well as stream function data as it goes from Grashoff number of 10^3 to 10^5. There is slight rise in plume for Grashoff number of 10^6. For Prandtl number of hundred apart from the figure of Grashoff number 10^6 showing convection effect, the temperature and stream function of Grashoff number 10^5 also shows significant natural convection effect.
- ✓ The dilatant fluid having viscosity index of 1.4 and Prandtl number of 1 as seen above for n=.6 that there is slight or no change in stream function as well as temperature profile for Grashoff number from 10^3 to 10^5 but slight rise in plume for Grashoff number of 10^6. For Prandtl number of 100, in going from Grashoff number of 10^3 to 10^6, the effect of buoyancy keeps on increases, it can be seen in temperature as well as stream function.

For Cuboid inside Cylinder co-axially

- ✓ As was seen for triangle, for blockage of 10% and for Pr=1 on going from Grashoff number of 10^3 to 10^6, the increase in plume rising above is seen in temperature profile. In stream function it can be seen aero foil type of shape formation due to the effect of natural convection increasing as seen in Grashoff number of 10^5.
- ✓ For 20% and 30% blockage for Prandtl number 1 it can be seen the effect of natural convection from Grashoff number 10^5 and above.
- ✓ The result for Pr=100 and viscosity index of 0.2 for all the geometries is same as seen above for triangle blockage with same parameters.
- ✓ For all blockages i.e. 10%, 20% & 30%, for viscosity index of 0.6 and Prandtl number of 1, it can be seen almost no change in temperature as well as stream function data as it go from Grashoff number of 10^3 to 10^5. There is slight rise in plume for Grashoff number of 10^6. For Prandtl number of hundred apart from the figure of Grashoff number 10^6 showing convection effect, the temperature and stream function of Grashoff number 10^5 also shows significant natural convection effect.
- ✓ For viscosity index of 1.4 and Prandtl number of 1 and for all geometries it do not see any effect of natural convection while increasing Grashoff number from 10^3 to 10^4.
- ✓ For Prandtl number 100 while keeping viscosity index of 1.4 and for 10% and 20% blockage there is effect of natural convection while increasing Grashoff number but for 30% geometry there is absolute no sign of any change in mode of heat transfer is seen.

Co-axial cylinders

- ✓ For all blockages i.e. 10%, 20% & 30%, for viscosity index of 0.2, 0.6, 1.4 and Prandtl number of 1,it can be seen almost no change in temperature as well as stream function data as it goes from Grashoff number of 10^3 to 10^5. There is slight rise in plume for Grashoff number of 10^6. For Prandtl number of hundred apart from the figure of Grashoff number 10^6 showing convection effect, the temperature and stream function of Grashoff number 10^5 also shows significant natural convection effect.
- ✓ For Pr=100 and viscosity index of 0.2 and all the geometries, it can be seen only significant natural convection in Grashoff number =10^6 and rest same as above.
- ✓ For Pr=100 and viscosity index of 0.6 and all the geometries, it can be seen only significant natural convection in Grashoff number =10^5 and 10^6 and rest same as above.
- ✓ Increase in buoyancy effect is seen as it increase Grashoff number from 10^3 to 10^6 for Prandtl number of 100 and viscosity index of 1.4

CHAPTER 8

REFERENCES

[1] H K Versteeg, W Malalasekera. An Introduction to Computational Fluid Dynamics (THE FINITE VOLUME METHOD). Glasgow: Pearson Education Limited; 2007.

[2] http://www.mathematik.uni-dortmund.de/~kuzmin/cfdintro/cfd.html

[3] R Bhaskaran, L Collins. Introduction to CFD Basics. Cornell University –sibly school of Mechanical and aerospace engineering. 2002 - Erac.ntut.edu.tw.

[4] T.H. KUEHN, R. J. GOLDSTEIN, An experimental and theoretical study of natural convection in the annulus between horizontal concentric cylinders, J. Fluid Mech. (1976), vol. 74, part 4 , pp. 695-719

[5] Zi-Tao Yu et al., Transient natural convective heat transfer from a heated triangular Cylinder to its air-filled coaxial cylindrical enclosure, Int. J. of Heat and Mass Transfer 53 (2010) 4296–4303

[6] https://en.wikipedia.org/wiki/Finite_volume_method

[7] https://en.wikipedia.org/wiki/Convective_heat_transfer

[8] F.P. Incropera and D.P. Dewitt, Fundamentals of Heat Transfer, Wiley, New York (1981)

[9] https://en.wikipedia.org/wiki/Non-Newtonian

[10] Mohammad Ali Hazar, Ali Akbar abbasian, Numerical analysis of the natural convection in horizontal cylindrical annuli, International Academic Journal of Vol. 3, No. 5, 2016, pp. Science and Engineering